

The species-specific role of caspase-8 as a regulator of necroptosis

Dissertation

zur Erlangung des Doktorgrades

der Mathematisch-Naturwissenschaftlichen Fakultät

der Christian-Albrechts-Universität zu Kiel

vorgelegt von

Carina Saggau

Kiel

2018

Erster Gutachter:	Prof. Dr. Dieter Adam
Zweiter Gutachter:	Prof. Dr. Axel Scheidig
Tag der mündlichen Prüfung:	11.12.2018
Zum Druck genehmigt:	11.12.2018

I. Table of contents

I.	Table of contents	3
II.	Abbreviations	6
III.	List of Figures	8
IV.	List of Tables	10
1.	Summary	11
	Zusammenfassung.....	12
2.	Introduction	14
2.1	Caspase-dependent programmed cell death – apoptosis.....	14
2.2	Non-apoptotic cell death.....	15
2.2.1	Necroptosis.....	16
2.2.2	Necroptotic signaling.....	17
2.3	Necroptosis and relevant molecules of the presented dissertation	19
2.3.1	Necroptosis and the caspases-8 and -10.....	19
2.3.2	Necroptosis and HtrA2/Omi	21
2.4	Aims of the presented dissertation	21
3.	Materials and Methods	24
3.1	Materials.....	24
3.1.1	Technical equipment	24
3.1.2	Reagents and chemicals	25
3.1.3	Antibodies.....	27
3.1.4	siRNAs and constructs	28
3.1.5	Cell lines.....	29
3.2	Methods	30
3.2.1	Transfection	30
3.2.2	Cytotoxicity assay – propidium iodide staining	31
3.2.3	Determination of protein concentrations	31
3.2.4	Preparation of whole cell lysates.....	31
3.2.5	Western blot analysis	32
3.2.6	Immunoprecipitation.....	32
3.2.7	Generation of knockout cell lines with the CRISPR/Cas9 system.....	33
3.2.8	Purification of TNF ligands.....	33

I. Table of contents

3.2.9	Immunomagnetic isolation of TNF receptosomes	33
3.2.10	Mitochondria isolation and LC-MS/MS analysis	34
4.	Results	35
4.1	Caspase-8 and caspase-10 as key mediators regulating TNF-induced necroptosis	35
4.1.1	Genetic ablation of caspase-8 in murine L929Ts cells leads to increased cell death ..	35
4.1.2	Genetic ablation of caspase-8 in two different human cell lines protects cells from necroptosis	38
4.1.3	Genetic ablation of caspase-10 in two different human cell lines leads to increased cell death	40
4.1.4	The additional downregulation of other components of the necrosome alters the effect of caspases-8 and -10 within the necroptotic signaling pathway	42
4.1.5	The additional downregulation of caspase-10 in human cells cannot override the effect of caspase-8.....	44
4.1.6	Reconstitution of CRISPR/Cas knockout cell lines with enzymatically active and inactive mutant forms of caspases-8 and -10.....	45
4.1.7	Analyses of the composition of the necrosome in caspase-8- and caspase-10-deficient human cells.....	47
4.1.8	The effect caused by the deletion of caspase-8 in human cells can be overcome upon usage of the Smac mimetic birinapant.....	49
4.2	The serine protease HtrA2/Omi as a key mediator regulating TNF-induced necroptosis	50
4.2.1	Analyses of DBC1, PDXDC1 and VPS4B as potential downstream mediators of HtrA2/Omi during necroptosis	50
4.2.2	Analyses of PMPCA, PSA1 and LONP1 as potential downstream mediators of HtrA2/Omi during necroptosis	52
4.2.3	Analyses of moesin and stathmin as potential downstream mediators of HtrA2/Omi during necroptosis	53
4.2.4	Analyses of Inhibitor of apoptosis proteins cIAP1 and XIAP as potential downstream mediators of HtrA2/Omi during necroptosis	54
4.2.5	Identification of new potential substrates of HtrA2/Omi by mass spectrometric analysis.....	57
4.2.6	Conclusion	57
5.	Discussion	59
5.1	Necroptosis is differentially regulated by caspase-8 in mice and in humans	59
5.2	Caspase-10 in humans cannot substitute the function that is held by caspase-8 in mice.....	60
5.3	Identification of downstream mediators of the serine protease HtrA2/Omi	62

I. Table of contents

5.4	Biological relevance of the obtained results of this thesis and future perspectives.....	65
6.	References	66
7.	List of publications	79
8.	Eidesstattliche Erklärung	80
9.	Danksagung	81
10.	Wissenschaftlicher Werdegang	82

II. Abbreviations

AIF	apoptosis-inducing factor
Apaf-1	apoptotic protease activating factor 1
ATCC	American Type Culture Collection
ATP	adenosine-5'-triphosphate
BAX	Bcl-2-associated X protein
Bcl-2	B-cell CLL/lymphoma-2
BSA	bovine serum albumin
Cas9	CRISPR-associated 9
caspase	cysteine-aspartate protease
Casp/CASP	caspases
CFLAR	caspase-8 and FADD-like apoptosis regulator
c-FLIP	cellular FLICE-inhibitory protein
ciAP	cellular inhibitor of apoptosis proteins
CHX	cycloheximide
CL	cardiolipin
CRISPR	clustered regularly interspaced short palindromic repeats
ctrl	control
CYLD	cylindromatosis
DAI	DNA-dependent activator of interferon regulatory factors
DAMPs	damage associated molecular patterns
DBC1	deleted in bladder cancer protein 1
DD	death domain
DISC	death-inducing signaling complex
DMSO	dimethyl sulfoxide
Dox	doxycycline
EDTA	ethylenediaminetetraacetic acid
FACS	fluorescence-activated cell sorting
FADD	Fas-associated death domain protein
Fas	First apoptosis signal
FCS	fetal calf serum
FLICE	FADD-like IL-1 β -converting enzyme
GFP	green fluorescent protein
GSK	N(6-(isopropylsulfonyl)quinolin-4-yl)benzo[d]thiazol-5-amine
HB	homogenization buffer
HRP	horseradish peroxidase
HtrA2	high-temperature requirement protein A2
IAPs	inhibitor of apoptosis proteins
IFNs	interferons
IP	immunoprecipitation
KO	knockout
LAMP-2	lysosome-associated membrane glycoprotein 2
LONP1	Lon protease 1
LUBAC	linear ubiquitin chain assembly complex
MEF	mouse embryonic fibroblast
MLKL	mixed lineage kinase domain-like protein
MSN	moesin
MTCH2	mitochondrial carrier homologue 2
mut	mutant
Nec-1s	necrostatin-1s

II. Abbreviations

NF- κ B	nuclear factor- κ B
NSA	necrosulfonamide
PAGE	polyacrylamide gel electrophoresis
PARP-1	poly (ADP-ribose)-polymerase 1
PBS	phosphate buffered saline
PDXDC1	pyridoxal dependent decarboxylase domain containing protein 1
PI	propidium iodide
PMPCA (MPP-A)	mitochondrial-processing peptidase subunit alpha
PSA1	proteasome subunit alpha type-1
RHIM	RIP homotypic interaction motif
RIPK	receptor-interacting protein kinase
RN	regulated necrosis
Ros	reactive oxygen species
RT	room temperature
SD	standard deviation
SDS	sodium dodecyl sulphate
siRNA	small interfering RNA
Smac	second mitochondrial-derived activator of caspases
STMN1	stathmin 1
TLR	Toll-like receptor
TNF	tumor necrosis factor
TNF-R	tumor necrosis factor receptor
TRADD	TNF-associated death domain protein
TRAF2	TNF-R-associated factor 2
TRAIL-R	TNF related apoptosis-inducing ligand-receptor
UCH-L1	ubiquitin C-terminal hydrolase 1
VPS4B	vacuolar protein sorting 4 homolog B
WT	wild type
XIAP	X-linked inhibitor of apoptosis protein
zVAD-fmk	benzyloxycarbonyl-Val-Ala-Asp-fluoromethylketone

Commonly used abbreviations are not listed.

III. List of Figures

- Figure 1: Apoptotic signaling
- Figure 2: Forms of regulated cell death and their core pathway proteins
- Figure 3: Necroptotic signaling
- Figure 4: Phylogeny of caspase-8
- Figure 5: Relevant molecules of the presented dissertation and their role within the necroptotic signaling pathway
- Figure 6: Generation of caspase-8-deficient L929Ts cells
- Figure 7: Inhibition of cell death in response to Nec-1s and GSK'872 in L929Ts CRISPR/Cas clones deficient for caspase-8
- Figure 8: Determining the effect of the genetic ablation of caspase-8 on TNF-induced necroptosis in the L929Ts caspase-8 $-/-$ clone B3
- Figure 9: Generation of caspase-8-deficient U-937 and HT-29 cells
- Figure 10: Inhibition of cell death in response to treatment with Nec-1s and GSK'872 in U-937 and HT-29 CRISPR/Cas clones deficient for caspase-8
- Figure 11: Determining the effect of the genetic ablation of caspase-8 on TNF-induced necroptosis in the U-937 caspase-8 $-/-$ clone A7
- Figure 12: Determining the effect of the genetic ablation of caspase-8 on TNF-induced necroptosis in the HT-29 caspase-8 $-/-$ clone F11
- Figure 13: Generation of caspase-10-deficient U-937 and HT-29 cells
- Figure 14: Inhibition of cell death in response to treatment with Nec-1s and GSK'872 in U-937 and HT-29 CRISPR/Cas clones deficient for caspase-10
- Figure 15: Determining the effect of the genetic ablation of caspase-10 on TNF-induced necroptosis in the U-937 caspase-10 $-/-$ clone A3
- Figure 16: Determining the effect of the genetic ablation of caspase-10 on TNF-induced necroptosis in the HT-29 caspase-10 $-/-$ clone G14
- Figure 17: Additional downregulation of core components of the necrosome in the L929Ts caspase-8 $-/-$ clone B3
- Figure 18: Additional downregulation of core components of the necrosome in the U-937 caspase-8 $-/-$ clone A7 and the U-937 caspase-10 $-/-$ clone A3
- Figure 19: Additional downregulation of core components of the necrosome in the HT-29 caspase-8 $-/-$ clone F11 and the HT-29 caspase-10 $-/-$ clone G14
- Figure 20: Reconstitution of the L929Ts caspase-8 $-/-$ clone B3 with active mouse caspase-8, active human caspase-8 and an inactive mutant form of human caspase-8
- Figure 21: Reconstitution of the HT-29 caspase-8 $-/-$ clone F11 with active and inactive mutant forms of human and mouse caspase-8
- Figure 22: Reconstitution of the HT-29 caspase-10 $-/-$ clone G14 with active and inactive mutant forms of caspase-10
- Figure 23: Analyses of the assembly of the necrosome in wild type HT-29 cells and the HT-29 caspase-8 $-/-$ clone F11 via immunoprecipitation
- Figure 24: Analyses of the assembly of the necrosome in wild type U-937 cells, the U-937 caspase-8 $-/-$ clone A7 and the U-937 $-/-$ clone A3 via immunoprecipitations
- Figure 25: Analyses of magnetically isolated receptosomes from wild type HT-29 and U-937 cells
- Figure 26: The Smac mimetic birinapant overcomes the protection from necroptosis caused by the deletion of caspase-8 in human HT-29 cells
- Figure 27: Western blot analyses of DBC1, PDXDC1 and VPS4B as downstream mediators of HtrA2/Omi during necroptosis
- Figure 28: Downregulation by siRNA of DBC1, PDXDC1 and VPS4B in HtrA2/Omi wild type MEF
- Figure 29: Downregulation by siRNA of LONP1, PSA1 and PMPCA in L929Ts and HT-29 wild type cells

III. List of Figures

- Figure 30: Western blot analyses of moesin and stathmin as downstream mediators of HtrA2/Omi during necroptosis
- Figure 31: Western blot analyses of XIAP as downstream mediator of HtrA2/Omi during necroptosis
- Figure 32: Western blot analyses of cIAP1 as downstream mediator of HtrA2/Omi during necroptosis
- Figure 33: The Smac mimetic birinapant overcomes the protection from necroptosis caused by the deletion of HtrA2/Omi

IV. List of Tables

- Table 1: List of all utilized primary and secondary antibodies
- Table 2: List of all utilized constructs and siRNAs
- Table 3: List of potential substrates of HtrA2/Omi during necroptosis which were identified by mass spectrometric analysis

1. Summary

In contrast to apoptosis, the molecular mechanisms of the necroptotic signaling pathway remain to a certain proportion unknown. Since necroptosis is associated to various diseases, a precise knowledge of the necroptotic signaling pathway is essential for the development of new therapeutic strategies. The aim of this dissertation was to therefore gain a deeper insight into molecular and cellular events of TNF-induced necroptosis.

In the first part of the thesis, murine L929Ts cells deficient for caspase-8 as well as human HT-29 and U-937 cells deficient for caspase-8 or caspase-10 were generated by employing the CRISPR/Cas9 technology. It was shown that genetic ablation of caspase-8 in murine L929Ts cells enhances necroptosis (as shown in many studies worldwide for murine cells), whereas genetic ablation of caspase-8 in human U-937 and HT-29 cells protects the cells from TNF-induced necroptosis. The identification of those opposing effects of caspase-8 on necroptosis in mouse and man are essential for the attempt to develop new clinical strategies by targeting necroptosis through caspase-8. It is noteworthy that humans express caspase-8 and caspase-10, while caspase-10 was lost in mice over the course of evolution. In the presented dissertation, it was demonstrated that genetic ablation of caspase-10 in human cells exacerbates necroptosis, supporting the hypothesis that caspase-10 in humans can substitute the function that is held by caspase-8 in mice. Furthermore, experiments aimed at the identification of differences in the composition of necrosomes in wild type vs. caspase-8- or caspase-10-deficient U-937 and HT-29 cells found that caspase-10 associates with caspase-8 during TNF-induced necroptosis. Furthermore, genetic ablation of caspase-8 prevents the recruitment of caspase-10. Genetic ablation of caspase-8 disrupts the assembly of the necrosome while genetic ablation of caspase-10 promotes at least the recruitment of RIPK1 and RIPK3, which are core proteins of the necroptotic cell death machinery. The reconstitution of cells genetically deficient for caspase-8, with active and inactive forms of human and mouse caspase-8, confirmed a species-specific role of caspase-8 in the suppression of necroptosis. It was demonstrated that the reconstitution of human caspase-8-deficient HT-29 cells with active human caspase-8 enhances necroptosis, while reconstitution with active mouse caspase-8 does not enhance but rather protects the cells from TNF-induced necroptosis. Additionally, data obtained in this thesis revealed that the enzymatic activity of human and mouse caspase-8, as well as the enzymatic activity of caspase-10, are required for their function within the necroptotic signaling pathway. In summary, it can be stated that all data obtained in this thesis consistently point to a differential proteolytic regulation of necroptosis by caspase-8 in mice and in humans.

The serine protease HtrA2/Omi has been identified as a key mediator regulating TNF-induced necroptosis. Pharmacological inhibition or genetic deletion of HtrA2/Omi protects cells from necroptosis, but the underlying molecular mechanism is still unknown. In the second part of this thesis, several potential substrates (e.g., LONP1, PSA1, PMPCA, DBC1, PDXDC1 and VPS4B) of HtrA2/Omi were therefore analyzed by Western blot analysis and

siRNA knockdown experiments. In the course of the work of this doctoral thesis, it was discovered that one of the inhibitor of apoptosis proteins (IAPs), named XIAP, is cleaved by HtrA2/Omi during necroptosis. Moreover, it was demonstrated that the effect caused by the genetic deletion of HtrA2/Omi could be neutralized upon usage of the IAP-deleting Smac mimetic birinapant, supporting the hypothesis that HtrA2/Omi mediates TNF-induced necroptosis by proteolytic cleavage of IAPs. In addition, by mass spectrometric analyses from mitochondrial fractions of necroptotic wild type and HtrA2/Omi-deficient mouse embryonic fibroblasts, 17 potential downstream mediators of HtrA2/Omi were identified.

Zusammenfassung

Im Gegensatz zur Apoptose ist der molekulare Mechanismus des nekroptotischen Signalweges nur teilweise aufgeklärt. Da Nekroptose mit vielen verschiedenen Krankheiten in Verbindung steht, ist es essentiell, genaue Erkenntnis über den Signalweg der Nekroptose zu erlangen, um neue therapeutische Strategien entwickeln zu können. Daher war das Ziel der vorliegenden Dissertation, einen tieferen Einblick in molekulare und zelluläre Prozesse der TNF-induzierten Nekroptose zu gewinnen.

Im ersten Teil dieser Arbeit wurden sowohl Caspase-8-defiziente L929Ts Mauszellen als auch Caspase-8- oder Caspase-10-defiziente humane HT-29 und U-937 Zellen mittels CRISPR/Cas9 Technologie generiert. Es wurde gezeigt, dass genetische Deletion von Caspase-8 in L929Ts Mauszellen Nekroptose verstärkt (wie auch bereits in vielen Studien in Mauszellen weltweit gezeigt), wohingegen genetische Deletion von Caspase-8 in humanen U-937 und HT-29 Zellen die Zellen vor TNF-induzierter Nekroptose schützt. Die Identifikation dieser gegensätzlichen Effekte von Caspase-8 auf Nekroptose in Mäusen und im Menschen ist entscheidend für die Entwicklung neuer klinischer Strategien, wenn man versucht Nekroptose über Caspase-8 zu manipulieren. Nennenswert an dieser Stelle ist, dass der Mensch Caspase-8 und Caspase-10 exprimiert, während Caspase-10 in Mäusen im Verlauf der Evolution verloren gegangen ist. In der vorliegenden Dissertation wurde gezeigt, dass genetische Deletion von Caspase-10 in humanen Zellen Nekroptose begünstigt, was die Hypothese unterstützt, dass Caspase-10 im Menschen die Funktion, welche der Caspase-8 in Mäusen zugeschrieben ist, übernimmt. Des Weiteren haben Experimente mit dem Ziel zur Identifikation von Unterschieden in der Komposition des „Nekrosoms“ von Wildtyp vs. Caspase-8-defizienten U-937 und HT-29 Zellen ergeben, dass Caspase-10 und Caspase-8 während TNF-induzierter Nekroptose assoziieren und dass die genetische Deletion von Caspase-8 die Rekrutierung von Caspase-10 verhindert. Die genetische Deletion von Caspase-8 stört die Bildung des „Nekrosoms“, während die genetische Deletion von Caspase-10 zumindest die Rekrutierung von RIPK1 und RIPK3 begünstigt, welche Hauptkomponenten des nekroptotischen Zelltodes sind. Die Rekonstitution von Caspase-8-defizienten Zellen mit aktiven und inaktiven Formen von humaner und muriner Caspase-8 bestätigte eine spezie-spezifische Rolle der Caspase-8 in Bezug auf ihre unterdrückende Funktion auf Nekroptose. Es wurde demonstriert, dass die Rekonstitution von humanen Caspase-8-defizienten HT-29

Zellen mit humaner Caspase-8 Nekroptose verstärkt, während die Rekonstitution mit muriner Caspase-8 Nekroptose vermindert. Außerdem ergaben die innerhalb dieser Arbeit gewonnenen Daten, dass die enzymatische Aktivität von Caspase-8 und -10 essentiell für ihre Funktion innerhalb des nekroptotischen Signalweges ist. Zusammenfassend kann gesagt werden, dass alle Daten, welche innerhalb der vorliegenden Arbeit generiert wurden, übereinstimmend auf einen Unterschied in der proteolytischen Regulation der Nekroptose durch Caspase-8 in der Maus und im Menschen hindeuten.

Die Serinprotease HtrA2/Omi wurde als Schlüsselmediator identifiziert, welche die TNF-induzierte Nekroptose reguliert. Pharmakologische Inhibition oder genetische Deletion von HtrA2/Omi schützen Zellen vor Nekroptose, aber der zugrundeliegende Mechanismus ist bislang unbekannt. Im zweiten Teil dieser Arbeit wurden daher verschiedene potentielle Substrate (z.B. LONP1, PSA1, PMPCA, DBC1, PDXDC1 und VPS4B) der Serinprotease HtrA2/Omi mittels Western Blot Analyse und „siRNA-Knockdown“ Experimenten untersucht. Im Verlauf der vorliegenden Dissertation wurde herausgefunden, dass einer der Apoptose-Inhibitoren (IAPs) mit dem Namen XIAP während der Nekroptose von HtrA2/Omi gespalten wird. Des Weiteren wurde gezeigt, dass der Effekt, welcher durch die genetische Deletion von HtrA2/Omi hervorgerufen wurde, durch den Einsatz des IAP-abbauenden Smac-Mimetikums Birinapant aufgehoben werden konnte, was die Hypothese unterstützt, dass HtrA2/Omi die TNF-induzierte Nekroptose durch die proteolytische Spaltung der IAPs reguliert. Zusätzlich wurden durch massenspektrometrische Analysen mitochondrialer Fraktionen, welche aus nekroptotischen Wildtyp und HtrA2/Omi-defizienten embryonalen Mausfibroblasten gewonnen wurden, 17 neue potentielle Substrate „Downstream“ von HtrA2/Omi identifiziert.

2. Introduction

2.1 Caspase-dependent programmed cell death – apoptosis

Apoptosis was first described in a study by Kerr and colleagues in 1972 and became the best-studied form of cell death (Kerr *et al.* 1972). Apoptosis normally serves as a homeostatic mechanism to maintain cell populations in tissues (Grootjans *et al.* 2017). Apart from that, apoptosis can also occur as a defense mechanism against pathogens or harmful agents (Norbury and Hickson 2001). During apoptosis, cells undergo morphological changes like cell shrinkage, chromatin condensation, nuclear condensation and fragmentation, plasma membrane blebbing, DNA fragmentation and separation of cell fragments into apoptotic bodies. These apoptotic bodies are subsequently phagocytosed by macrophages or by surrounding cells. Since apoptotic cells do not release their cellular components into the environment, there is no inflammatory reaction associated with apoptosis (Kerr *et al.* 1972, Savill and Fadok 2000, Elmore 2007, Poon *et al.* 2014, Nagata *et al.* 2017).

To date, there exist two main apoptotic pathways: the extrinsic pathway (death receptor pathway) and the intrinsic pathway (mitochondrial pathway) (Green and Llambi 2015) (Figure 1). The extrinsic apoptotic pathway is triggered by external signals via death receptors that are members of the tumor necrosis factor (TNF) receptor gene superfamily (e.g., TNF receptor 1 (TNF-R1), TNF related apoptosis-inducing ligand receptors (TRAIL-R1/2), First apoptosis signal receptor (Fas)) (Galluzzi *et al.* 2018). In the aftermath of ligand binding, cytoplasmic adapter proteins like TNF-associated death domain protein (TRADD) and Fas-associated death domain protein (FADD) are recruited to the receptor, followed by activation of initiator caspases-8 and -10 and effector caspases-3, -6 and -7 (Pfeffer and Singh 2018). Death receptor-mediated apoptosis can be inhibited by a protein called cellular FLICE-inhibitory protein (c-FLIP) which binds to FADD and caspase-8 (Hughes *et al.* 2016, Shindo *et al.* 2016). The intrinsic apoptotic pathway is activated via intracellular stimuli such as DNA damage, hypoxia or oxidative stress (Galluzzi *et al.* 2018). These stimuli lead to changes of the inner mitochondrial membrane and the loss of the mitochondrial transmembrane potential (Elmore 2007). This eventually results in the release of cytochrome c, second mitochondrial-derived activator of caspases (Smac) and high-temperature requirement protein A2 (HtrA2/Omi) from mitochondria (Pfeffer and Singh 2018). Cytochrome c binds and activates the apoptotic protease activating factor 1 (Apaf-1) and the initiator caspase-9, forming a protein complex called “apoptosome”, which then leads to the activation of effector caspases-3, -6 and -7 (Green and Llambi 2015). The control of the intrinsic apoptotic pathway occurs through members of the B-cell lymphoma-2 (Bcl-2) family (Sprick and Walczak 2004, Zaman *et al.* 2014).

Apoptosis can be regulated via inhibitor of apoptosis proteins (IAPs), which function as E3 ubiquitin ligases. The group of IAPs comprises cellular inhibitor of apoptosis proteins 1 (cIAP1), cellular inhibitor of apoptosis proteins 2 (cIAP2) and X-linked inhibitor of apoptosis proteins (XIAP). IAPs negatively regulate cell death by inhibiting caspases (Silke and Meier

2013). The activity of IAPs is blocked, when endogenous IAP antagonists such as Smac are released from mitochondria, binding to selected BIR domains of the IAPs and neutralizing these proteins, thus leading to activation of caspases and the induction of apoptosis (Fulda and Vucic 2012, Fuchs and Steller 2015).

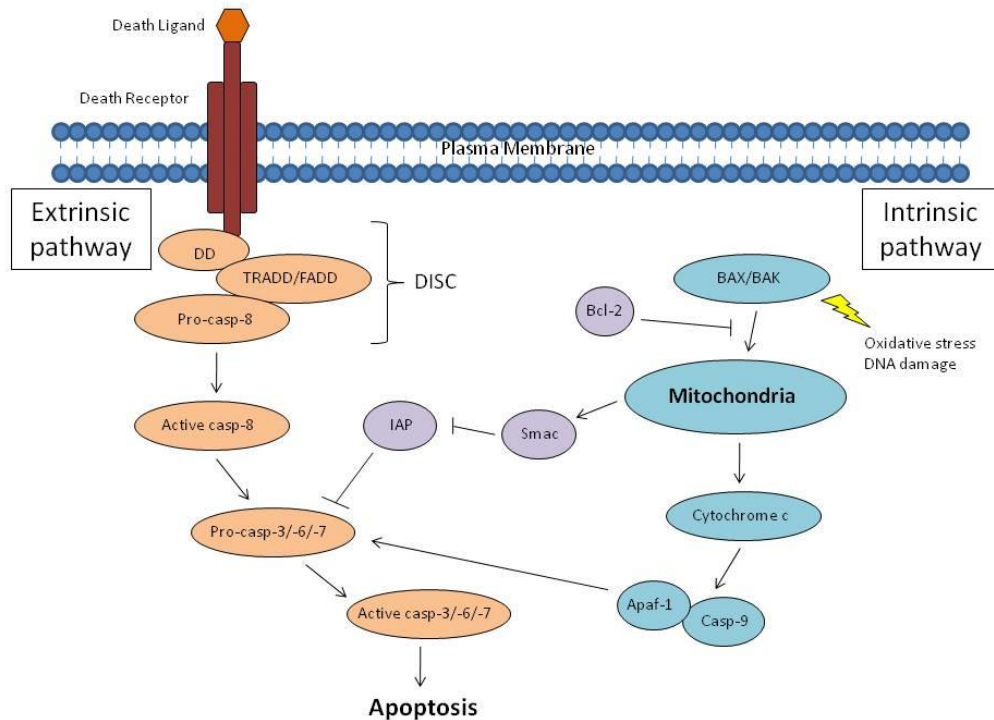


Figure 1: Apoptotic signaling. There exist two main apoptotic pathways: the extrinsic and the intrinsic apoptotic pathway. The extrinsic pathway is induced by ligation of death ligands to their receptor, leading to formation of the death-inducing signaling complex (DISC), consisting of death-domain proteins like TRADD/FADD and pro-caspase-8. Subsequently, activated caspase-8 cleaves and activates the effector caspases-3, -6 and -7. The intrinsic pathway is activated by cellular stress, which leads to activation of BAX/BAK and thus to permeabilization of the mitochondria and release of cytochrome c and Smac. Cytochrome c leads to formation of the apoptosome by oligomerizing caspase-9 and Apaf-1, which results in activation of the effector caspases -3, -6 and -7. The release of Smac supports the execution of both apoptotic pathways by inhibiting IAPs. **Figure modified from Zaman *et al.* 2014.**

2.2 Non-apoptotic cell death

In the last few decades, various forms of non-apoptotic regulated cell death were discovered, i.e., necroptosis (Degterev *et al.* 2005), ferroptosis (Dixon *et al.* 2012), pyroptosis (Cookson and Brennan 2001), pyronecrosis (Willingham *et al.* 2007), NETosis/ETosis (Brinkman *et al.* 2004) and parthanatos (Andrabi *et al.* 2008) and were summarized as “regulated necrosis” (RN) (Grootjans *et al.* 2017) (Figure 2). In contrast to apoptosis, all these forms of non-apoptotic regulated cell death share the same morphological features, such as cell swelling and loss of cell membrane integrity (Weinlich *et al.* 2017). This breakdown of the plasma membrane leads to the release of the cytoplasmic contents in the environment and therefore to an inflammatory reaction (Sun and Wang 2014).

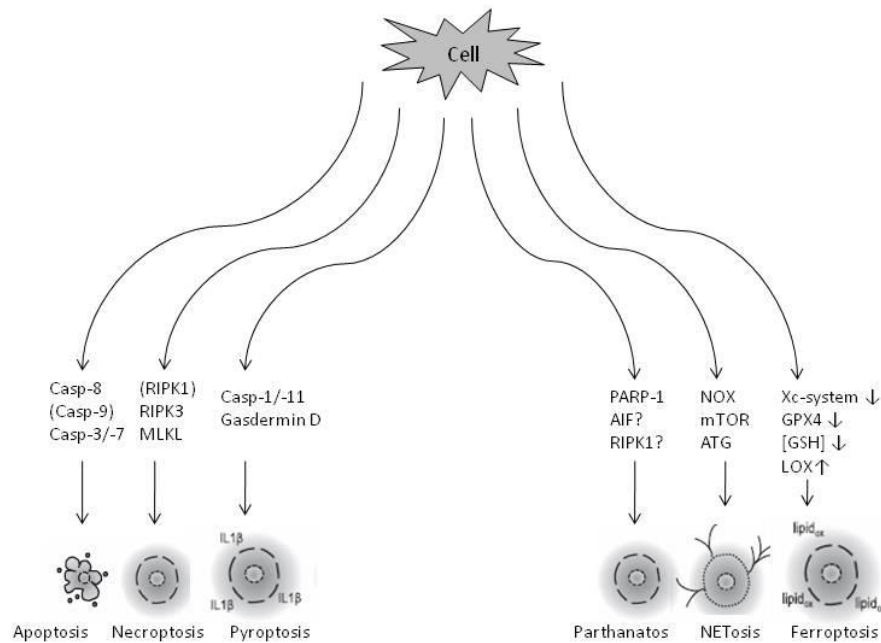


Figure 2: Forms of regulated cell death and their core pathway proteins.

Casp – caspases, RIPK – receptor-interacting protein kinase, MLKL – mixed lineage kinase-like, IL1 β – interleukin-1 β , PARP – poly-(ADP ribose)-polymerase, AIF – apoptosis-inducing factor, NOX – NADPH oxidase, mTOR – mechanistic target of rapamycin, ATG – autophagy-related, Xc-system – cystin/glutamate antiporter, GPX4 – glutathione peroxidase 4, GSH – reduced glutathione, LOX – lipoxygenase, lipid_{ox} – peroxidized (phospho)lipids **Figure modified from Grootjans *et al.* 2017.**

2.2.1 Necroptosis

TNF-induced necroptosis is the most intensively studied subtype of regulated necrosis and will also be the main topic of the presented dissertation. Apart from TNF, necroptosis can be triggered by other members of the TNF receptor superfamily, such as Fas, TRAIL-R1/2 or DR3 and DR6. In addition, necroptosis can be initiated by various other triggers (e.g., Toll-like receptors (TLR) 3 and 4, intracellular RNA and DNA sensors, interferons (IFNs), DNA damage, ionizing radiation, reactive oxygen species (ROS), calcium overload) (Seifert and Miller 2017, Annibaldi and Meier 2018).

In 2005, the term necroptosis was introduced for the first time and described as a form of non-apoptotic cell death with necrotic cell death morphology that is triggered by the TNFR receptor family (Degterev *et al.* 2005). Within this study, necrostatin-1, a specific inhibitor of necroptosis that inhibits receptor-interacting protein kinase 1 (RIPK1), was identified. By using RIPK1 inhibitors or animal models lacking receptor-interacting protein kinase 3 (RIPK3) or mixed lineage kinase domain-like protein (MLKL) (core components of the necroptotic signaling pathway), the majority of knowledge about necroptosis was ascertained (Sun and Wang 2014). TNF-induced necroptosis depends on RIPK1 (Holler *et al.* 2000, Degterev *et al.*

2008) and RIPK3, interacting through their RIP homotypic interaction motif (RHIM) (Cho *et al.* 2009, He *et al.* 2009, Zhang *et al.* 2009). MLKL is also essential for necroptosis and, together with RIPK1 and RIPK3, forms a complex called necrosome (Sun *et al.* 2012, Zhao *et al.* 2012, Murphy *et al.* 2013, Alvarez-Diaz *et al.* 2016).

Necroptosis can act as a back-up cell death program when the apoptotic cell death machinery fails (e.g., after virus infection) (Conrad *et al.* 2016). Since there are only a few hints that necroptosis occurs under physiological conditions, the biological relevance of necroptosis seems to be primarily related to pathophysiological conditions and diseases (Grootjans *et al.* 2017). These include: inflammatory bowel disease (Pierdomenico *et al.* 2014), Gaucher's disease (Vitner *et al.* 2014), multiple sclerosis (Ofengeim *et al.* 2015), Alzheimer's disease (Qinli *et al.* 2013), Huntington's disease (Zhu *et al.* 2011), ischemia-reperfusion injury (Rosenbaum *et al.* 2010), sepsis (Linkermann *et al.* 2012), chronic alcoholic (Wang *et al.* 2016) and non-alcoholic liver disease (Afonso *et al.* 2015), acute kidney injury (Linkermann *et al.* 2013), atherosclerosis (Lin *et al.* 2013), amyotrophic lateral sclerosis (ALS) (Ito *et al.* 2016) or viral (Guo *et al.* 2015, Huang *et al.* 2015, Nogusa *et al.* 2015), bacterial (Robinson *et al.* 2012, Roca *et al.* 2013, Kitur *et al.* 2015) and parasitic infection (Osborn *et al.* 2010). Necroptotic cells release damage associated molecular patterns (DAMPs), thus mobilizing the host immune response and contributing to physiological immunosurveillance (Murakami *et al.* 2014, Sun and Wang 2014, Pearson and Murphy 2017). It is also known that necroptosis plays a role in cancer (Aaes *et al.* 2016), and recently has been shown to facilitate metastasis by promoting inflammation (Najafov *et al.* 2017). In a study by Seifert and colleagues, necroptosis was found to cause macrophage-induced suppression of T cell immunity in pancreatic ductal adenocarcinoma, which leads to tumor cell metastasis (Seifert *et al.* 2016). In a different study, tumor cells induced necroptosis in endothelial cells to promote tumor cell extravasation and metastasis (Strilic *et al.* 2016). Upon use of the necroptosis inhibitor Nec-1 or upon endothelial cell-specific deletion of RIPK3 or MLKL in mice, necroptosis and therefore tumor cell extravasation and metastasis were reduced (Najafov *et al.* 2017). In a further study, it was reported that apoptosis-resistant colorectal tumors could be reduced in size by induction of necroptosis in mice (He *et al.* 2017). Targeting necroptosis might therefore be a potential therapeutic strategy. Nowadays, necroptosis can be blocked by targeting RIPK1 (necrostatin-1s (Nec-1s (R-7-Cl-O-Nec-1))) (Takahashi *et al.* 2012), RIPK3 (GSK'840, GSK'843, GSK'872, GW'39B and dabrafenib) (Kaiser *et al.* 2013, Li *et al.* 2014, Rodriguez *et al.* 2015) or MLKL (necrosulfonamide (NSA), inhibits only human but not rodent MLKL) (Sun *et al.* 2012, Conrad *et al.* 2016).

2.2.2 Necroptotic signaling

Upon ligation of TNF to TNF-R1, the so-called complex I is formed (Figure 3). This complex consists of TNF-R1, TRADD, TNF-R-associated factor 2 (TRAF2), RIPK1, the linear ubiquitin chain assembly complex (LUBAC) and the E3 ligases cellular inhibitor of apoptosis protein 1 and 2 (cIAP1/2). Formation of complex I shifts cells toward survival programs (Brenner *et al.* 2015). cIAP1/2 encourage ubiquitination of themselves and RIPK1 with K63 chains (Witt and

Vucic 2017). When Smac is released from the mitochondria, it binds to cIAP1/2. Subsequently, cIAP1/2 are inactivated and degraded, leading to dissociation of RIPK1 from the plasma membrane (Du *et al.* 2000). The K63-linked polyubiquitin chain on RIPK1 is subsequently removed by cylindromatosis (CYLD) (Moquin *et al.* 2013). RIPK1 then binds to FADD, which leads to the recruitment of pro-caspase-8 and formation of complex IIb (Sun and Wang 2014, Pasparakis and Vandenabeele 2015). Activated caspase-8 subsequently cleaves downstream caspases inducing apoptosis and, at the same time, blocks necroptosis by cleaving and inactivating RIPK1 and RIPK3 (Li *et al.* 2012, Feltham *et al.* 2017). When caspase-8 is inhibited or deleted and cellular levels of RIPK3 and MLKL are high enough (Moujalled *et al.* 2013), necroptosis is induced and the necrosome is assembled (Pasparakis and Vandenabeele 2015). RIPK1 and RIPK3 interact through their homotypic interaction motif (RHIM) domains, leading to auto-phosphorylation of RIPK3 at the serine 227 site (Ser232 for mouse RIPK3) and recruitment of pseudokinase MLKL (Chen *et al.* 2013).

The activation of RIPK3 is the key initiation step for necroptosis. There are several different triggers that can induce necroptosis via direct interaction with RIPK3. Toll-like receptors 3 and 4, for example, directly activate RIPK3 via the RHIM-containing protein TRIF (Galluzzi *et al.* 2018) and the RHIM-containing cellular protein DNA-dependent activator of interferon regulatory factors (DAI) might also be able to activate RIPK3 directly (Sun and Wang 2014).

Activated RIPK3 then leads to phosphorylation of its substrate MLKL at Thr357 and Ser358 in humans and Ser345 in mice (Wang *et al.* 2014, Rodriguez *et al.* 2015). RIPK3-mediated phosphorylation induces a conformational change in MLKL, which leads to exposure of its N-terminal four-helix bundle domain. Subsequently, MLKL is oligomerized and translocates to the membranes where it provokes cell rupture (Murphy *et al.* 2013, Cai *et al.* 2014, Chen *et al.* 2014, Hildebrand *et al.* 2014). MLKL is labeled as the executioner of necroptosis, but the exact mechanism of MLKL permeabilizing the membranes is still a matter of debate. One possibility is that the phosphorylation and oligomerization of MLKL enables the N-terminal four-helix bundle to bind to both phosphatidylinositol phosphates (PIPs) and the mitochondria-specific lipid cardiolipin (CL) (Dondelinger *et al.* 2014, Wang *et al.* 2014). A second suggestion is that MLKL interacts with the kinase transient receptor potential cation channel, subfamily M, member 7 (TRPM7), which leads to extracellular Ca²⁺ influx and therefore to plasma membrane damage and the execution of necroptosis (Cai *et al.* 2014, Murphy *et al.* 2014, Hildebrand *et al.* 2014). Another claim is that MLKL translocates to lipid rafts of the plasma membrane, leading to Na⁺ influx and execution of necroptotic cell death (Chen *et al.* 2014).

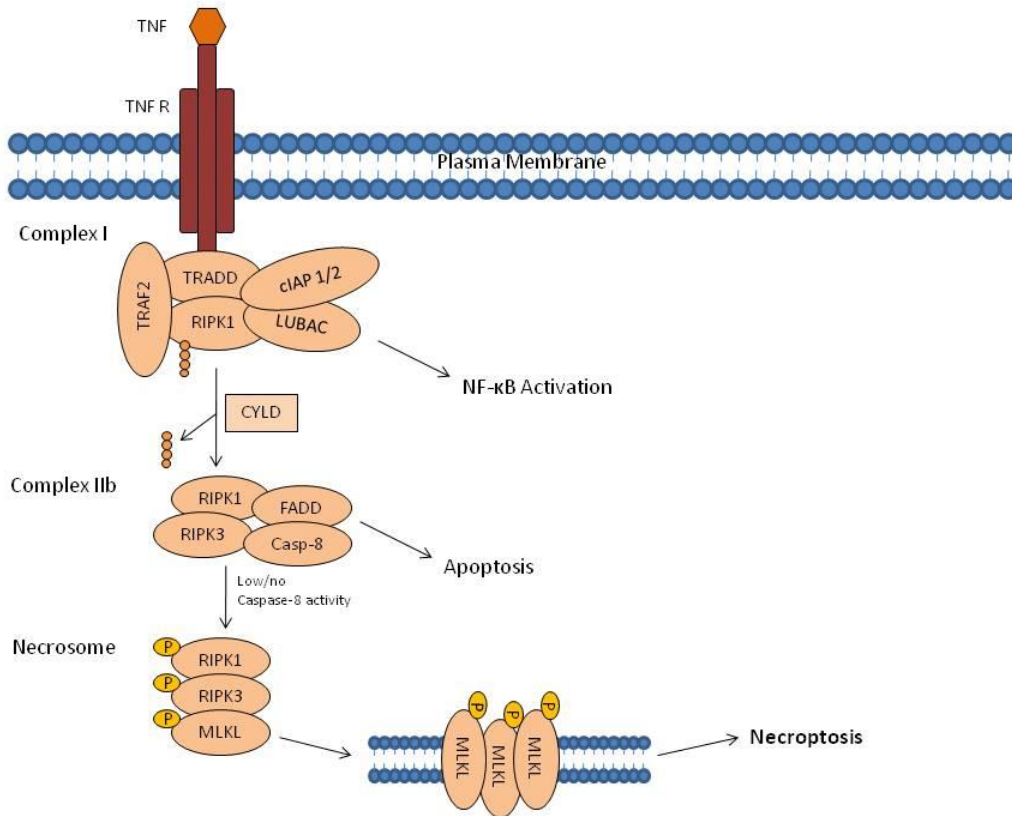


Figure 3: Necroptotic signaling. Ligation of TNF to TNF-R1 leads to formation of the so called complex I, consisting of TRADD, TRAF2, RIPK1, cIAP 1/2 and LUBAC and shifting cells toward survival programs. cIAP 1/2 encourage ubiquitination of themselves and RIPK1. When cIAP 1/2 are inactivated, RIPK1 dissociates from the plasma membrane. Subsequently, the polyubiquitin chain on RIPK1 is removed by CYLD, leading to formation of the complex IIb. Active caspase-8 induces apoptosis and at the same time blocks necroptosis by cleaving and inactivating RIPK1 and RIPK3. When caspase-8 activity is low or completely absent, RIPK1 and RIPK3 become activated by phosphorylation and the necrosome is assembled. Auto-phosphorylation of RIPK3 leads to recruitment and phosphorylation of MLKL. MLKL translocates to the membranes, causing cell rupture and inducing necroptosis. **Figure modified from Fuchslocher *et al.* 2017.**

2.3 Necroptosis and relevant molecules of the presented dissertation

2.3.1 Necroptosis and the caspases-8 and -10

Caspases are cysteine proteases that cleave cellular substrates at specific aspartate residues (Los *et al.* 1999). Caspases can be subdivided into initiator and effector caspases. Effector caspases have a small prodomain and cleave various cellular substrates. In contrast, initiator caspases have a long prodomain and activate downstream effector caspases. Caspases-8 and -10 belong to the group of initiator caspases (Fischer *et al.* 2006, Galluzzi *et al.* 2016). While caspase-8 is known to be a key mediator of apoptosis (Hughes *et al.* 2016, Feltham *et al.* 2017, Keller *et al.* 2018), little is understood about the function of its homolog caspase-10. Although both caspases share overlapping substrate specificities (Fischer *et al.* 2006), controversy exists as to whether caspase-10 can substitute the function of caspase-8 (Mühlethaler-Motte *et al.* 2011). Both caspases share, together with c-FLIP, the same gene locus on chromosome 2q33-34 (Fischer *et al.* 2006) and both caspases are recruited to and activated at the DISC (Mühlethaler-Mottet *et al.* 2011). Various studies have shown that

caspase-8 inhibits necroptosis (He *et al.* 2009, Sakamaki *et al.* 2014). Inhibition or deletion of caspase-8 therefore leads to formation of the necrosome and the induction of necroptosis (Sun and Wang 2014, Grootjans *et al.* 2017). How caspase-8 prevents necroptosis is still not completely understood but, to date, the likeliest mechanism seems to be caspase-8-mediated cleavage and inactivation of RIPK1 and RIPK3 (Feltham *et al.* 2017). The amount of different c-FLIP isoforms interacting with caspase-8 (Hughes *et al.* 2016) or the fact that caspase-8 cleaves cylindromatosis (CYLD), which is responsible for the deubiquitination and activation of RIPK1-dependent necroptosis (O'Donnell *et al.* 2011), seem to be additional or alternative mechanisms. c-FLIP is a catalytically inactive homolog of caspase-8. Due to alternative splicing, a long form c-FLIP (c-FLIP_L) and a short form c-FLIP (c-FLIP_S) exist (Hughes *et al.* 2016). c-FLIP_L is described as an inhibitor of both apoptosis and necroptosis (Budd *et al.* 2006, Vanlangenakker *et al.* 2012, Hughes *et al.* 2016), whereas c-FLIP_S blocks apoptosis and simultaneously promotes necroptosis (Hughes *et al.* 2016, Shindo *et al.* 2016).

In contrast to caspase-8, little is known about the impact of caspase-10 for necroptosis. Recently, caspase-10 was identified as a negative regulator of caspase-8-mediated cell death by reducing DISC association and activation of caspase-8 (Horn *et al.* 2017). In another study, it was suggested that caspase-10 mediates IFN γ -induced- and RIPK1-dependent cell death when cells fail to undergo caspase-8-dependent apoptosis and classic necroptosis (Tanzer *et al.* 2017). While humans express both caspase-8 and caspase-10, caspase-10 was lost in rodents (e.g., mice) over the course of their evolution (Salvesen and Walsh 2014, Sakamaki *et al.* 2015) (Figure 4). This leads to the assumption that the caspases-8 and -10 might have a species-specific role within the necroptotic signaling pathway. Ultimately, the role of caspase-10 for necroptosis remains unknown.

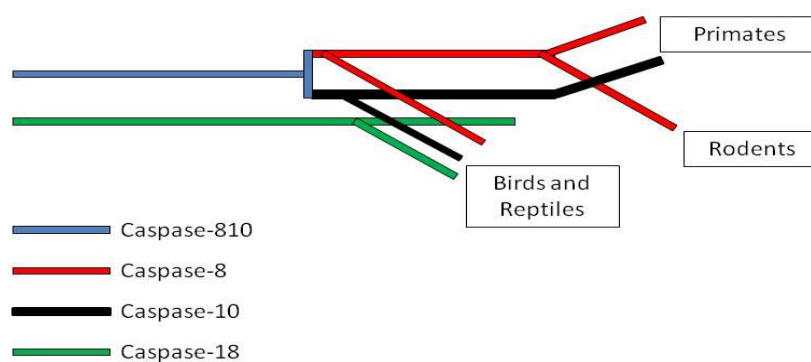


Figure 4: Phylogeny of caspase-8. Caspase-8 and caspase-10 branched from the same ancestor caspase, which is called caspase-810 in this schematic. Birds and Reptiles express three caspases: caspase-18, caspase-8 and caspase-10. Primates lost caspase-18, while rodents lost both caspase-18 and caspase-10. **Figure modified from Salvesen and Walsh 2014.**

2.3.2 Necroptosis and HtrA2/Omi

HtrA2/Omi is a mitochondrial serine protease, identified as the mammalian homolog of the bacterial HtrA endoprotease (van Loo *et al.* 2002), and is involved in the degradation of misfolded proteins during cellular stress (Gray *et al.* 2000). HtrA2/Omi is highly conserved from bacteria to mammals (van Loo *et al.* 2002). It has been reported that during apoptosis, HtrA2/Omi is released from the mitochondria to the cytosol, binding to and deactivating IAPs (e.g., cIAP1, cIAP2, XIAP), and thus leading to activation of caspases and the induction of apoptosis (van Loo *et al.* 2002, Srinivasula *et al.* 2003, Yang *et al.* 2003, Vande Walle *et al.* 2010). Although it is known that serine protease inhibitors, such as tosylphenylanylchloromethyl ketone (TPCK), can inhibit necroptosis (Egger *et al.* 2003), the identification of relevant serine proteases for necroptosis and their substrates has long been unsuccessful. In 2013, Sosna and colleagues identified HtrA2/Omi as a key mediator regulating TNF-induced necroptosis, where they demonstrated that upon usage of the specific HtrA2/Omi inhibitor Ucf-101, several cell lines were protected from TNF-induced necroptosis (Sosna *et al.* 2013). In addition, mouse embryonic fibroblasts from HtrA2/Omi-deficient mice were analyzed and also exhibited full protection against necroptosis (Sosna *et al.* 2013). In contrast to apoptosis, it is described that HtrA2/Omi is not released from mitochondria during TNF-induced necroptosis (van Loo *et al.* 2002, Blink *et al.* 2004). In conclusion, it seems as if HtrA2/Omi does not interact directly with members of the necrosome but via indirect mechanisms from within the mitochondria.

Sosna and colleagues have also identified the deubiquitinating enzyme ubiquitin C-terminal hydrolase 1 (UCH-L1) as a substrate of HtrA2/Omi (Sosna *et al.* 2013). Since UCH-L1 is not expressed ubiquitously (Meyer-Schwesinger *et al.* 2011), but restricted to several chosen tissues, there must be additional substrates or mechanisms through which HtrA2/Omi mediates necroptosis. To conclude, there is demonstrable evidence that HtrA2/Omi plays a major role within the necroptotic signaling pathway, but the exact underlying mechanism remains unknown.

2.4 Aims of the presented dissertation

In contrast to apoptosis, the characterization of the necroptotic signaling pathway is still ongoing. The primary aim of the presented dissertation was therefore to get a better understanding of the regulation of the necroptotic signaling pathway. Since necroptosis is associated to various diseases, it is important to understand its detailed initiation and execution mechanisms at the molecular level. Precise knowledge about necroptotic signaling can then open up new therapeutic opportunities. This thesis therefore pursues two major goals: (A) to get more insight into the proteolytic regulation of necroptosis by the initiator caspases-8 and -10 and (B) to unravel the exact mechanism through which HtrA2/Omi mediates necroptosis (Figure 5).

(A) As described above, according to the available literature, caspase-8 functions as inhibitor of necroptosis by cleaving and inactivating RIPK1 and RIPK3 (Moriwaki *et al.* 2015).

Thus, when caspase-8 is inhibited or deleted, necroptosis is induced (Sun and Wang 2014, Grootjans *et al.* 2017). Paradoxically, in a small interfering RNA (siRNA) screen for proteases participating in necroptosis (performed by Susann Voigt during her PhD thesis in the group of Prof. Dr. Dieter Adam), caspase-8 did not enhance but rather protected from necroptosis in different human cell lines. At this point it should be mentioned, that, to date, almost all studies concerning caspase-8 and the induction of necroptosis have been conducted in mice. Together with the fact that humans express caspases-8 and -10, while caspase-10 was lost in rodents over the course of evolution (Salvesen and Walsh 2014, Sakamaki *et al.* 2015), this led to the hypothesis that caspase-8 might play a species-specific role for necroptosis. In addition, it was hypothesized that caspase-10 in humans might substitute the function that is held by caspase-8 in mice. Therefore, one main goal of the presented dissertation is to further investigate the species-specific role of caspases-8 and -10 for necroptosis by analyzing the composition of human necrosomes. To achieve this, different human and murine cell lines deficient for caspases-8 or -10 will be generated by employing the CRISPR/Cas9 technology. In a second step, knockout cell lines will be stably reconstituted with enzymatically active and inactive mutant forms of caspase-8 and caspase-10. This will be followed by analyses of the composition of the necrosomes via Western blot analysis, immunoprecipitation and magnetic isolation of TNF receptors. Furthermore, it will be clarified whether downregulation of other components of the necrosome will alter the effects of caspases-8 and -10 within the necroptotic signaling pathway.

(B) In contrast to apoptosis, the role of HtrA2/Omi for necroptosis is largely unknown. As described previously, inhibition or genetic ablation of HtrA2/Omi completely protects cells from TNF-induced necroptosis (Sosna *et al.* 2013), but the underlying mechanism is still not figured out. UCH-L1 has been identified as a substrate of HtrA2/Omi (Sosna *et al.* 2013), but since UCH-L1 is only expressed in certain tissues (Meyer-Schwesinger *et al.* 2011), there must be other substrates through which HtrA2/Omi mediates necroptosis. To identify such substrates, mitochondrial fractions of necroptotic wild type and HtrA2/Omi-deficient mouse embryonic fibroblasts (MEF) will be isolated and further analyzed by mass spectrometry in collaboration with Prof. Dr. Andreas Tholey (Institute for Experimental Medicine, Kiel). HtrA2/Omi-deficient L929Ts cells were generated with the CRISPR/Cas9 system by Johaiber I. Fuchslocher Chico during his PhD thesis in the group of Prof. Dr. Dieter Adam and are available as a further tool to investigate the role of HtrA2/Omi in necroptosis. In addition, both L929Ts cells and MEF deficient for HtrA2/Omi were stably reconstituted with HtrA2/Omi by Johaiber I. Fuchslocher Chico. Within his PhD thesis, he could also show that HtrA2/Omi seems to be linked to necroptosis upstream of RIPK3 and MLKL. Since it is known that during apoptosis, HtrA2/Omi deactivates IAPs (e.g., cIAP1/2, XIAP), leading to activation of caspases and the induction of apoptosis (van Loo *et al.* 2002, Srinivasula *et al.* 2003, Yang *et al.* 2003, Vande Walle *et al.* 2010), it will be clarified within the presented dissertation if HtrA2/Omi also mediates necroptosis by proteolytic cleavage of IAPs. Western blot analyses, as well as cytotoxicity assays will therefore be performed. Since dysregulation of IAPs has been associated to various cancers, tumor cell survival and chemo-resistance, IAPs have

been used as anticancer drug targets. Consequently, a group of small pharmacological inhibitors of IAPs labeled as Smac mimetics were designed and utilized in clinical trials for cancer treatment (Silke and Meier 2013). With the aid of birinapant, a Smac mimetic, binding to and inhibiting the activity of IAPs, it will be clarified if the effect of the previously described knockout cell lines can be overcome.

Several cellular proteins cleaved during necroptosis (Mitochondrial-processing peptidase subunit alpha (MPP-A, also called PMPCA), proteasome subunit alpha type-1 (PSA1), Lon protease 1 (LONP1), moesin (MSN) and stathmin (STMN1)) have been identified in a proteomic screen performed by Susann Voigt, which will be further investigated by Western blot analysis within the presented dissertation. Since deleted in bladder cancer protein 1 (DBC1), pyridoxal dependent decarboxylase domain containing protein 1 (PDXDC1) and vacuolar protein sorting 4 homolog B (VPS4B) were identified as substrates of HtrA2/Omi during apoptosis (Vande Walle *et al.* 2007), these proteins will also be studied in the context of necroptosis by Western blot analysis within this thesis.

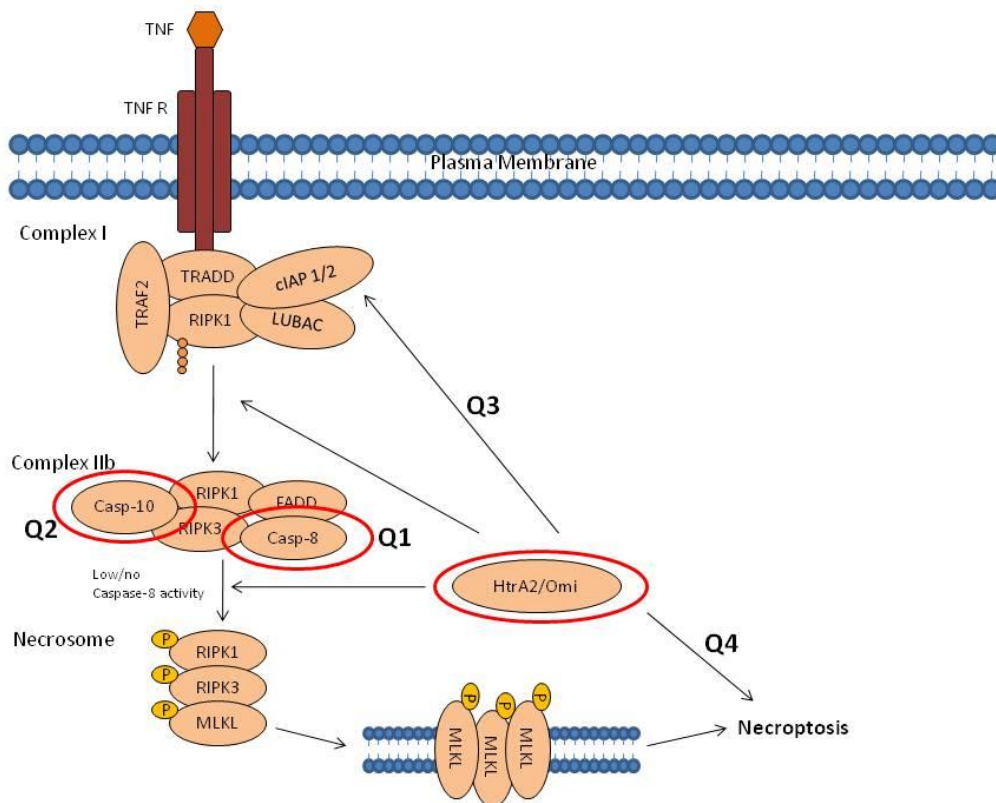


Figure 5: Relevant molecules of the presented dissertation and their role within the necroptotic signaling pathway.

Question 1: Does caspase-8 have a species-specific role within the necroptotic signaling pathway (Q1)?

Question 2: Does caspase-10 in humans substitute the function that is held by caspase-8 in mice (Q2)?

Question 3: Does HtrA2/Omi mediate necroptosis by proteolytic cleavage of IAPs (Q3)?

Question 4: Does HtrA2/Omi mediate necroptosis through different unknown substrates (Q4)?

3. Materials and Methods

3.1 Materials

3.1.1 Technical equipment

Company	Equipment
AGFA, Düsseldorf, Germany	CP1000 X-ray processor
BD Biosciences, Heidelberg, Germany	FACS Calibur flow cytometer Software: BD CellQuest™ Pro V.4.0.2 5 ml Polystyrene round-bottom FACS tubes
Beckman Coulter, Krefeld, Germany	TL-100 Ultracentrifuge, SW-32 rotor Ultra clear™ Centrifuge tube, 11 x 60 mm
Bender & Hobein, Zurich, Switzerland	Vortex Genie 2™
Biometra, Göttingen, Germany	Power Pack P25T
Bio-Rad, Munich, Germany	Gene Pulser Xcell™ Mini PROTEAN Tetra System Glass Plates 1.0 mm , 10-well comb
BRAND, Wertheim, Germany	Neubauer counting chamber
Branson Ultrasonics, Danbury, CT, USA	W-450 Sonication device
Corning Incorporated, Corning, NY, USA	Tissue Culture Dish 100 x 20 mm
Eppendorf, Hamburg, Germany	Refrigerated Centrifuge 5417R Pipettes (2, 10, 20, 100, 200 and 1,000 µl)
GE Healthcare, Munich, Germany	HiTrap™ Protein GHP 1 ml columns Hyperfilm™ Nitrocellulose blotting membrane 0.2 µm Whatman™ filtering paper Grade 3 CHR
GFL, Wunstorf, Germany	Water bath 1003
Gilson, Middleton, WI, USA	Minipuls 3 peristaltic pump Pipettes (10, 20, 100, 200 and 1,000 µl)
Greiner Bio-One, Frickenhausen, Germany	15 and 50 ml Tubes Serological pipettes (1, 5, 10, 25 and 50 ml) 6- and 12-well plates Cell culture flasks (50, 250 and 650 ml)
Heidolph Instruments, Schwabach, Germany	Polymax 1040 shaker

3. Materials and Methods

Heraeus, Osterode, Germany	LaminAir® HB2472K Megafuge 1.0R Megafuge 16R
Hettich, Tuttlingen, Germany	Mikro 200R centrifuge
Hirschmann Laborgeräte, Eberstadt, Germany	Pipetus®
Hoock, Kiel, Germany	Magnetic device: HOKImag 1
IKA Labortechnik, Staufen, Germany	IKA® RCT basic magnetic mixer IKA® HS 260 basic shaker
Kern & Sohn, Balingen, Germany	KERN 440-47N precision scales
Kisker, Mühlhausen, Germany	X-Ray cassette 24 x 30 cm
Lonza Group, Basel, Switzerland	Amaxa Biosystems Nucleofector™ 2b Device
Miltenyi Biotec, Bergisch Gladbach, Germany	μ columns OctoMACS™ Separator
National Labnet CO, Edison, NJ, USA	Mini Centrifuge C-1200
Sartorius Group, Göttingen, Germany	Precision scales A120S-D1
Stuart, Stone, Staffordshire, UK	Roller mixer SRT9
Tecan Group, Männedorf, Germany	Infinite M200 ELISA Microplate Reader, Software: i-Control 1.3
Thermo Fisher Scientific, Waltham, MA, USA	HERAcell 240i CO ₂ Incubator 96-well plate
Xylem Analytics (WTW), Weilheim, Germany	pH 325 pH meter
Zeiss, Göttingen, Germany	Axiovert 100 microscope

3.1.2 Reagents and chemicals

Company	Reagent/Chemical
Abcam, Cambridge, UK	Mitochondria Isolation Kit for Cultured Cells
Bachem AG, Bubendorf, Switzerland	zVAD-fmk
BASF BioResearch, Ludwigshafen, Germany	TNF (2mg/ml)
Biochrom, Berlin, Germany	L-glutamine PBS Dulbecco w/o Ca ²⁺ McCoy's modified medium 10 x Trypsin/EDTA penicillin/streptomycin
Biovision, Milpitas, CA, USA	RIPK1 Inhibitor Nec-1s

3. Materials and Methods

Cell Signaling Technology, Danvers, MA, USA	LumiGLO®
GE Healthcare, Munich, Germany	Ammonium persulfate TEMED
Heirler Cenovis, Radolfzell, Germany	Skimmed milk powder
Horizon Discovery, Cambridge, UK	Trans-Lentiviral shRNA Packaging Kit with Calcium Phosphate
Lonza Group, Basel, Switzerland	Amaxa® Cell Line Nucleofector® Kit V, R, C and Primary fibroblasts
Merck KGaA, Darmstadt, Germany	β-mercaptoethanol Dimethyl sulfoxide Glycerol 85 % (v/v) RIPK3 Inhibitor GSK'872
Miltenyi Biotec, Bergisch-Gladbach, Germany	μMACS Protein G microbeads
PAN Biotech, Aidenbach, Germany	Click's RPMI 1640
Promega, Madison, WI, USA	Cell Titer-Glo® Luminescent Viability Assay
R&D Systems, Minneapolis, Canada	Birinapant
Roche Diagnostics, Mannheim, Germany	Protease Inhibitor Cocktail Tablets
Roth, Karlsruhe, Germany	Ethanol Glycine Hydrogen peroxide 30 % (v/v) Methanol Sodium chloride 99.8 % (w/v) Tris
Santa Cruz Biotechnology, Heidelberg, Germany	Puromycindihydrochloride
Serva, Heidelberg, Germany	Acrylamide/bis-solution Dodecylsulfate-Na-salt in pellets Trypan blue solution
Sigma-Aldrich, Munich, Germany	Cycloheximide Optiprep™ Density Gradient Medium Propidium Iodide Tween®20
Thermo Fisher Scientific, Waltham, MA, USA	NP-40 detergent Pierce™ BCA Protein Assay Kit BSA standard PageRuler™ Prestained Protein Ladder

Freestyle™ 293 medium (Life Technologies)
Accutase (Life Technologies)
Fetal bovine serum (Life Technologies)
Sodium pyruvate (Life Technologies)
Doxycycline hyclate (MP Biomedicals)

3.1.3 Antibodies

Table 1: List of all utilized primary and secondary antibodies

Target protein	Used dilution	Company/Article number
primary antibodies		
β-Actin, AC-15	1:10,000	Sigma-Aldrich, Munich, Germany / A1978
Cleaved Caspase-3, D175	1:1,000	Cell Signaling Technology, Danvers, MA, USA / 9661
Caspase-8, 1C12, human	1:1,000	Cell Signaling Technology, Danvers, MA, USA / 9746
Caspase-8, murine	1:1,000	Cell Signaling Technology, Danvers, MA, USA / 4927
Caspase-10	1:1,000	Abcam, Cambridge, UK / ab177475
clAP-1, 1E1-1-10	1:1,000	Enzo Life Sciences, Farmingdale, NY, USA / ALX-803-335
DBC1	1:1,000	Cell Signaling Technology, Danvers, MA, USA / 5693
Flip Dave-2	1:1,000	AdipoGen Life Sciences, Liestal, Switzerland / AG-20B-0005
HtrA2	1:2,000	OriGene Europe-Acris Antibodies, Herford, Germany / 15775-1-AP
Lamp-2, CD1076	1:2,000	Southern Biotech, Birmingham, AL, USA / 9840-01
LONP1	1:1,000	Abcam, Cambridge, UK / ab103809
Moesin	1:1,000	Abcam, Cambridge, UK / ab151542
PARP-1	1:2,000	Cell Signaling Technology, Danvers, MA, USA / 9542
PDXDC1	1:1,500	Proteintech (Thermo Scientific), Waltham, MA, USA / 21021-1-AP
pMLKL, EPR9514, human	1:1,000	Abcam, Cambridge, UK / ab187091
pMLKL, EPR9515(2), murine	1:1,000	Abcam, Cambridge, UK / ab196436
PMPCA	1:1,000	Abcam, Cambridge, UK / ab140171
PSA	1:1,000	Abcam, Cambridge, UK / ab53774
RIPK1	1:1,000	BD Biosciences, Heidelberg, Germany / 610459

3. Materials and Methods

RIPK3, E1Z1D, human	1:1,000	Cell Signaling Technology, Danvers, MA, USA / 13526
RIPK3, murine	1:1,000	Abcam, Cambridge, UK / ab56164
Stathmin1, EP1573Y	1:5,000	Abcam, Cambridge, UK / ab52630
TNF-R1, H5	1:500	Santa Cruz Biotechnology, Heidelberg, Germany / sc-8436
VPS4B	1:3,000	Abcam, Cambridge, UK / ab102687
hILP/XIAP	1:2,000	BD Transduction Laboratories, Heidelberg, Germany / 610717
secondary antibodies		
Goat anti-mouse IgG peroxidase-conjugated	1:10,000	Jackson ImmunoResearch Europe, Suffolk, UK
Goat anti-mouse light chain, HRP conjugate	1:10,000	Merck KGaA, Darmstadt, Germany / AP200P
Goat anti-rabbit IgG peroxidase-conjugated	1:10,000	Jackson ImmunoResearch Europe, Suffolk, UK
Mouse anti-rabbit light chain, HRP conjugate	1:10,000	Merck KGaA, Darmstadt, Germany / MAB201P
Goat anti-rat IgG peroxidase-conjugated	1:10,000	Jackson Immuno Research Europe, Suffolk, UK

3.1.4 siRNAs and constructs

Table 2: List of all utilized constructs and siRNAs

Construct	Vector	Company/Source
CASP8 CRISPR/Cas human CASP8 CRISPR/Cas mouse CASP10 CRISPR/Cas human	pCMV-Cas9-GFP CRISPR/Cas	Sigma-Aldrich, Munich, Germany
FC-tagged TNF (TNF60-FC)	pCR3 TM	Obtained from Harald Wajant, Würzburg, Germany
Human CASP8 WT Human CASP8 mutated (inactive) Mouse Casp8 WT Mouse Casp8 mutated (inactive) Human CASP10 WT Human CASP10 mutated (inactive)	pTRIPZ-N-HA	Thermo Fisher Scientific, Waltham, MA, USA
Mouse Casp8 WT Human Casp8 WT Human Casp8 mutated (C36S)	pCMV6-Entry pEGFP-N1 pEGFP-N1	Obtained from Francis Chan, Worcester, MA, USA
Product	Catalogue number	Company
siGENOME Human CASP8 (A)	D-003466-01	Horizon Discovery, Cambridge, UK
siGENOME Human CASP8 (B)	D-003466-02	Horizon Discovery, Cambridge, UK
siGENOME Human CASP8 (C)	D-003466-07	Horizon Discovery, Cambridge, UK
siGENOME Mouse Casp8	D-043044-01	Horizon Discovery, Cambridge, UK
siGENOME Human CASP10 (A)	D-004402-02	Horizon Discovery, Cambridge, UK

siGENOME Human CASP10 (B)	D-004402-01	Horizon Discovery, Cambridge, UK
siGENOME Human CFLAR	M-003772-06	Horizon Discovery, Cambridge, UK
Silencer [®] Select Mouse cflar	4390771	Thermo Scientific, Waltham, MA, USA
ON-TARGETplus Mouse Dbc1 (Ccar2)	J-047837-05-0002	Horizon Discovery, Cambridge, UK
ON-TARGETplus Human LONP1	J-003979-06-0002	Horizon Discovery, Cambridge, UK
ON-TARGETplus Mouse Lonp1	J-054897-09-0002	Horizon Discovery, Cambridge, UK
ON-TARGETplus Mouse Pdxdc1	J-042274-09-0002	Horizon Discovery, Cambridge, UK
ON-TARGETplus Human PMPCA	J-008734-08-0002	Horizon Discovery, Cambridge, UK
ON-TARGETplus Mouse Pmpca	J-055541-05-0002	Horizon Discovery, Cambridge, UK
ON-TARGETplus Human PSA1 (KLK3)	J-005914-14-0002	Horizon Discovery, Cambridge, UK
ON-TARGETplus Mouse PSA1 (Klkb1)	J-046987-09-0002	Horizon Discovery, Cambridge, UK
siGENOME Human RIPK1	D-004445-03	Horizon Discovery, Cambridge, UK
Silencer [®] Select Mouse Ripk1	16104	Thermo Scientific, Waltham, MA, USA
siGENOME Human RIPK3	D-003534-01	Horizon Discovery, Cambridge, UK
Silencer [®] Select Mouse Ripk3	4390771	Thermo Scientific, Waltham, MA, USA
ON-TARGETplus Mouse Vps4b	J-044487-05-0002	Horizon Discovery, Cambridge, UK

3.1.5 Cell lines

The TRAIL-sensitive murine fibrosarcoma cell line L929Ts was generated in the laboratory of Prof. Dr. Dieter Adam (Kiel University, Kiel, Germany) and has been described previously (Thon *et al.* 2006). HtrA2/Omi-deficient mouse embryonic fibroblasts (MEF) and their wild type counterparts have been described earlier (Martins *et al.* 2004) and were kindly provided by Prof. Dr. Thomas Langer, Cologne. Hamster embryonic kidney cells constitutively expressing the simian virus (SV40) large T antigen cells (HEK293T) were originally obtained from the American Type Culture Collection (ATCC, Manassas, VA, USA).

The human leukemia-derived U-937 and the human colorectal HT-29 cancer cells, being a gift from Prof. Dr. Holger Kalthoff (Kiel University, Kiel, Germany), were originally obtained from the American Type Culture Collection (ATCC, Manassas, VA, USA). Within this present work, caspase-8-deficient HT-29, U-937 and L929Ts cells were generated by employing the CRISPR/Cas system. Using the CRISPR/Cas technology, caspase-10-deficient HT-29 and U-937 cells were also generated within this thesis.

MEF and HEK293T cells were cultivated in DMEM supplemented with 10 % (v/v) heat-inactivated fetal calf serum (FCS), 50 µg/ml penicillin/streptomycin and 50 µM β-mercaptoethanol in 0.9 % (w/v) NaCl. L929Ts and U-937 cells were maintained in Click's/RPMI 1640 (50/50 % v/v) supplemented with 10 % (v/v) heat-inactivated FCS, 2 mM L-glutamine, 50 µg/ml penicillin/streptomycin and 50 µM β-mercaptoethanol in 0.9 % (w/v) NaCl, whereas HT-29 cells were cultivated in McCoy's modified medium supplemented with 10 % (v/v) FCS, 2 mM L-glutamine, 50 µg/ml penicillin/streptomycin and 1 mM sodium

pyruvate. For detachment of the cells, either accutase or phosphate buffered saline (PBS) containing 0.5 % (v/v) trypsin and 0.2 % (v/v) EDTA was used. For long-term storage, cells were resuspended in FCS containing 10 % (v/v) DMSO and frozen in liquid nitrogen. All cell lines were cultivated with 5 % (w/v) CO₂ at 37 °C.

3.2 Methods

3.2.1 Transfection

3.2.1.1 Nucleofection

U-937 cells were transfected using the Amaxa® cell line kit C according to manufacturer's instructions. 1×10^6 were pelleted and resuspended in 100 µl Solution C. Afterwards, this cell suspension was transferred into a cuvette and mixed with 150 pmol siRNA or 2-5 µg DNA. For the transfection of U-937 cells, the Nucleofector® Program W-001 was used. Afterwards, cells were resuspended in 6 ml prewarmed culture medium in 6-well plates for 24-48 h.

L929Ts cells were transfected as described above using the Amaxa® cell line kit V in combination with the Nucleofector® Program T-20. For HT-29 cells, the Amaxa® cell line kit R was used in combination with the Nucleofector® Program W-17.

3.2.1.2 Electroporation

HEK293T cells were transfected with a Gene Pulser™ X Cell electroporation device from Bio-Rad. 2×10^6 cells were pelleted and mixed with 10 µg DNA and 200 µl cell-specific medium without supplements (10 % (v/v) FCS, 50 µg/ml penicillin/streptomycin, β-mercaptoethanol in 0.9 % (w/v) NaCl). This mixture was transferred into a prewarmed 0.2 µm cuvette and electroporation was performed with predefined standard settings for HEK293 cells (pulse length 25 ms, voltage 110 V).

3.2.1.3 Transfection with pTRIPZ lentiviral inducible constructs

For transfection, the Dharmacon™ Trans-Lentiviral Packaging Kit was used. For producing lentiviral particles, HEK293T cells were grown to 70 % confluence. The cells were seeded in 2 ml DMEM (10 % (v/v) FCS, 50 µg/ml penicillin/streptomycin, 1 mM sodium pyruvate) onto 6-well plates at a density of 1.2×10^6 cells per well. Afterwards the cells were incubated at 37 °C with 5 % (w/v) CO₂ overnight. The next day, 6 µg of the respective pTRIPZ lentiviral construct was mixed with 4.3 µl trans-lentiviral packaging mix and filled up with sterile water to a total volume of 135 µl. 15 µl CaCl₂ were added to the diluted DNA. The reagents were mixed thoroughly and while vortexing, 150 µl 2 x HBSS were added drop-wise and incubated for 3 min at RT. The total volume (300 µl) of the transfection mix was added drop-wise to the HEK293T cells and the cells were incubated for 16 h at 37 °C with 5 % (w/v) CO₂. After 16 h, the calcium phosphate-containing medium was removed and replaced with 2 ml of reduced serum medium (DMEM supplemented with 5 % (v/v) FCS, 2 mM L-glutamine and 50 µg/ml penicillin/streptomycin). After another 48 h of incubation at 37 °C with 5 % (w/v) CO₂, the

viral particle-containing supernatant was collected and centrifuged at 1,600 x g for 10 min at 4 °C. Finally, the supernatant was sterile filtered and stored at -80 °C until further use.

Human HT-29 cells and murine L929Ts cells were seeded in 25 cm² cell culture flasks in 4 ml cell line specific medium at a density of 5 x 10⁵ cells. The viral particle-containing supernatant was thawed, mixed with 5 µg/ml polybrene and added to the cells. After 3 h, 2 ml cell line-specific medium was added and the next day the viral particle-containing medium was removed and replaced with fresh cell line-specific medium supplemented with puromycindihydrochloride (L929Ts: 6 µg/ml puromycin, HT29: 0.75 µg/ml puromycin). After approximately 3 weeks of cultivation with regular media change, the cells were analyzed via Western blot for stable expression of the desired protein. Since the pTRIPZ vector is an inducible vector, cells were incubated for 24 h with 1 µg/ml doxycycline for induction of the protein expression.

3.2.2 Cytotoxicity assay – propidium iodide staining

For flow cytometric analysis, cells were seeded onto 12-well plates at a density of 1 x 10⁵/ml (or 5 x 10⁴/ml for HT-29 cells) per well. Suspension cells were stimulated immediately whereas adherent cells were left in the incubator overnight followed by stimulation the next day. All following steps were performed on ice. Adherent cells were detached with accutase, washed once with cold PBS/5 mM EDTA and centrifuged at 400 x g for 5 min at 4 °C. The supernatant was discarded and the cell pellet was stained with 4 µg/ml propidium iodide (PI). Cells were then analyzed for loss of membrane integrity with the help of a FACS Calibur flow cytometer at red fluorescence.

3.2.3 Determination of protein concentrations

For protein quantitation, the Pierce™ BCA Protein Assay kit was used according to the manufacturer's instructions. Absorbance was measured at 562 nm with an Infinite M200 microplate reader. The total protein concentration of whole cell lysates was calculated from a protein standard (Albumin standard 2 mg/ml).

3.2.4 Preparation of whole cell lysates

Adherent cells were washed once with prewarmed PBS, detached with accutase or trypsin/EDTA and centrifuged at 400 x g for 5 min at 4 °C. Suspension cells were centrifuged immediately as outlined above. The supernatant was discarded and the cell pellet was washed once with cold PBS before being lysed in TNE buffer (50 mM Tris pH 8.0, 1 % (v/v) NP-40, 150 mM NaCl, 3 mM EDTA, 1 mM sodium orthovanadate, 5 mM sodium fluoride and complete protease inhibitor cocktail) for 10 min on ice. Afterwards, the samples were centrifuged at 20,800 x g for 10 min at 4 °C.

3.2.5 Western blot analysis

A sodium dodecyl sulfate polyacrylamide gel electrophoresis (SDS-PAGE) was performed to separate the proteins according to their molecular mass. The separating gel was poured with 30 % (w/v) acrylamide, 0.375 mM Tris/HCL pH 8.8, 0.1 % (w/v) SDS in 20 % (v/v) glycerol, 1 % (v/v) APS and 1 % (v/v) TEMED. The amount of acrylamide (10-15 % (w/v)) used for preparing the separating gel was dependent on the molecular weight of the target protein.

Samples were diluted in 5 x sample buffer (10 % (v/v) β -mercaptoethanol, 125 mM Tris/HCl pH 6.8, 4 % (w/v) SDS, 20 % (v/v) glycerol, 0.02 % (w/v) bromophenol blue) to a final volume of 25 μ l. The samples were denatured by boiling for 4 min at 100 °C. Afterwards, equal amounts of protein were loaded into the gel lanes and electrophoresis was performed at 25 mA per gel for 1 h. To enable the identification of the molecular mass of the target proteins, the PageRuler™ Prestained Protein Ladder was used.

The proteins were transferred by wet blotting to a nitrocellulose membrane for 1 h at 100 V. Afterwards, the membrane was blocked for 1 h at RT under constant gentle agitation using a blocking solution consisting of 5 % (w/v) milk-powder in PBS and 0.1 % (v/v) Tween 20 (PBS/T). Finally, the membrane was incubated in the primary antibody, which was diluted in the blocking solution, at 4 °C overnight. The next day, the membrane was washed 2 x 15 min in PBS/T under constant gentle agitation and incubated in the secondary antibody (diluted 1:10,000 in the blocking solution) for 1 h at RT. This was followed by two more washing steps with PBS/T. The membrane was developed using LumiGLO® reagent. For detection of the chemiluminescence signals, Hyperfilm ECL was used. The exposure time varied from 5 seconds up to 60 min.

For detection of a second protein on the same membrane, any remaining peroxidase activity from the secondary antibodies was inactivated with 15 % (v/v) H₂O₂ for 60 min, followed by 2 washing steps à 15 min in PBS/T and incubation in the new primary and secondary antibodies as described above.

3.2.6 Immunoprecipitation

For immunoprecipitation, Miltenyi μ MACS columns were used. 500 μ g cell lysate from stimulated cells was incubated with 1 or 2 μ g antibody and 50 μ l Protein G Microbeads for 45 minutes on ice. μ MACS columns were placed in the magnetic field of the OctoMACS™ Separator and prepared by rinsing with 200 μ l of lysis buffer. Afterwards, the cell lysate was given onto the μ MACS columns and allowed to run through, followed by 3 washing steps with 200 μ l lysis buffer each. Then, the columns were rinsed with 100 μ l high-salt wash buffer (50 mM Tris/HCl pH 8.0, 1 M NaCl, 1 % (v/v) NP-40, 2 mM EDTA), followed by a last washing step with 100 μ l lysis buffer.

For elution, 20 μ l of 1 x SDS gel loading buffer was preheated to 95 °C, given onto the μ MACS columns and incubated for 5 minutes at RT. Then, additional 30 μ l of preheated 1 x SDS gel loading buffer were given onto the μ MACS columns and collected in a fresh tube.

Subsequently, the eluted immunoprecipitate was analyzed by Western blot.

3.2.7 Generation of knockout cell lines with the CRISPR/Cas9 system

For the generation of knockout cell lines with the CRISPR/Cas9 system, 1×10^6 cells were transfected with 2-5 μg DNA (CRISPR/Cas9 vector expressing Cas9, the customized gRNA and GFP, cell line-specific) by nucleofection as described above. After 48 h the cells were selected using a FACS Aria cell sorter. GFP was used as a marker to identify the transfected cells. 96-well plates were prepared with 100 μl prewarmed medium per well in which single cells were seeded by the sorter. After approximately 4-6 weeks, cell colonies were visible and transferred to 12-well plates. The cells were expanded and further analyzed via Western blot.

3.2.8 Purification of TNF ligands

2×10^6 HEK293T cells were transfected with 10 μg TNF60-FC-ligand DNA via electroporation (see above). Three independently performed transfections were pooled into 100 ml prewarmed FreeStyle[®] medium and left in the incubator overnight. The next day, 50 $\mu\text{g}/\text{ml}$ penicillin and 50 $\mu\text{g}/\text{ml}$ streptomycin was added to the medium, followed by two more days of cultivation. Afterwards, the supernatant was collected, sterile filtered and 10 $\mu\text{g}/\text{ml}$ of a protease inhibitor cocktail were added. The cells were left in the incubator for three more days with fresh Freestyle[®] medium supplemented with 50 $\mu\text{g}/\text{ml}$ penicillin, 50 $\mu\text{g}/\text{ml}$ streptomycin and 1 mg/ml G418 to select for transfected cells. Also this supernatant was collected, sterile filtered and supplemented with 10 $\mu\text{g}/\text{ml}$ of a protease inhibitor cocktail. Finally, both supernatants were pooled and Hi Trap[™] Protein G HP 1 ml columns were used for purification of the TNF ligand according to the manufacturer's protocols.

3.2.9 Immunomagnetic isolation of TNF receptors

The receptor isolation was executed via a free-flow magnetic chamber (HOKImag 1, invented by Tchikov and Schütze, 2008; now manufactured by HOOK GmbH, Kiel).

HT-29 cells were grown to 80 % confluence, detached with accutase, pooled and centrifuged at 400 x g for 5 min at 4 °C. 2×10^8 cells per time-point were prestimulated for 20 min with 20 μM zVAD and 5 $\mu\text{g}/\text{ml}$ CHX on ice. All following steps were performed at 4 °C unless otherwise stated. Afterwards, the cells were incubated for another 30 min with 100 ng/ml TNF60-Fc. Hereafter, 25 μl Protein G Microbeads were added and the cells were left for further 30 min on ice. The cells were then resuspended in 30 ml PBS in a 50 ml Falcon tube and centrifuged for 5 min at 1,500 rpm. The supernatant was discarded and the cell pellet was resuspended in 5-7 ml McCoy's medium without supplements and incubated for different time-points at 37 °C for internalization of the TNF receptors. Subsequently, the reaction was stopped by adding 30 ml ice-cold PBS. The cells were centrifuged for 5 min at 1,500 rpm, followed by a washing step with homogenization buffer (HB: 15 mM HEPES, 250 mM sucrose and 0.5 mM MgCl_2 at pH 7.4). The cells were then homogenized by

ultrasonication using a Branson W-450 sonication device equipped with a cup-resonator. For this purpose, the cell pellet was resuspended in 850 μ l HB supplemented with 10 μ g/ml protease inhibitor cocktail and 0.5 μ l benzonase. The cells were sonicated for 40 sec with a constant duty cycle (output control: 2.5) and centrifuged for 4 min at 400 x g. 500 μ l of the supernatant was collected in a fresh microtube. The pellet was resuspended in the remaining supernatant, sonicated once again for 40 sec, centrifuged and pooled with the collected supernatant. After that, the homogenate was centrifuged for 4 min at 400 x g and 750 μ l of the supernatant were loaded to the HOKImag 1 device. The cell lysate was incubated for 1 h in the magnetic field and washed for 20 min with HB using a peristaltic pump (0.5 ml/min). Finally, the magnetic fraction was collected in a fresh microtube, centrifuged at 14,000 rpm for 30 min and analyzed by Western blot.

3.2.10 Mitochondria isolation and LC-MS/MS analysis

For isolation of mitochondria, the Mitochondria Isolation Kit for cultured cells (Abcam, UK) was used. Murine embryonic wild type fibroblasts (MEF) and HtrA2-deficient MEF were seeded at a density of 3×10^6 cells in 650 ml cell culture flasks (2 flasks for each cell line). 48 h later, cells were stimulated for 30 min with 1 μ g/ml CHX and 20 μ M zVAD, followed by stimulation with 100 ng/ml TNF for 4 h. Afterwards, cells were collected and pelleted by centrifugation at 1300 rpm for 5 min. In order to weaken the cell membranes, the cell pellet was frozen and thawed 3 times in liquid nitrogen. Hereafter, the pellet was resuspended in 2 ml reagent A and incubated for 10 min on ice, followed by a transfer into a precooled Dounce Homogenizer. The cells were homogenized with 30 strokes using pestle B and then centrifuged at 1,000 x g for 10 min at 4 °C. The supernatant was saved in a fresh microtube and the pellet was resuspended in 2 ml reagent B, followed by homogenization with 20 strokes using pestle B of the precooled Dounce Homogenizer. The cells were once more centrifuged at 1,000 x g for 10 min at 4 °C. The cell pellet was discarded and the two supernatants were pooled and centrifuged again at 12,000 x g for 15 min at 4 °C. At last, the supernatant was discarded and the pellet was resuspended in 500 μ l of reagent C supplemented with 5 μ l protease inhibitors and frozen at -80 °C.

The LC-MS/MS analysis was executed by Prof. Dr. Andreas Tholey and Dr. Diego Yepes (Institute for Experimental Medicine, Kiel).

4. Results

4.1 Caspase-8 and caspase-10 as key mediators regulating TNF-induced necroptosis

In the literature, it has been described that inhibition or deletion of caspase-8 promotes the formation of the necrosome and the induction of necroptosis (Sun and Wang 2014, Grootjans *et al.* 2017). In a human siRNA screen for proteases participating in necroptosis (performed by Susann Voigt during her PhD thesis in the group of Prof. Dr. Dieter Adam), downregulation of caspase-8 surprisingly seemed to protect from rather than enhancing cell death. Since so far, almost all studies concerning caspase-8 and the induction of necroptosis have been performed in mice, the focus of this work was to clarify if caspase-8 holds a species-specific role within the necroptotic signaling pathway. Besides, humans express a homolog of caspase-8, the caspase-10, which was lost in rodents in the course of evolution. Therefore, one additional goal of this thesis was to determine if caspase-10 in humans can substitute the function that is held by caspase-8 in mice. Throughout this thesis, necroptosis was primarily induced by TNF/zVAD/(CHX). When TNF binds to one of the two TNF-receptors, the default pathway leads to cell survival via activation of nuclear factor- κ B (NF- κ B) (Brenner *et al.* 2015). Therefore, most of the cell lines had to be treated with TNF in combination with cycloheximide (CHX) to induce cell death. CHX is a protein synthesis inhibitor that sensitizes cells for cell death. The pan-caspase inhibitor zVAD-fmk was used to inhibit caspases, primarily caspase-8, and thus to prevent an interfering induction of apoptosis.

4.1.1 Genetic ablation of caspase-8 in murine L929Ts cells leads to increased cell death

First of all, murine caspase-8-deficient L929Ts cells were generated by employing the CRISPR/Cas9 technology (Figure 6A). Flow cytometry was performed to measure loss of membrane integrity as a readout for cell death and it could be confirmed that cell death is enhanced when caspase-8 is genetically ablated. All caspase-8 $-/-$ clones showed increased cell death in comparison to wild type cells (Figure 6B).

4. Results

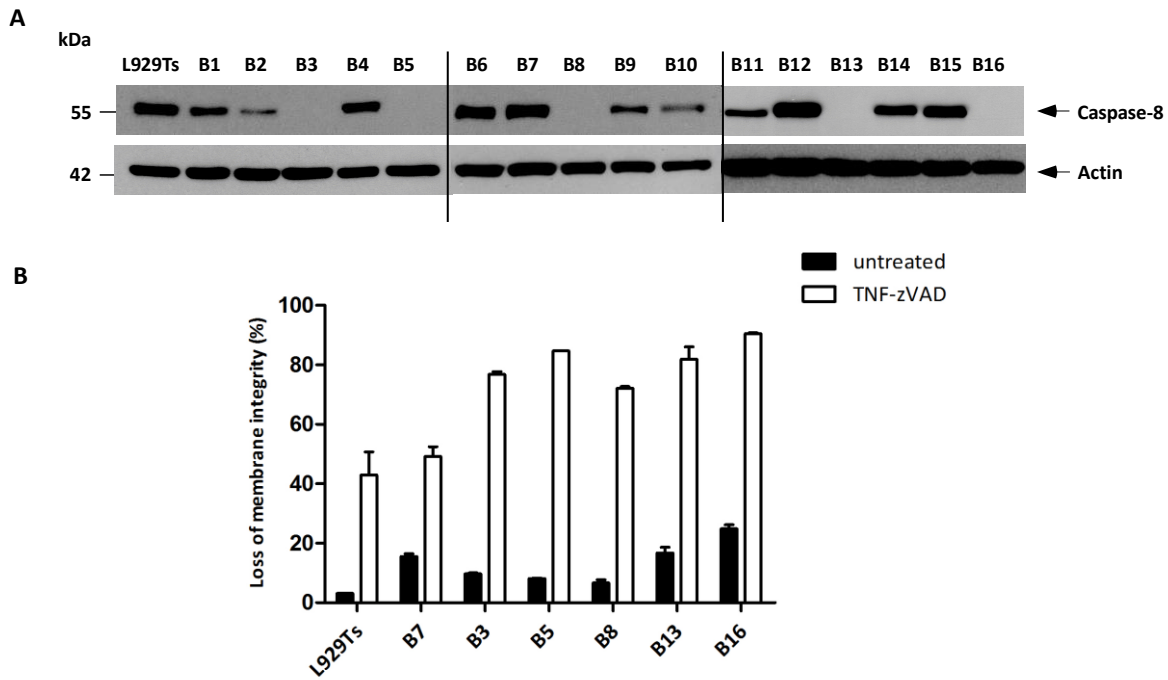


Figure 6: Generation of caspase-8-deficient L929Ts cells. (A) Western blot analyses were performed of whole cell lysates from wild type L929Ts cells and CRISPR/Cas candidate clones. The blots were incubated with an antibody detecting the full length form of caspase-8 (55 kDa) to determine which of the generated clones is deficient for caspase-8. Arrows indicate the position of the analyzed proteins. Detection of actin served as a loading control. **(B)** Flow cytometric analyses of all CRISPR/Cas clones deficient for caspase-8 (B3, B5, B8, B13, B16) in comparison to wild type and control L929Ts (B7) cells were performed to determine the effect on TNF-induced necroptosis caused by the deletion of caspase-8. Cells were left untreated or stimulated with 20 μ M zVAD-fmk (prestimulation for 30 min) and 100 ng/ml TNF for 5 h to induce necroptosis. Representative data from one out of three experiments are shown and error bars indicate SD from three measurements.

To ascertain that the cells were dying through necroptosis and not another form of regulated cell death, cells were treated with two different specific necroptosis inhibitors (Nec-1s and GSK'872). Nec-1s is a RIPK1 inhibitor and GSK'872 is a RIPK3 inhibitor and both inhibitors were able to completely block cell death (Figure 7). GSK alone can induce apoptosis. As shown in Figure 7 only L929Ts wild type cells showed enhanced cell death upon treatment with GSK, indicating that caspase-8-deficient cells are not able to die through apoptosis anymore. Clone B3 was selected for further studies throughout this dissertation.

In L929Ts wild type cells and the caspase-8 $-/-$ clone B3, necroptosis was induced over a time course via treatment with TNF/zVAD, and Western blot analyses for PARP-1 and caspase-3 cleavage as markers for apoptosis and pMLKL as a marker for necroptosis were performed. For the caspase-8-deficient cells, the signal for pMLKL appeared faster and more pronounced in comparison to wild type cells (Figure 8), supporting that the deletion of caspase-8 enhances necroptosis. Moreover, the caspase-8 $-/-$ clone B3 showed no signal for cleaved caspase-3 and cleaved PARP-1 (Figure 8), indicating once more that these cells are not able to die through apoptosis anymore.

4. Results

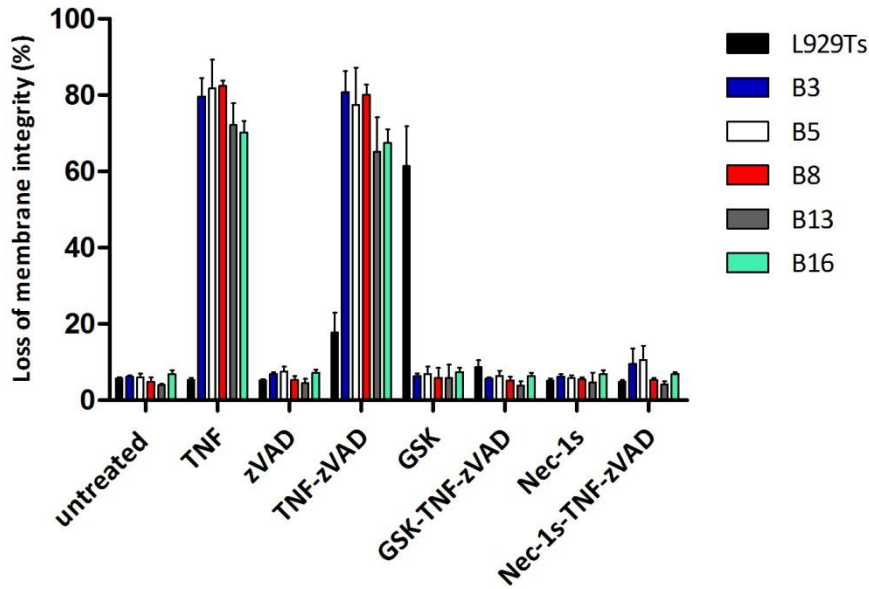


Figure 7: Inhibition of cell death in response to treatment with Nec-1s and GSK'872 in L929Ts CRISPR/Cas clones deficient for caspase-8. Flow cytometric analyses of all CRISPR/Cas clones deficient for caspase-8 (B3, B5, B8, B13, B16) and L929Ts wild type cells were performed. Cells were left untreated or stimulated with 20 μ M zVAD-fmk (prestimulation for 30 min) and 100 ng/ml TNF for 5 h to induce necroptosis. Cells were additionally treated with 50 μ M Nec-1s (RIK1 inhibitor) or 10 μ M GSK'872 (RIPK3 inhibitor) to clarify if the cells die through necroptosis or another form of regulated cell death. Representative data from one out of three experiments are shown and error bars indicate SD from three measurements.

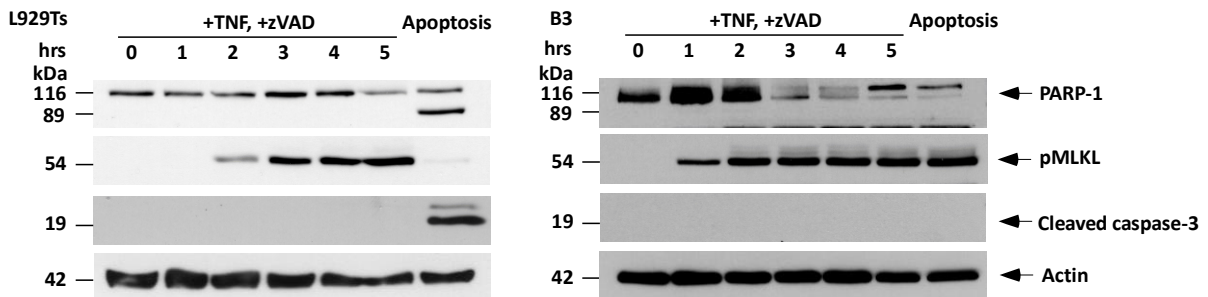


Figure 8: Determining the effect of the genetic ablation of caspase-8 on TNF-induced necroptosis in the L929Ts caspase-8 $-/-$ clone B3. Wild type L929Ts cells and the L929Ts caspase-8 $-/-$ clone B3 were left untreated or stimulated with 20 μ M zVAD-fmk (prestimulation for 30 min) and 100 ng/ml TNF over a time course from 1 to 5 h to induce necroptosis. As a control, cells were additionally treated with 100 ng/ml TNF and 2 μ g/ml CHX for 4 h to induce apoptosis. Western blot analyses were performed of whole cell lysates. The blots were incubated with an antibody detecting the full length form (116 kDa) and the apoptotic cleavage fragment of PARP-1 (89 kDa, present only in the apoptotic lysate in L929Ts cells). Western blots were also generated from whole cell lysates incubated with antibodies detecting pMLKL (54 kDa, necroptotic marker) and the apoptotic cleavage fragment of caspase-3 (19 kDa, present only in the apoptotic lysate in L929Ts cells). Arrows indicate the position of the analyzed proteins. Detection of actin served as a loading control.

4.1.2 Genetic ablation of caspase-8 in two different human cell lines protects cells from necroptosis

Human caspase-8-deficient U-937 and HT-29 cells were generated with the help of Jaqueline Klausewitz (Kiel University, Kiel, Germany) using the CRISPR/Cas9 technology (Figure 9A and C). In contrast to the murine cells, all human caspase-8 $-/-$ clones were not more sensitive, but rather protected against cell death in comparison to wild type cells, even though the differences for HT-29 cells were not that distinct as for U-937 cells (Figure 9B and D).

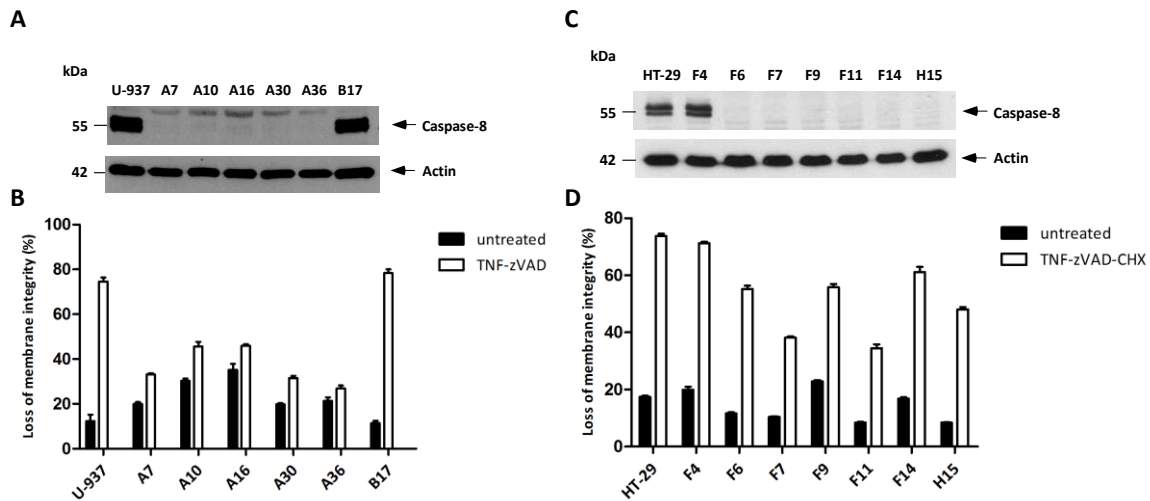


Figure 9: Generation of caspase-8-deficient U-937 and HT-29 cells. (A) Western blot analyses were performed of whole cell lysates from wild type U-937 cells and CRISPR/Cas candidate clones. The blots were incubated with an antibody detecting the full length form of caspase-8 (55 kDa) to determine which of the generated clones is deficient for caspase-8. (B) Flow cytometric analyses of all U-937 CRISPR/Cas clones deficient for caspase-8 (A7, A10, A16, A30, A36) in comparison to wild type and control (B17) U-937 cells were performed to determine the effect on TNF-induced necroptosis caused by the deletion of caspase-8. Cells were left untreated or stimulated with 50 μ M zVAD-fmk (prestimulation for 30 min) and 100 ng/ml TNF for 24 h to induce necroptosis. The experiment was performed by Jaqueline Klausewitz. (C) Western blot analyses were performed of whole cell lysates from wild type HT-29 cells and CRISPR/Cas candidate clones. The blots were incubated with an antibody detecting the full length form of caspase-8 (55 kDa) to determine which of the generated CRISPR/Cas clones is deficient for caspase-8. Arrows indicate the position of the analyzed proteins. Detection of actin served as a loading control. (D) Flow cytometric analysis of all HT-29 CRISPR/Cas clones deficient for caspase-8 (F6, F7, F9, F11, F14, H15) in comparison to wild type and control (F4) HT-29 cells were performed to determine the effect on TNF-induced necroptosis caused by the deletion of caspase-8. Cells were left untreated or stimulated with 20 μ M zVAD-fmk (prestimulation for 30 min), 5 μ g/ml CHX (prestimulation for 30 min) and 100 ng/ml TNF for 24 h to induce necroptosis. Representative data from one out of three experiments are shown and error bars indicate SD from three measurements.

Clones A7 (U-937 cells) and F11 (HT-29 cells) were selected for further studies throughout this dissertation. As described above for the murine cells, two different specific necroptosis inhibitors were used and both were able to fully inhibit cell death (Figure 10A and B), indicating that the cells died through necroptosis and not another form of regulated cell death.

4. Results

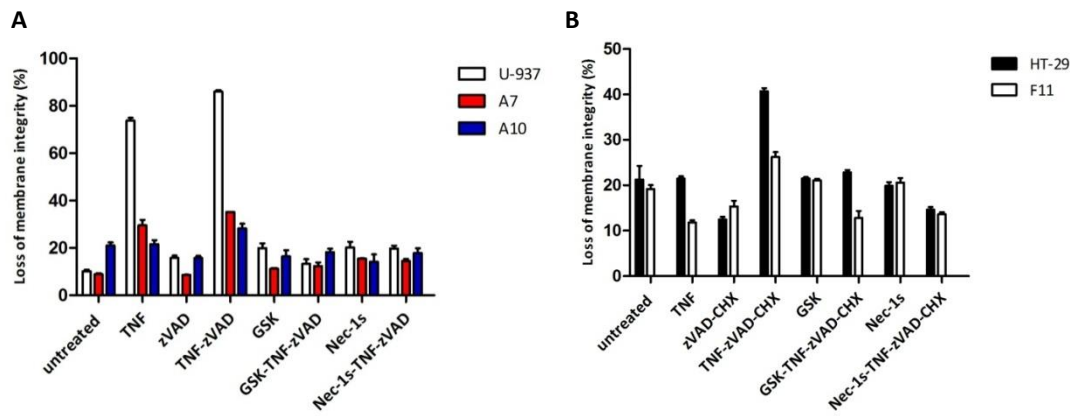


Figure 10: Inhibition of cell death in response to treatment with Nec-1s and GSK'872 in U-937 and HT-29 CRISPR/Cas clones deficient for caspase-8. (A) Flow cytometric analyses of U-937 CRISPR/Cas clones deficient for caspase-8 (A7, A10) and U-937 wild type cells were performed. Cells were left untreated or stimulated with 50 μ M zVAD-fmk (prestimulation for 30 min) and 100 ng/ml TNF for 24 h to induce necroptosis. Cells were additionally treated with 50 μ M Nec-1s (RIK1 inhibitor) or 10 μ M GSK'872 (RIPK3 inhibitor) to clarify if the cells die through necroptosis or another form of regulated cell death. The experiment was performed by Jaqueline Klausewitz. **(B)** Flow cytometric analyses of the HT-29 CRISPR/Cas clone F11 deficient for caspase-8 and HT-29 wild type cells were performed. Cells were left untreated or stimulated with 20 μ M zVAD-fmk (prestimulation for 30 min), 5 μ g/ml CHX (prestimulation for 30 min) and 100 ng/ml TNF for 24 h to induce necroptosis. Cells were additionally treated with 50 μ M Nec-1s (RIK1 inhibitor) or 10 μ M GSK'872 (RIPK3 inhibitor) to clarify if the cells die through necroptosis or another form of regulated cell death. Representative data from one out of three experiments are shown and error bars indicate SD from three measurements.

Western blot analyses showed that in caspase-8-deficient U-937 cells, the signal for pMLKL as a marker for necroptosis appeared less pronounced in comparison to wild type cells (Figure 11), confirming the causal relationship between the deletion of caspase-8 and the protection of these cells against necroptosis. For the HT-29 caspase-8 $-/-$ clone F11, this was even more distinct, showing an extremely delayed and less pronounced signal for pMLKL in comparison to wild type cells (Figure 12). For both human cell lines, the caspase-8 $-/-$ clones showed either no signal or at least a less pronounced signal for cleaved caspase-3 and cleaved PARP-1 (Figure 11, Figure 12), indicating a resistance against apoptosis due to deletion of caspase-8.

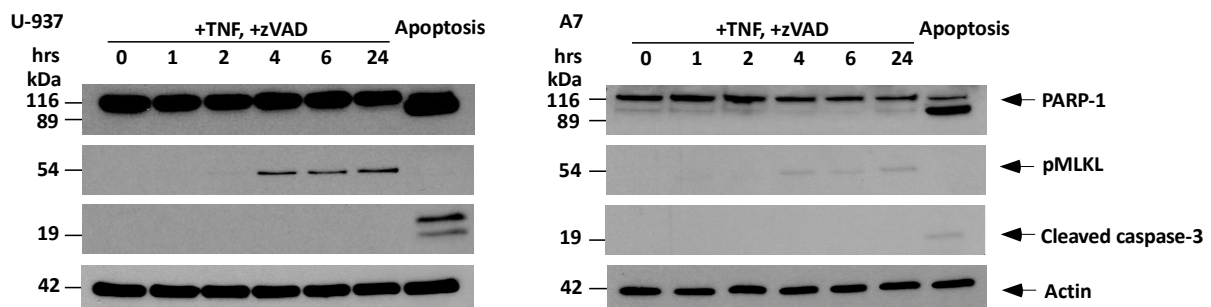


Figure 11: Determining the effect of the genetic ablation of caspase-8 on TNF-induced necroptosis in the U-937 caspase-8 $-/-$ clone A7. Wild type U-937 cells and the U-937 caspase-8 $-/-$ clone A7 were left untreated or stimulated with 50 μ M zVAD-fmk (prestimulation for 30 min) and 100 ng/ml TNF over a time course from 1 to 24 h to induce necroptosis. As a control, cells were additionally treated with 100 ng/ml TNF and 0.1 μ g/ml CHX for 4 h to induce apoptosis. Western blot analyses were performed of whole cell lysates. The blots were incubated with an antibody detecting the full length form (116 kDa) and the apoptotic cleavage fragment of PARP-1 (89 kDa). Western blots were also generated from whole cell lysates incubated with antibodies detecting pMLKL (54 kDa, necroptotic marker) and the apoptotic cleavage fragment of caspase-3 (19 kDa). Arrows indicate the position of the analyzed proteins. Detection of actin served as a loading control.

4. Results

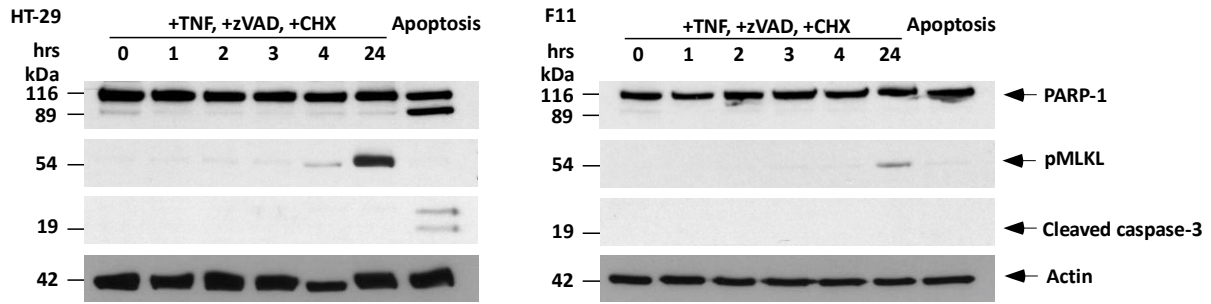


Figure 12: Determining the effect of the genetic ablation of caspase-8 on TNF-induced necroptosis in the HT-29 caspase-8 $-/-$ clone F11. Wild type HT-29 cells and the HT-29 caspase-8 $-/-$ clone F11 were left untreated or stimulated with 20 μ M zVAD-fmk (prestimulation for 30 min), 5 μ g/ml CHX (prestimulation for 30 min) and 100 ng/ml TNF over a time course from 1 to 24 h to induce necroptosis. As a control, cells were additionally treated with 100 ng/ml TNF and 5 μ g/ml CHX for 4 h to induce apoptosis. Western blot analyses were performed of whole cell lysates. The blots were incubated with an antibody detecting the full length form (116 kDa) and the apoptotic cleavage fragment of PARP-1 (89 kDa). Western blots were also generated from whole cell lysates incubated with antibodies detecting pMLKL (54 kDa, necroptotic marker) and the apoptotic cleavage fragment of caspase-3 (19 kDa). Arrows indicate the position of the analyzed proteins. Detection of actin served as a loading control.

4.1.3 Genetic ablation of caspase-10 in two different human cell lines leads to increased cell death

Human caspase-10-deficient U-937 and HT-29 cells were generated by employing the CRISPR/Cas system (Figure 13A and C). In contrast to the human caspase-8 $-/-$ clones, all obtained caspase-10 $-/-$ clones showed increased cell death in comparison to wild type cells (Figure 13B and D).

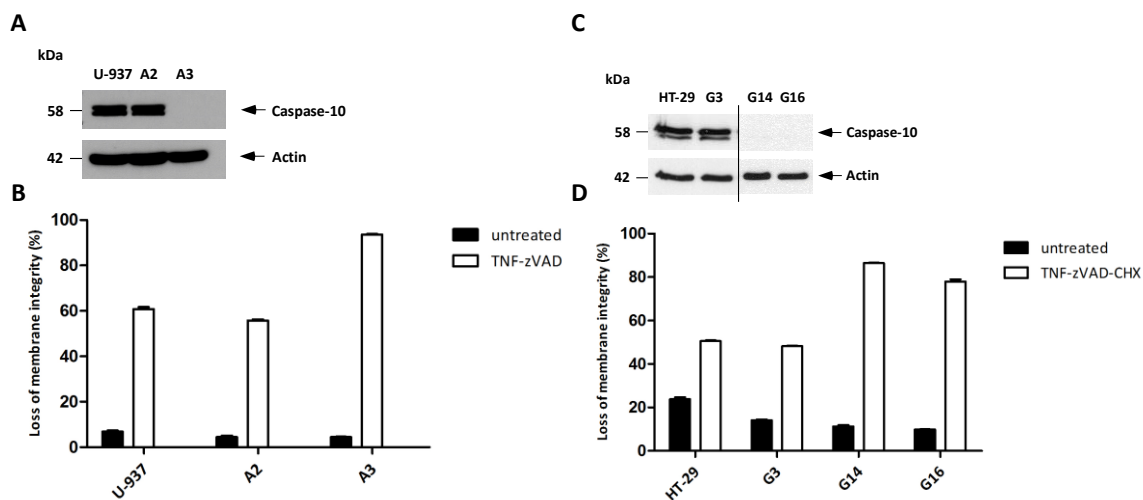


Figure 13: Generation of caspase-10-deficient U-937 and HT-29 cells. (A) Western blot analyses were performed of whole cell lysates from U-937 wild type cells and CRISPR/Cas candidate clones. The blots were incubated with an antibody detecting the full length form of caspase-10 (58 kDa) to determine which of the generated CRISPR/Cas clones is deficient for caspase-10. (B) Flow cytometric analyses of the U-937 caspase-10 $-/-$ clone A3 in comparison to wild type and control (A2) U-937 cells were performed to determine the effect on TNF-induced necroptosis caused by the deletion of caspase-10. Cells were left untreated or stimulated with 50 μ M zVAD-fmk (prestimulation for 30 min) and 100 ng/ml TNF for 24 h to induce necroptosis. (C) Western blot analyses were performed of whole cell lysates from HT-29 wild type cells and CRISPR/Cas candidate clones. The blots were incubated with an antibody detecting the full length form of caspase-10 (58 kDa) to determine which of the generated CRISPR/Cas clones is deficient for caspase-10. Arrows indicate the position of the analyzed proteins. Detection of actin served as a loading control. (D) Flow cytometric analyses of all HT-29 CRISPR/Cas clones deficient for caspase-10 (G14, G16) in comparison to wild type and control (G3) HT-29 cells were performed to determine the effect on TNF-induced necroptosis caused by the deletion of caspase-10. Cells were left untreated or stimulated with 20 μ M zVAD-fmk (prestimulation for 30 min), 5 μ g/ml CHX (prestimulation for 30 min) and 100 ng/ml TNF for 24 h to induce necroptosis. Representative data from one out of three experiments are shown and error bars indicate SD from three measurements.

4. Results

Once again, the cells were treated with two different specific necroptosis inhibitors to make sure that the cells undergo necroptosis and not another form of regulated cell death. Both inhibitors were able to block cell death (Figure 14A and B).

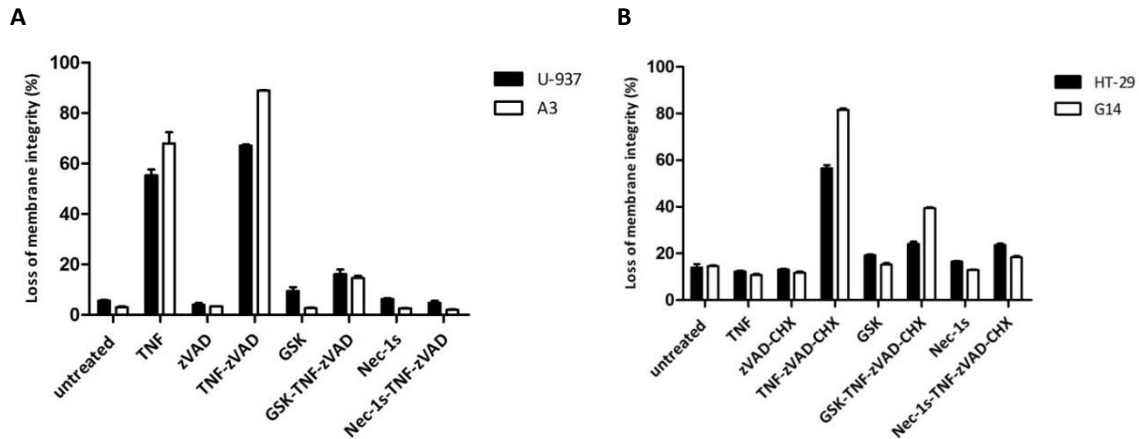


Figure 14: Inhibition of cell death in response to treatment with Nec-1s and GSK'872 in U-937 and HT-29 CRISPR/Cas clones deficient for caspase-10. (A) Flow cytometric analyses of wild type U-937 cells and the U-937 caspase-10 $-/-$ clone A3 were performed. Cells were left untreated or stimulated with 50 μ M zVAD-fmk (prestimulation for 30 min) and 100 ng/ml TNF for 24 h to induce necroptosis. Cells were additionally treated with 50 μ M Nec-1s (RIK1 inhibitor) or 10 μ M GSK'872 (RIPK3 inhibitor) to clarify if the cells die through necroptosis or another form of regulated cell death. (B) Flow cytometric analyses of wild type HT-29 cells and the caspase-10 $-/-$ clone G14 were performed. Cells were left untreated or stimulated with 20 μ M zVAD-fmk (prestimulation for 30 min), 5 μ g/ml CHX (prestimulation for 30 min) and 100 ng/ml TNF for 24 h to induce necroptosis. Cells were additionally treated with 50 μ M Nec-1s (RIK1 inhibitor) or 10 μ M GSK'872 (RIPK3 inhibitor) to clarify if the cells die through necroptosis or another form of regulated cell death. Representative data from one out of three experiments are shown and error bars indicate SD from three measurements.

Western blot analyses for PARP-1 and caspase-3 cleavage as markers for apoptosis and pMLKL as a marker for necroptosis looked quite similar in the HT-29 caspase-10 $-/-$ clone G14 and its wild type counterpart (Figure 16). For the U-937 caspase-10 $-/-$ clone A3, the signal for pMLKL appeared faster and more pronounced (Figure 15), supporting the observed effect of caspase-10-deficient cells showing increased cell death.

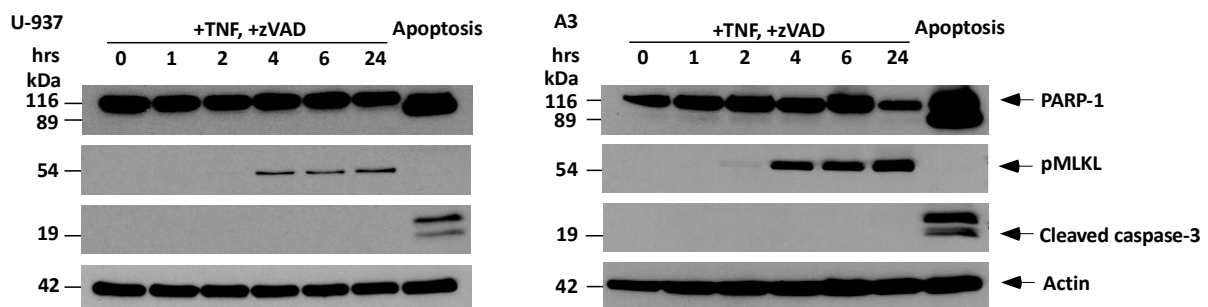


Figure 15: Determining the effect of the genetic ablation of caspase-10 on TNF-induced necroptosis in the U-937 caspase-10 $-/-$ clone A3. As part of the same experiment as shown in Figure 11, the U-937 caspase-10 $-/-$ clone A3 was left untreated or stimulated with 20 μ M zVAD-fmk (prestimulation for 30 min) and 100 ng/ml TNF over a time course from 1 to 24 h to induce necroptosis. As a control, cells were additionally treated with 100 ng/ml TNF and 0.1 μ g/ml CHX for 4 h to induce apoptosis. Western blot analyses were performed of whole cell lysates. The blots were incubated with an antibody detecting the full length form (116 kDa) and the apoptotic cleavage fragment of PARP-1 (89 kDa). Western blots were also generated from whole cell lysates incubated with antibodies detecting pMLKL (54 kDa, necroptotic marker) and the apoptotic cleavage fragment of caspase-3 (19 kDa). For clarity of presentation, the data are shown in a new figure, but with the same wild type U-937 blots as in Figure 11. Arrows indicate the position of the analyzed proteins. Detection of actin served as a loading control.

4. Results

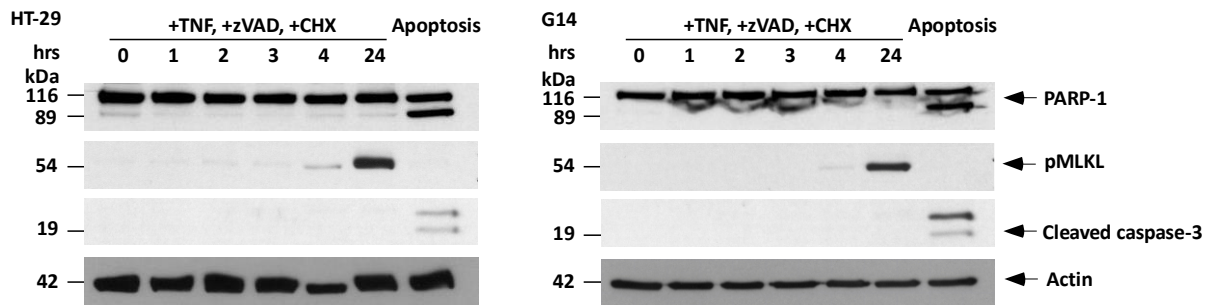


Figure 16: Determining the effect of the genetic ablation of caspase-10 on TNF-induced necroptosis in the HT-29 caspase-10 $-/-$ clone G14. As part of the same experiment as shown in Figure 12, the HT-29 caspase-10 $-/-$ clone G14 was left untreated or stimulated with 20 μ M zVAD-fmk (prestimulation for 30 min), 5 μ g/ml CHX (prestimulation for 30 min) and 100 ng/ml TNF over a time course from 1 to 24 h to induce necroptosis. As a control, cells were additionally treated with 100 ng/ml TNF and 5 μ g/ml CHX for 4 h to induce apoptosis. Western blot analyses were performed of whole cell lysates. The blots were incubated with an antibody detecting the full length form (116 kDa) and the apoptotic cleavage fragment of PARP-1 (89 kDa). Western blots were also generated from whole cell lysates incubated with antibodies detecting pMLKL (54 kDa, necroptotic marker) and the apoptotic cleavage fragment of caspase-3 (19 kDa). For clarity of presentation, the data are shown in a new figure, but with the same wild type HT-29 cell blots as in Figure 12. Arrows indicate the position of the analyzed proteins. Detection of actin served as a loading control.

In mouse caspase-8-deficient cells, core components of the necrosome, e.g., RIPK1, RIPK3 and CFLAR, were additionally downregulated via siRNA (Figure 17A). As expected, flow cytometric assays of the L929Ts caspase-8 $-/-$ clone B3 showed that additional downregulation of RIPK1 and RIPK3 decreased cell death under necroptotic conditions, whereas the additional downregulation of CFLAR had almost no effect on cell death (Figure 17B). RIPK1 and RIPK3 are core components of the necrosome and are essential for the induction of necroptosis (Li *et al.* 2012). Necroptosis can therefore only occur to a limited extent, when one of these proteins is missing. Since CFLAR, as a regulator of caspase-8, is blocking apoptosis and necroptosis (Hughes *et al.* 2016, Shindo *et al.* 2016), its downregulation would typically enhance necroptosis. In caspase-8-deficient L929Ts cells, cell death rates had already reached the maximum, which is why the downregulation of CFLAR did not further increase necroptosis.

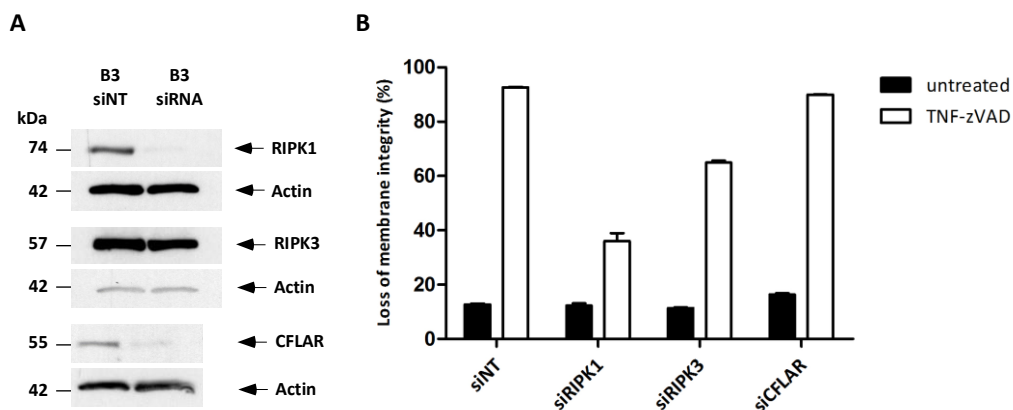


Figure 17: Additional downregulation of core components of the necrosome in the L929Ts caspase-8 $-/-$ clone B3. (A) Control Western blots of the untreated L929Ts caspase-8 $-/-$ clone B3, transfected with siRNAs specific for either RIPK1, RIPK3 or CFLAR (siRIPK1, siRIPK3, siCFLAR) or control siRNA (siNT) were performed to verify the efficiency of the siRNA knockdown. Detection of actin served as a loading control. (B) In parallel, flow cytometric analyses of the L929Ts caspase-8 $-/-$ clone B3 were performed. After 48 h, cells were left untreated or stimulated with 20 μ M zVAD-fmk (prestimulation for 30 min) and 100 ng/ml TNF. Representative data from one out of three experiments are shown and error bars indicate SD from three measurements.

4. Results

In human caspase-8- or caspase-10-deficient cells, caspase-8 or -10 (where still present) were downregulated in addition to RIPK1, RIPK3 and CFLAR (Figure 18A, Figure 19A). For the downregulation of caspase-10, two different siRNAs (A and B) were used and for the downregulation of caspase-8, three different siRNAs (A, B and C) were used (Figure 18A, B and C, Figure 19A, B and C). In the U-937 caspase-8 $-/-$ clone A7, the downregulation (Figure 18A) of none of the core components except for CFLAR could overcome the effect triggered by the deletion of caspase-8 (Figure 18B) meaning that the cells were still protected from necroptosis. Cell death was increased when CFLAR was additionally downregulated in these cells (Figure 18B). In the HT-29 caspase-8 $-/-$ clone F11, the results were similar to the ones generated in mouse cells. The additional downregulation of RIPK1 and RIPK3 (Figure 19A) decreased cell death, whereas CFLAR slightly increased cell death (Figure 19B).

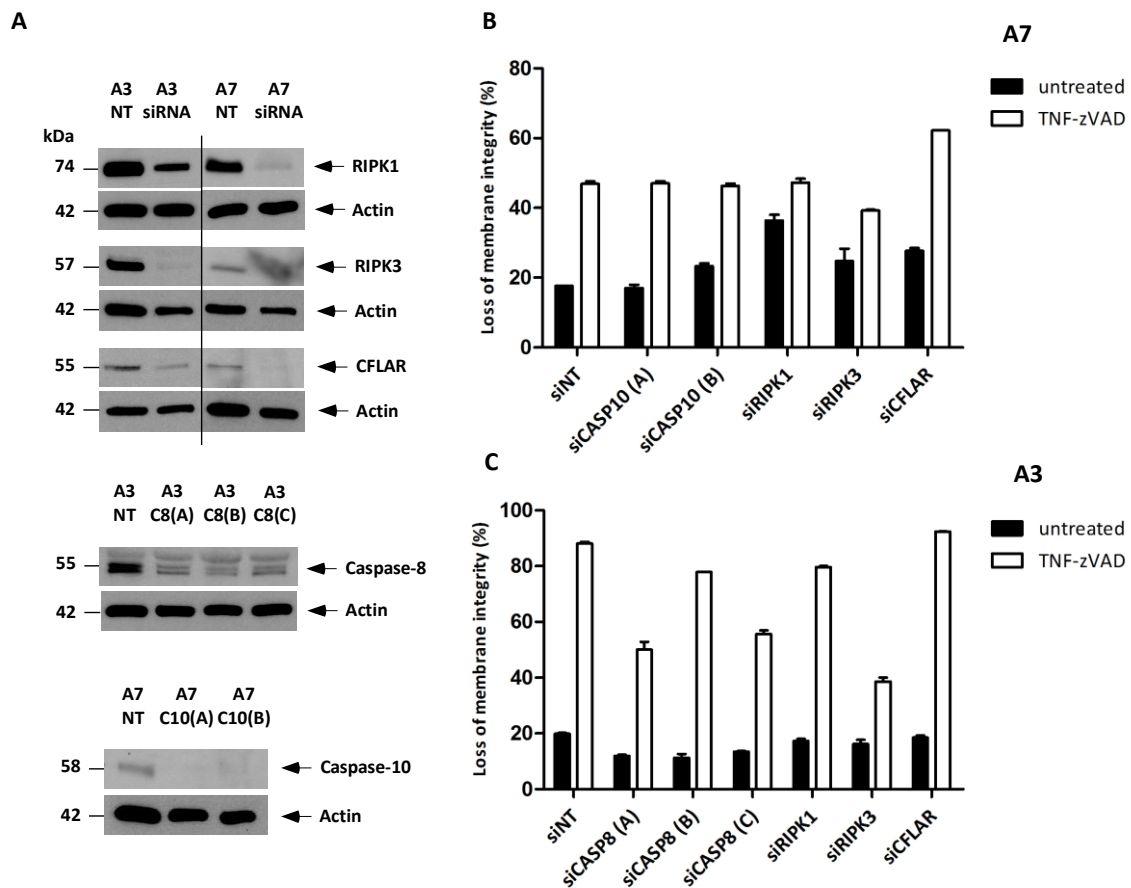


Figure 18: Additional downregulation of core components of the necrosome in the U-937 caspase-8 $-/-$ clone A7 and the U-937 caspase-10 $-/-$ clone A3. (A) Control Western blots of untreated caspase-8- (A7) or caspase-10-deficient (A3) U-937 cells, transfected with siRNAs specific for either RIPK1, RIPK3, caspase-10, caspase-8 or CFLAR (siRIPK1, siRIPK3, siCASP10 (A)/(B), siCASP8 (A)/(B)/(C), siCFLAR) or control siRNA (siNT) were performed to verify the efficiency of the siRNA knockdown. Detection of actin served as a loading control. The experiment was performed by Jaqueline Klauswitz. **(B)** In parallel, flow cytometric analyses of the U-937 caspase-8 $-/-$ clone A7 were performed. After 48 h, cells were left untreated or stimulated with 50 μ M zVAD-fmk (prestimulation for 30 min) and 100 ng/ml TNF. **(C)** In parallel, flow cytometric analyses of the U-937 caspase-10 $-/-$ clone A3 were performed. After 48 h, cells were left untreated or stimulated with 50 μ M zVAD-fmk (prestimulation for 30 min) and 100 ng/ml TNF. Representative data from one out of three experiments are shown and error bars indicate SD from three measurements.

4. Results

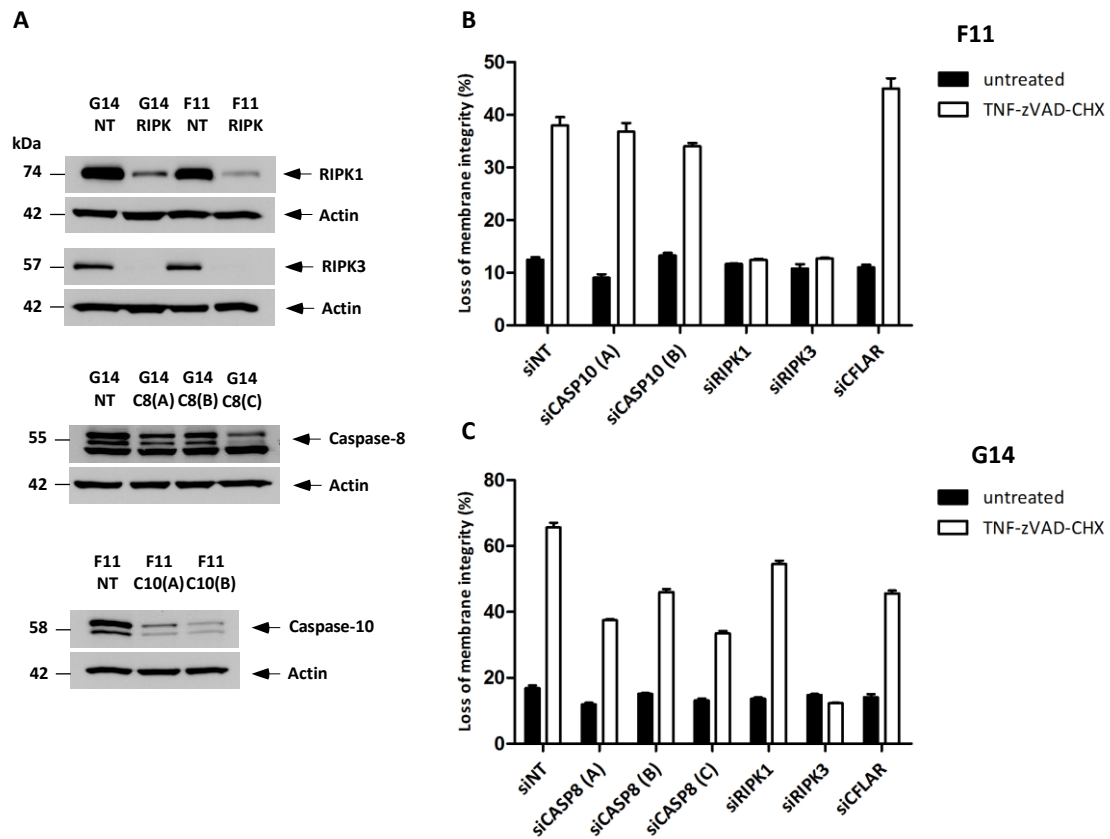


Figure 19: Additional downregulation of core components of the necrosome in the HT-29 caspase-8^{-/-} clone F11 and the HT-29 caspase-10^{-/-} clone G14. (A) Control Western blots of untreated caspase-8^{-/-} (F11) or caspase-10^{-/-} (G14) HT-29 cells, transfected with siRNAs specific for either RIPK1, RIPK3, caspase-10 or caspase-8 (siRIPK1, siRIPK3, siCASP10 (A)/(B), siCASP8 (A)/(B)/(C) or control siRNA (siNT) were performed to verify the efficiency of the siRNA knockdown. Detection of actin served as a loading control. **(B)** In parallel, flow cytometric analysis of HT-29 caspase-8^{-/-} clone F11 were performed. After 48 h, cells were left untreated or stimulated with 20 μ M zVAD-fmk, 5 μ g/ml CHX (both prestimulated for 30 min) and 100 ng/ml TNF. **(C)** In parallel, flow cytometric analysis of the HT-29 caspase-10^{-/-} clone G14 were performed. After 48 h, cells were left untreated or stimulated with 20 μ M zVAD-fmk, 5 μ g/ml CHX (both prestimulated for 30 min) and 100 ng/ml TNF. Representative data from one out of three experiments are shown and error bars indicate SD from three measurements.

In human U-937 and HT-29 caspase-10-deficient cells, the additional downregulation of RIPK1 and RIPK3 (Figure 18A, Figure 19A) decreased cell death with RIPK3 showing the most distinct results concerning the protection of the cells (Figure 18C, Figure 19C). This is in line with the induction of necroptosis being dependent on RIPK1 and RIPK3 as outlined above (Li *et al.* 2012). In the HT-29 caspase-10^{-/-} clone G14, the additional downregulation of CFLAR decreased cell death (Figure 19C), whereas in the U-937 caspase-10^{-/-} clone A3 the additional downregulation of CFLAR only slightly increased cell death (Figure 18C). The latter can be explained by the fact that cell death rates had already reached a maximum as described above for caspase-8-deficient L929Ts cells.

4.1.5 The additional downregulation of caspase-10 in human cells cannot override the effect of caspase-8

In both human cell lines, caspase-10 was additionally downregulated in the caspase-8^{-/-} clones A7 and F11 via siRNA. For both caspase-8^{-/-} clones the results looked quite similar. The additional downregulation of caspase-10 had no effect on cell death meaning that the caspase-8-deficient cells were still protected against necroptosis (Figure 18B, Figure 19B).

Vice versa, when caspase-8 was additionally downregulated in the caspase-10 $-/-$ clones A3 and G14 the downregulation of caspase-8 decreased cell death in caspase-10-deficient cells (Figure 18C, Figure 19C). In all experiments, caspase-8 siRNA (B) showed the weakest effects on cell death (Figure 18C, Figure 19C).

4.1.6 Reconstitution of CRISPR/Cas knockout cell lines with enzymatically active and inactive mutant forms of caspases-8 and -10

Human and mouse caspase-8- and caspase-10-deficient cells were transiently or stably reconstituted with enzymatically active and inactive mutant forms of human and mouse caspase-8 and caspase-10 (Figure 20A, Figure 21A, Figure 22A). As a result, it should be established whether necroptosis is differentially regulated by caspase-8 in mice and in humans and whether the effects caused by the deletion of caspase-8 or caspase-10 can be reversed. After transiently transfecting the L929Ts caspase-8 $-/-$ clone B3 with active mouse caspase-8, the cells showed decreased cell death and behaved more like their wild type counterparts again (Figure 20B), indicating that the phenotype in these cells could be restored. In contrast, transfecting these cells with active or inactive human caspase-8 had absolutely no effect on cell death (Figure 20B), pointing to a difference between human and mouse caspase-8.

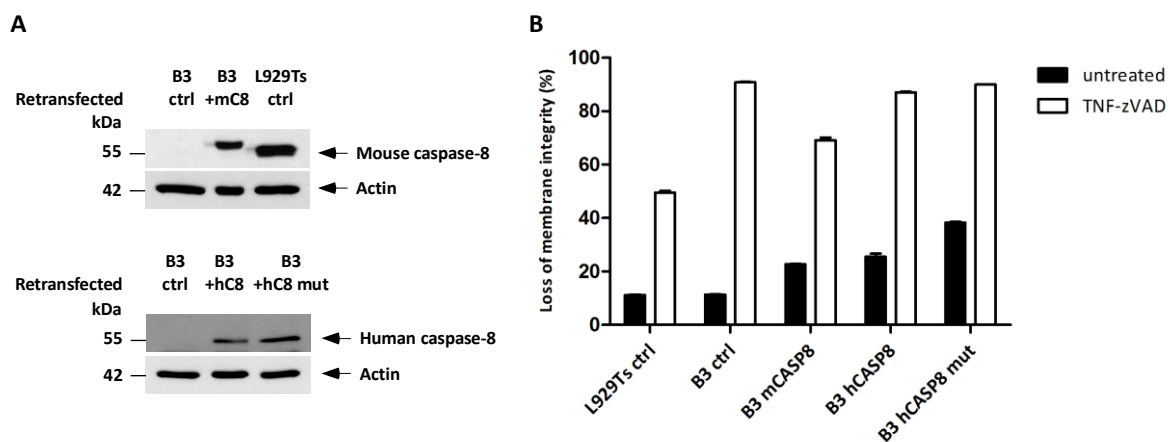


Figure 20: Reconstitution of the L929Ts caspase-8 $-/-$ clone B3 with active mouse caspase-8, active human caspase-8 and an inactive mutant form of human caspase-8. (A) Control Western blots of the transfected (mCASP8, hCASP8 and hCASP mut) but untreated L929Ts caspase-8 $-/-$ clone B3 were performed to verify the reconstitution of the respective proteins. Detection of actin served as a loading control. **(B)** In parallel, flow cytometric analyses of the L929Ts caspase-8 $-/-$ clone B3 transiently transfected with constructs encoding either mouse caspase-8, human caspase-8 (active or inactive) or the vector alone (ctrl) were performed. After 48 h, cells were left untreated or stimulated with 20 μ M zVAD-fmk (prestimulation for 30 min) and 100 ng/ml TNF. Representative data from one out of three experiments are shown and error bars indicate SD from three measurements.

In human cells, the pTRIPZ inducible lentiviral system had to be used for transfection (Figure 21A), because of the intrinsic toxicity of transiently or stably reconstituted active caspases. Within this system, doxycycline was used to induce caspase-8 and caspase-10 expression. Caspase-8-deficient HT-29 cells were transfected with the vector alone, as a control, which had no effect on cell death (Figure 21B). Both, inactive human and mouse caspase-8 mutant forms had no effect on cell death in caspase-8-deficient cells (Figure 21B). The transfection

4. Results

of human caspase-8-deficient cells with active human caspase-8 led to increased cell death (Figure 21B) and thus, to a similar behavior as one could observe for their wild type counterparts, meaning that the effect caused by the deletion of human caspase-8 could be neutralized by human active caspase-8. In contrast, the transfection with active mouse caspase-8 led to decreased cell death (Figure 21B), which was also shown in murine cells, supporting the hypothesis that necroptosis is differentially regulated by caspase-8 in mice and in humans.

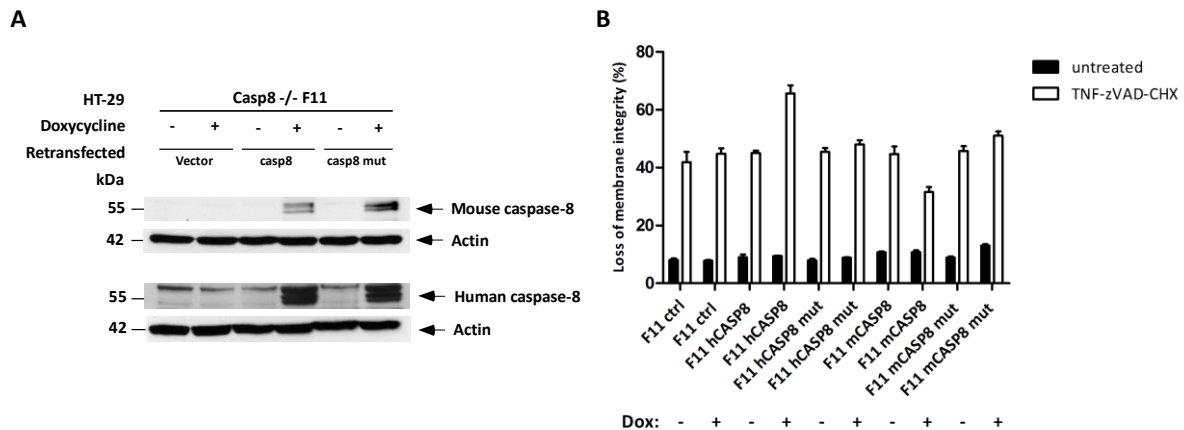
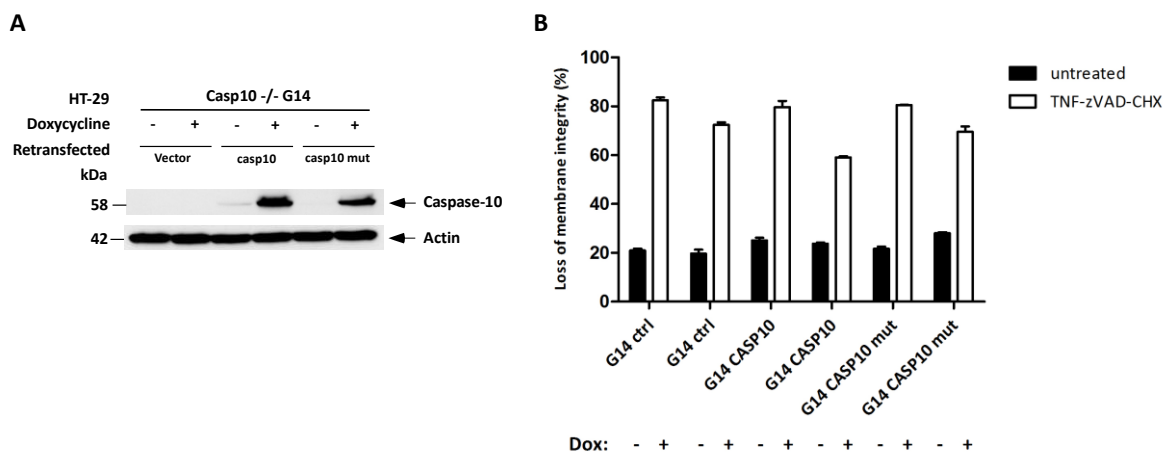


Figure 21: Reconstitution of the HT-29 caspase-8^{-/-} clone F11 with active and inactive mutant forms of mouse and human caspase-8. (A) Control Western blots of the transfected (mCASP8, mCASP mut, hCASP8 and hCASP8 mut) and doxycycline-treated or untreated HT-29 caspase-8^{-/-} clone F11 were performed to verify the reconstitution of the respective proteins. Detection of actin served as a loading control. (B) In parallel, flow cytometric analyses of the HT-29 caspase-8^{-/-} clone F11 stably transfected with the pTRIPZ lentiviral inducible system specific for either mouse caspase-8 (active or inactive), human caspase-8 (active or inactive) or the pTRIPZ vector alone (ctrl) were performed. After 24 h, cells were left untreated or stimulated with 1 µg/ml doxycycline to induce caspase-8 activity before necroptosis was induced by stimulating the cells with 20 µM zVAD-fmk, 5 µg/ml CHX (both prestimulated for 30 min) and 100 ng/ml TNF for further 24h. Representative data from one out of three experiments are shown and error bars indicate SD from three measurements.

The HT-29 caspase-10^{-/-} clone G14 was also reconstituted with active and inactive caspase-10 (Figure 22A). After transfection with active caspase-10, cell death was decreased and the cells behaved more like the wild type cells again. There was no effect on cell death after transfection with inactive caspase-10 (Figure 22B).



4. Results

Figure 22: Reconstitution of the HT-29 caspase-10 $-/-$ clone G14 with active and inactive mutant forms of caspase-10. (A) Control Western blots of the transfected (CASP10, and CASP10 mut) and doxycycline-treated or untreated HT-29 caspase-10 $-/-$ clone G14 were performed to verify the reconstitution of the respective proteins. Detection of actin served as a loading control. (B) In parallel, flow cytometric analyses of the HT-29 caspase-10 $-/-$ clone G14 stably transfected with the pTRIPZ lentiviral inducible system specific for either active caspase-10, inactive caspase-10 or the pTRIPZ vector alone (ctrl) were performed. After 24 h, cells were left untreated or stimulated with 1 μ g/ml doxycycline to induce caspase-10 activity before necroptosis was induced by stimulating the cells with 20 μ M zVAD-fmk, 5 μ g/ml CHX (both prestimulated for 30 min) and 100 ng/ml TNF for further 24h. Representative data from one out of three experiments are shown and error bars indicate SD from three measurements.

4.1.7 Analyses of the composition of the necrosome in caspase-8- and caspase-10-deficient human cells

As core components of the necrosome, RIPK1 and RIPK3 associate through their RIP homotypic interaction motifs (RHIM), which leads to auto-phosphorylation of RIPK3, recruitment of MLKL and thus to execution of necroptosis (Mompeàn *et al.* 2018). To clarify whether the deletion of caspase-8 or caspase-10 has an impact on the assembly of the necrosome, immunoprecipitations were performed from lysates of HT-29 and U-937 cells after induction of necroptosis, followed by Western blot analyses. For U-937 and HT-29 wild type cells, Western blot analyses of immunoprecipitations with caspase-8 revealed that caspase-8 associates with RIPK1, RIPK3 and caspase-10 during necroptosis and that the signal for all three proteins increased over time (Figure 23A, Figure 24A).

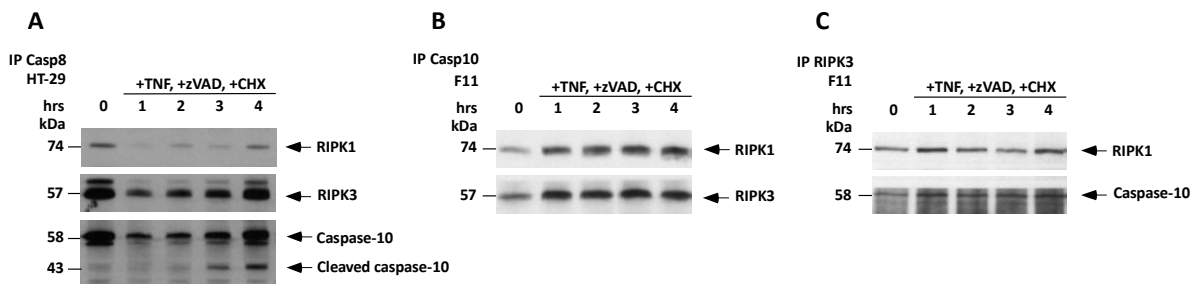


Figure 23: Analyses of the assembly of the necrosome in wild type HT-29 cells and the HT-29 caspase-8 $-/-$ clone F11 via immunoprecipitations. (A) Immunoprecipitations with caspase-8 were performed from whole cell lysates of necroptosis-induced (20 μ M zVAD, 5 μ g/ml CHX and 100 ng/ml TNF) wild type HT-29 cells over a time course from 1 to 4h. Western blots were generated from immunoprecipitates. The blots were incubated with antibodies detecting RIPK1 (74 kDa) RIPK3 (57 kDa), the full length form (58 kDa) and the cleavage fragment of caspase-10 (43 kDa). (B) Immunoprecipitations with caspase-10 were performed from whole cell lysates of the necroptosis-induced (20 μ M zVAD, 5 μ g/ml CHX and 100 ng/ml TNF) HT-29 caspase-8 $-/-$ clone F11 over a time course from 1 to 4h. Western blots were generated from immunoprecipitates. The blots were incubated with antibodies detecting RIPK1 (74 kDa) and RIPK3 (57 kDa). (C) Immunoprecipitations with RIPK3 were performed from whole cell lysates of the necroptosis-induced (20 μ M zVAD, 5 μ g/ml CHX and 100 ng/ml TNF) HT-29 caspase-8 $-/-$ clone F11 over a time course from 1 to 4h. Western blots were generated from immunoprecipitates. The blots were incubated with antibodies detecting RIPK1 (74 kDa) and caspase-10 (58 kDa). Arrows indicate the position of the analyzed proteins.

In contrast, Western blot analyses of immunoprecipitations with caspase-10 and RIPK3 in caspase-8-deficient cells showed no increase of any of the analyzed proteins (Figure 23B and C, Figure 24C and D) suggesting that the deletion of caspase-8 in human cells disrupts the assembly of the necrosome, thus preventing necroptosis. Furthermore, Western blot analyses of immunoprecipitations with caspase-8 in the U-937 caspase-10 $-/-$ clone A3 demonstrated that the increasing signal for RIPK1 and RIPK3 was much more pronounced in comparison to the wild type counterpart (Figure 24B).

4. Results

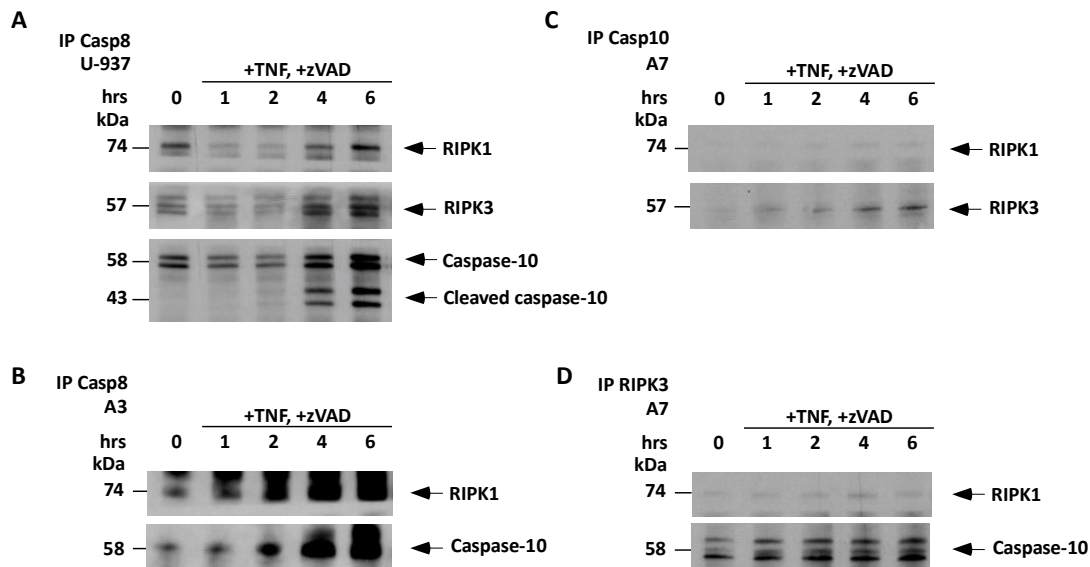


Figure 24: Analyses of the assembly of the necrosome in wild type U-937 cells, the U-937 caspase-8 $-/-$ clone A7 and the U-937 caspase-10 $-/-$ clone A3 via immunoprecipitations. (A) Immunoprecipitations with caspase-8 were performed from whole cell lysates of necroptosis-induced (50 μ M zVAD and 100 ng/ml TNF) wild type U-937 cells over a time course from 1 to 6 h. Western blots were generated from immunoprecipitates. The blots were incubated with antibodies detecting RIPK1 (74 kDa), RIPK3 (57 kDa), the full length form (58 kDa) and the cleavage fragment of caspase-10 (43 kDa). (B) Immunoprecipitations with caspase-8 were performed from whole cell lysates of the necroptosis-induced (50 μ M zVAD and 100 ng/ml TNF) U-937 caspase-10 $-/-$ clone A3 over a time course from 1 to 6 h. Western blots were generated from immunoprecipitates. The blots were incubated with antibodies detecting RIPK1 (74 kDa) and caspase-8 (55 kDa). (C) Immunoprecipitations with caspase-10 were performed from whole cell lysates of the necroptosis-induced (50 μ M zVAD and 100 ng/ml TNF) U-937 caspase-8 $-/-$ clone A7 over a time course from 1 to 6 h. Western blots were generated from immunoprecipitates incubated with antibodies detecting RIPK1 (74 kDa) and RIPK3 (57 kDa). (D) Immunoprecipitations with RIPK3 were performed from whole cell lysates of the necroptosis-induced (50 μ M zVAD and 100 ng/ml TNF) U-937 caspase-8 $-/-$ clone A7 over a time course from 1 to 6 h. Western blots were generated from immunoprecipitates. The blots were incubated with antibodies detecting RIPK1 (74 kDa) and caspase-10 (58 kDa). Arrows indicate the position of the analyzed proteins. The experiment was performed by Jaqueline Klausewitz.

The fact that caspase-10 and caspase-8 associate within the necroptotic signaling pathway was confirmed via additional Western blot analyses of lysates of magnetically isolated receptosomes from wild type U-937 and HT-29 cells (Figure 25).

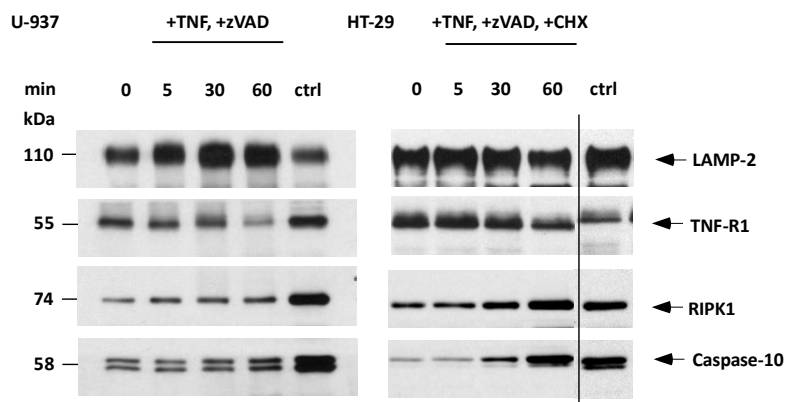


Figure 25: Analyses of magnetically isolated receptosomes from wild type HT-29 and U-937 cells. TNF-R1 magnetic fractions were derived from HT-29 and U-937 cells after stimulation with 100 ng/ml TNF60-Fc for the indicated times. 4 μ g of protein were analyzed by Western blot for presence of endogenous TNF-R1, RIPK1, caspase-10 and LAMP-2 as lysosomal marker. Whole cell lysates of untreated cells were used as control (ctrl). Arrows indicate the position of the analyzed proteins.

4.1.8 The effect caused by the deletion of caspase-8 in human cells can be overcome upon usage of the Smac mimetic birinapant

Birinapant is a biindole-based bivalent Smac mimetic, binding to and inhibiting the activity of IAPs, thus leading to activation of downstream caspases and the induction of apoptosis (Benetatos *et al.* 2014). In this context here, birinapant was used instead of CHX in combination with TNF and zVAD to induce necroptosis. In contrast to CHX, birinapant has clinical relevance, since it is used in clinical trials primarily for the therapy of hematological malignancies and solid tumors (Zhu *et al.* 2018). In HT-29 wild type cells and caspase-10 $-/-$ clone G14, necroptosis was slightly increased when CHX was exchanged for birinapant to induce necroptosis (Figure 26). In caspase-8-deficient cells the protection against necroptosis was completely abrogated upon usage of birinapant (Figure 26). When CHX and birinapant were used in combination, the results looked quite similar to the ones with TNF and zVAD in combination with birinapant alone. When caspase-8-deficient cells were treated with birinapant and TNF alone, cell death was extremely increased, which was not the case for caspase-10-deficient cells and wild type counterparts (Figure 26), supporting once more that treatment with birinapant can override the effect caused by the deletion of caspase-8. As described above, the birinapant-treated cells were additionally stimulated with Nec-1s and GSK'872 and both necroptosis inhibitors were able to completely block cell death (Figure 26), indicating that that the cells died through necroptosis.

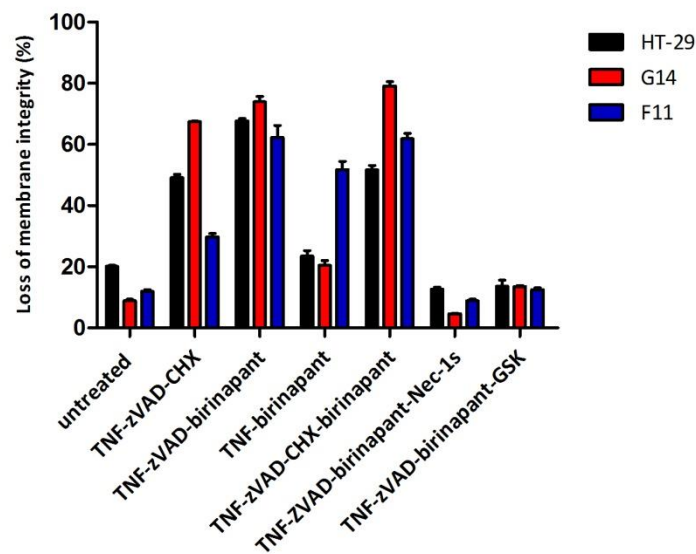


Figure 26: The Smac mimetic birinapant overcomes the protection from necroptosis caused by the deletion of caspase-8 in human HT-29 cells. Flow cytometric analyses of HT-29 CRISPR/Cas clones deficient for caspase-8 (F11) or caspase-10 (G14) and wild type HT-29 cells were performed. Cells were left untreated or stimulated with 20 μ M zVAD-fmk, 5 μ g/ml CHX (both prestimulated for 30 min) and 100 ng/ml TNF for 24 h to induce necroptosis. Cells were treated with 1 μ M birinapant instead of CHX or additional to CHX to induce necroptosis. Cells were additionally treated with Nec-1s (RIK1 inhibitor) or GSK'872 (RIPK3 inhibitor) to clarify if the cells die through necroptosis or another form of regulated cell death. Representative data from one out of three experiments are shown and error bars indicate SD from three measurements.

4.1.9 Conclusion

In accordance with the literature, genetic ablation of caspase-8 in murine cells led to increased cell death. In contrast, when caspase-8 was deleted in human cells, this led to protection of the cells against necroptosis, while the deletion of caspase-10 in human cells led to increased cell death. Additional downregulation of caspase-10 in caspase-8-deficient cells did not influence or even overcome the effect caused by the deletion of caspase-8. In contrast, additional downregulation of caspase-8 changed the effect caused by the deletion of caspase-10, indicating that caspase-10 in humans cannot substitute the function that is held by caspase-8 in mice. Reconstitution of HT-29, U-937 and L929Ts cells deficient for caspase-8 with enzymatically active and inactive mutant forms of human and mouse caspase-8 showed that there is a difference between human and mouse caspase-8. In human cells, the deletion of caspase-8 seemed to disrupt the assembly of the necrosome, thus preventing the induction of necroptosis. To conclude, all data obtained throughout this thesis consistently point to a differential proteolytic regulation of necroptosis by caspase-8 in mice and in humans.

4.2 The serine protease HtrA2/Omi as a key mediator regulating TNF-induced necroptosis

The serine protease HtrA2/Omi has been identified as a key mediator regulating TNF-induced necroptosis. Mouse embryonic fibroblasts deficient for HtrA2/Omi were completely protected from necroptosis (Sosna *et al.* 2013), but the underlying molecular mechanism remains unknown. As described above, UCH-L1 was identified as a substrate of HtrA2/Omi during necroptosis (Sosna *et al.* 2013), but since UCH-L1 is not expressed ubiquitously (Meyer-Schwesinger *et al.* 2011), there must be additional substrates or mechanisms through which HtrA2/Omi mediates necroptosis. Accordingly, several potential substrates of HtrA2/Omi were analyzed within this thesis.

4.2.1 Analyses of DBC1, PDXDC1 and VPS4B as potential downstream mediators of HtrA2/Omi during necroptosis

In a proteome-wide study, Vande Walle and colleagues have identified potential HtrA2/Omi substrates that are cleaved during apoptosis by mass spectrometry including the proteins DBC1, PDXDC1 and VPS4B (Vande Walle *et al.* 2007). VPS4B is described to be associated with intracellular protein trafficking, lysosomal degradation, virus budding and regulation of different stages of mitosis and cell division (Xu *et al.* 2017). DBC1 is reported to be involved in the induction of mitochondrial clustering and matrix condensation as well as the regulation of metabolism, apoptosis and RNA splicing (Vande Walle *et al.* 2007, Li *et al.* 2017). Moreover, DBC1 is described to function as an inhibitor of epigenetic regulators (e.g., methyltransferase SUV39H1, E3 ligase MDM2) (Moon *et al.* 2018). The function of PDXDC1 is unknown by now. All three proteins were further investigated as potential HtrA2/Omi

substrates during necroptosis by Western blot analyses and siRNA knockdown experiments within this thesis.

In a first experiment, L929Ts and HtrA2/Omi wild type MEF were compared with HtrA2/Omi-deficient counterparts and HtrA2/Omi-deficient MEF reconstituted with HtrA2/Omi with regard to necroptotic cleavage of DBC1, PDXDC1 and VPS4B. As shown in figure 25A and B, the signal for DBC1 was clearly decreased under necroptotic conditions in HtrA2/Omi wild type MEF and HtrA2/Omi-deficient MEF reconstituted with HtrA2/Omi, but not in L929Ts cells. For PDXDC1, there was no difference in either of the cell lines, except for a potential cleavage band appearing under necroptotic conditions in HtrA2/Omi wild type MEF and HtrA2/Omi-deficient MEF reconstituted with HtrA2/Omi (Figure 27A). The signal for VPS4B was more pronounced under necroptotic conditions in HtrA2/Omi wild type MEF and HtrA2/Omi-deficient MEF reconstituted with HtrA2/Omi (Figure 27A), but again this was not the case in L929Ts cells (Figure 27B).

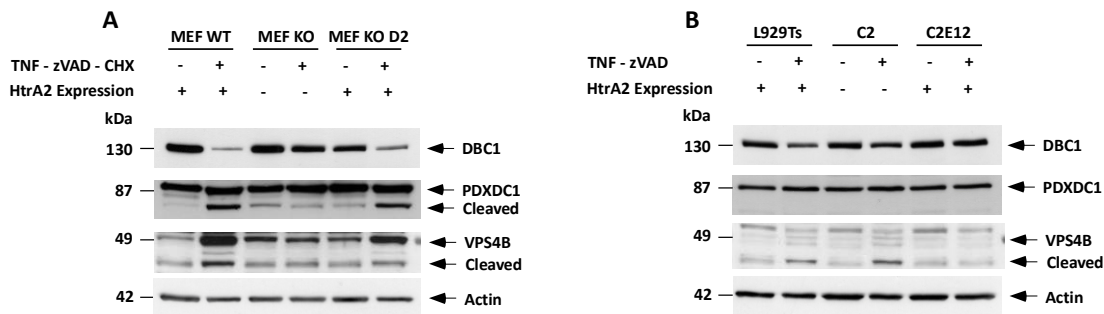


Figure 27: Western blot analyses of DBC1, PDXDC1 and VPS4B as downstream mediators of HtrA2/Omi during necroptosis. (A) HtrA2/Omi wild type MEF, HtrA2/Omi-deficient MEF and HtrA2/Omi-deficient MEF reconstituted with HtrA2/Omi (D2) were left untreated or stimulated with 20 μ M zVAD-fmk, 1 μ g/ml CHX (both prestimulated for 30 min) and 100 ng/ml TNF for 16 h to induce necroptosis. Western blot analyses were performed of whole cell lysates. The blots were incubated with antibodies detecting DBC1 (130 kDa), PDXDC1 (87 kDa) and VPS4B (49 kDa). **(B)** L929Ts wild type cells, HtrA2/Omi-deficient L929Ts cells (C2) and HtrA2/Omi-deficient L929Ts cells reconstituted with HtrA2/Omi (C2E12) were left untreated or stimulated with 20 μ M zVAD-fmk (prestimulated for 30 min) and 100 ng/ml TNF for 5 h to induce necroptosis. Western blot analyses were performed of whole cell lysates. The blots were incubated with antibodies detecting DBC1 (130 kDa), PDXDC1 (87 kDa) and VPS4B (49 kDa). Arrows indicate the position of the analyzed proteins. Detection of actin served as a loading control.

To clarify if the effects described above are due to an inefficient or absent cleavage by HtrA2/Omi or caused indirectly in HtrA2/Omi-deficient cells by their resistance against necroptosis, all three proteins were downregulated by siRNA in HtrA2/Omi wild type MEF (Figure 28A). The knockdown of none of the three proteins had any effect on cell death (Figure 28B), indicating that these proteins may not be critical for HtrA2/Omi-mediated necroptosis. However, since the efficiency of the knockdown was very weak (Figure 28A), it is not possible to draw a final conclusion concerning a direct cleavage by HtrA2/Omi and further experiments will be needed.

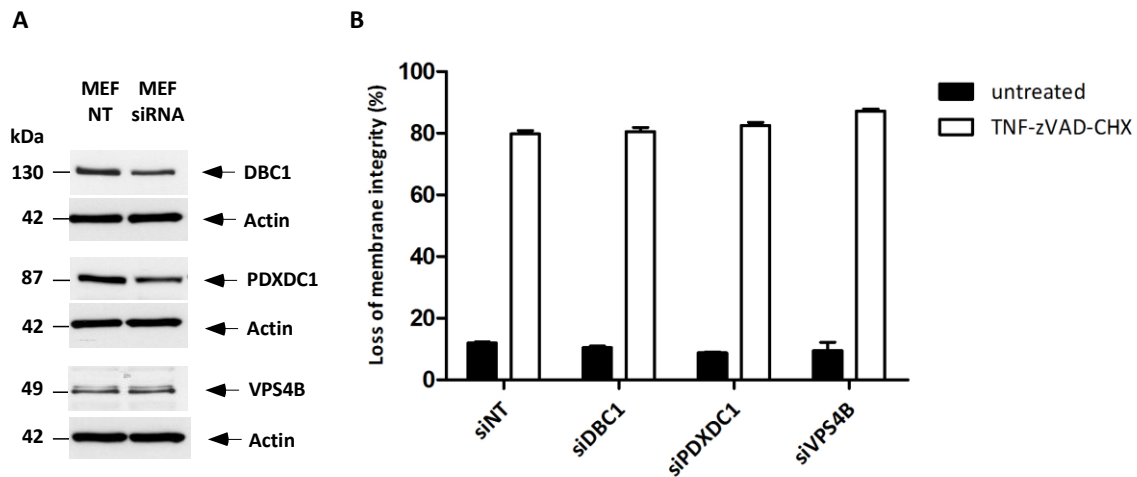


Figure 28: Downregulation by siRNA of DBC1, PDXDC1 and VPS4B in HtrA2/Omi wild type MEF. (A) Control Western blots of untreated HtrA2/Omi wild type MEF, transfected with siRNAs specific for either mouse DBC1, PDXDC1 or VPS4B (siDBC1, siPDXDC1 and siVPS4B) or control siRNA (siNT) were performed to verify the efficiency of the siRNA knockdown. Detection of actin served as a loading control. (B) In parallel, flow cytometric analyses of HtrA2/Omi wild type MEF were performed. After 48 h, cells were left untreated or stimulated with 20 μ M zVAD-fmk, 1 μ g/ml CHX (both prestimulated for 30 min) and 100 ng/ml TNF for 16 h to induce necroptosis. Representative data from one out of three experiments are shown and error bars indicate SD from three measurements.

4.2.2 Analyses of PMPCA, PSA1 and LONP1 as potential downstream mediators of HtrA2/Omi during necroptosis

In a proteomic screen performed by Susann Voigt, several proteases distinct from HtrA2/Omi that potentially also contribute to necroptosis have been previously identified. These proteases were further investigated by siRNA knockdown experiments within this thesis. Three potential candidates identified within the proteomic screens were PMPCA, PSA1 and LONP1. PMPCA is involved in the processing of mitochondrial proteins (Joshi *et al.* 2016) while LONP1 has been suggested to be correlated with mitochondrial gene expression and homeostasis (Matsushima *et al.* 2010). Mutations in both of these proteins have been described to cause mitochondrial disease (Joshi *et al.* 2016, Peter *et al.* 2018). As a subunit of the proteasome, PSA1 is involved in selective protein degradation and is suggested to be involved in tumorigenesis and tumor progression (Quin *et al.* 2017).

In L929Ts and HT-29 wild type cells, PMPCA, PSA1 and LONP1 were downregulated via siRNA (Figure 29A and C). If one of the three proteins would be a substrate or downstream mediator of the serine protease HtrA2/Omi, the downregulation should evoke a similar effect to the one caused by the deletion of HtrA2/Omi. This means that the cells should be protected against necroptosis. For both cell lines, the results looked quite similar, showing that the downregulation of none of the three proteins had any effect on cell death (Figure 29B and D), indicating that none of the proteins is a likely downstream mediator of HtrA2/Omi. Only the downregulation of LONP1 in HT-29 cells slightly decreased cell death in comparison to control (Figure 29D). However, the efficiency of the knockdown was again very weak (Figure 29A and C), and further experiments will be needed to draw a final conclusion.

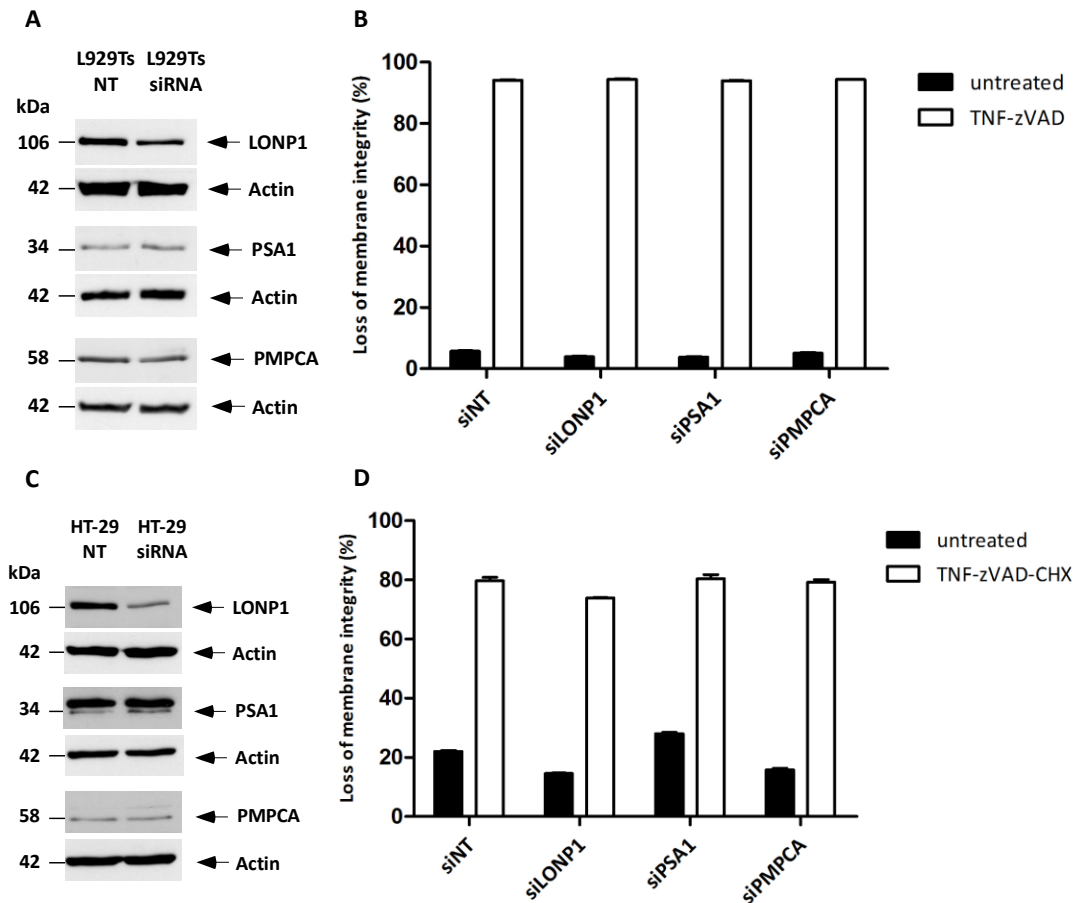


Figure 29: Downregulation by siRNA of LONP1, PSA1 and PMPCA in L929Ts and HT-29 wild type cells. (A) Control Western blots of untreated L929Ts cells, transfected with siRNAs specific for either mouse LONP1, PSA1 or PMPCA (siLONP1, siPSA1 and siPMPCA) or control siRNA (siNT) were performed to verify the efficiency of the siRNA knockdown. (B) In parallel, flow cytometric analyses were performed. After 48 h, cells were left untreated or stimulated with 20 μ M zVAD-fmk (prestimulated for 30 min) and 100 ng/ml TNF for 5 h to induce necroptosis. (C) Control Western blots of untreated HT-29 cells, transfected with siRNAs specific for either human LONP1, PSA1 or PMPCA (siLONP1, siPSA1 and siPMPCA) or control siRNA (siNT) were performed to verify the efficiency of the siRNA knockdown. Detection of actin served as a loading control. (D) In parallel, flow cytometric analyses were performed. After 48 h, cells were left untreated or stimulated with 20 μ M zVAD-fmk, 5 μ g/ml CHX (both prestimulated for 30 min) and 100 ng/ml TNF for 24 h to induce necroptosis. Representative data from one out of three experiments are shown and error bars indicate SD from three measurements.

4.2.3 Analyses of moesin and stathmin as potential downstream mediators of HtrA2/Omi during necroptosis

Moesin and stathmin have been identified within a proteomic screen for cellular proteins cleaved during necroptosis performed by Susann Voigt. Both proteins were further investigated via Western blot analyses within this thesis. Moesin and stathmin both have been described to be correlated with metastasis and poor prognosis, when overexpressed in tumors. Under physiological conditions, these proteins are involved in the regulation of cell division, cell growth, cell adhesion and cellular morphology (Barros *et al.* 2018, Yan *et al.* 2018).

HtrA2/Omi wild type MEF were compared with HtrA2/Omi-deficient MEF by Western blot. As shown in figure 28, there was no difference for the signal of moesin between the two cell lines. In contrast, the signal for stathmin was less pronounced under necroptotic conditions in HtrA2/Omi wild type MEF (Figure 30), suggesting that stathmin is cleaved by HtrA2/Omi

during necroptosis. However, to finally elucidate if the observed difference between the two cell lines is due to a lack of cleavage by HtrA2/Omi or indirectly caused by the necroptosis resistance of HtrA2/Omi-deficient cells, further experiments will be needed.

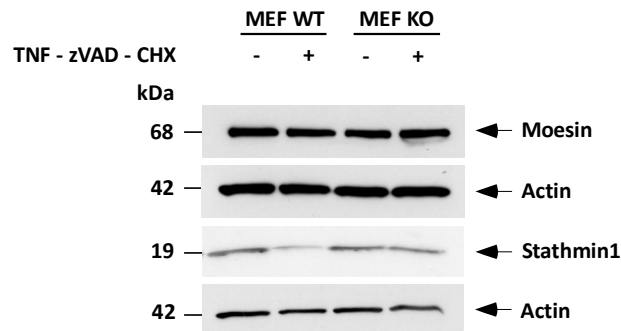


Figure 30: Western blot analyses of moesin and stathmin as downstream mediators of HtrA2/Omi during necroptosis. HtrA2/Omi wild type MEF and HtrA2/Omi-deficient MEF were left untreated or stimulated with 20 μ M zVAD-fmk, 1 μ g/ml CHX (both prestimulated for 30 min) and 100 ng/ml TNF for 16 h to induce necroptosis. Western blot analyses were performed of whole cell lysates. The blots were incubated with antibodies detecting moesin (68 kDa) and stathmin (19 kDa). Arrows indicate the position of the analyzed proteins. Detection of actin served as a loading control.

4.2.4 Analyses of Inhibitor of apoptosis proteins cIAP1 and XIAP as potential downstream mediators of HtrA2/Omi during necroptosis

For apoptosis, it is common knowledge that HtrA2/Omi is released from mitochondria, binding to and deactivating IAPs (van Loo *et al.* 2002, Srinivasula *et al.* 2003, Yang *et al.* 2003, Vande Walle *et al.* 2010).

Therefore, two different IAPs, cIAP1 and XIAP, were investigated as potential downstream mediators of HtrA2/Omi during necroptosis by Western blot analysis. Under necroptotic conditions induced by TNF, zVAD and CHX, HtrA2/Omi wild type MEF showed a signal for a cleavage band of XIAP after 16 hours (Figure 31). This signal for the cleavage band of XIAP was even more pronounced and appeared faster when the cells were additionally treated with birinapant (Figure 31). Birinapant is a Smac mimetic, binding to IAPs and leading to degradation of cIAP1 and cIAP2 and to inhibition of XIAP, which then leads to activation of downstream caspases during apoptosis (Benetatos *et al.* 2014, Brands *et al.* 2017). In HtrA2/Omi-deficient MEF, the signal for the cleavage band of XIAP was completely absent (Figure 31), suggesting that XIAP is cleaved by HtrA2/Omi during necroptosis.

4. Results

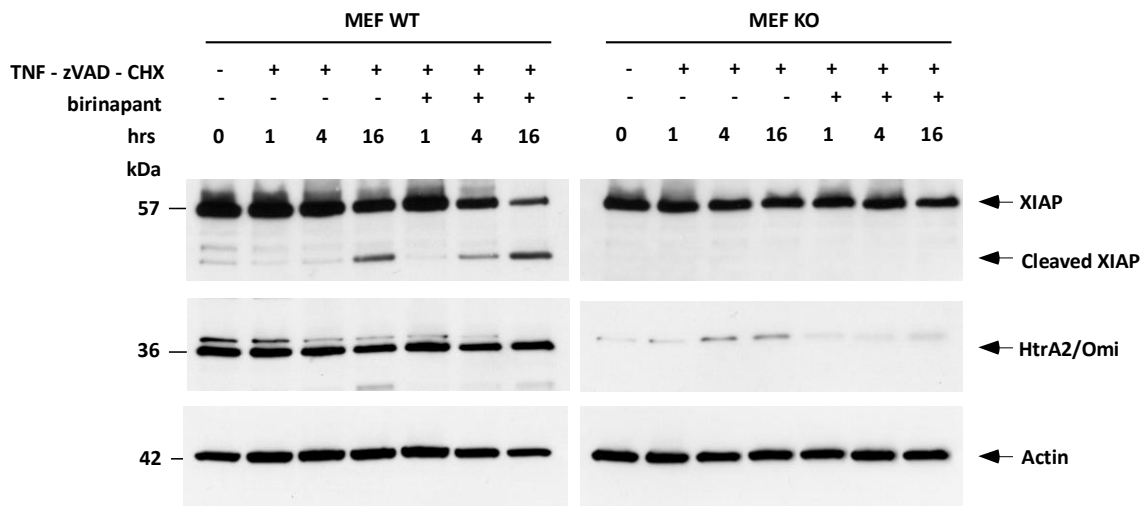


Figure 31: Western blot analyses of XIAP as a downstream mediator of HtrA2/Omi during necroptosis. HtrA2/Omi wild type MEF and HtrA2/Omi-deficient MEF were left untreated or stimulated with 20 μ M zVAD-fmk, 1 μ g/ml CHX (both prestimulated for 30 min) and 100 ng/ml TNF over a time course from 1 to 16 h to induce necroptosis. In parallel, cells were additionally treated with 1 μ M birinapant (prestimulated for 30min). Western blot analyses were performed of whole cell lysates. The blots were incubated with antibodies detecting XIAP (57 kDa) and HtrA2/Omi (36 kDa). Arrows indicate the position of the analyzed proteins. Detection of actin served as a loading control.

A similar experiment was performed for cIAP1. Since cIAP1 is degraded by birinapant, the signal for cIAP1 was completely absent in all three cell lines when the cells were additionally treated with birinapant (Figure 32). Surprisingly, in HtrA2/Omi-deficient cells the signal for cIAP1 was less pronounced under necroptotic conditions in comparison to wild type counterparts and HtrA2/Omi-deficient cells reconstituted with HtrA2/Omi (Figure 32). Since inhibition of IAPs leads to increased cell death, but the HtrA2/Omi-deficient cells were protected against necroptosis, a stronger signal for cIAP1 in HtrA2/Omi-deficient cells would have been expected. In conclusion, HtrA2/Omi seems to influence the amount of cIAP1 present during necroptosis, but further experiments will be needed to conclusively address this point.

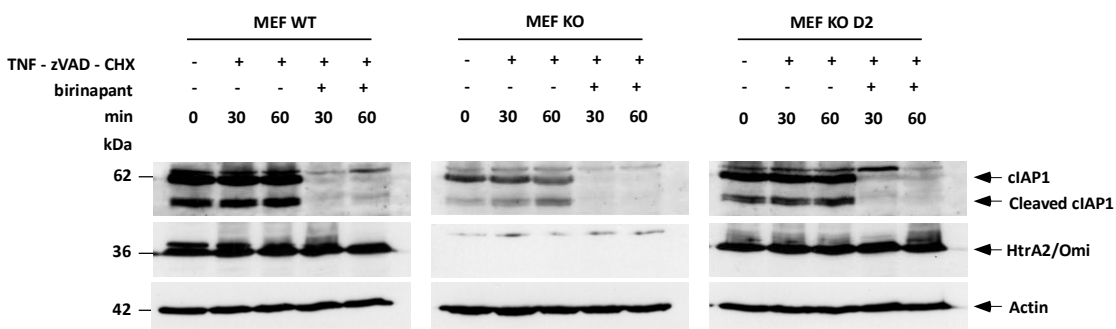


Figure 32: Western blot analyses of cIAP1 as downstream mediator of HtrA2/Omi during necroptosis. HtrA2/Omi wild type MEF, HtrA2/Omi-deficient MEF and HtrA2/Omi-deficient MEF reconstituted with HtrA2/Omi (D2) were left untreated or stimulated with 20 μ M zVAD-fmk, 1 μ g/ml CHX (both prestimulated for 30 min) and 100 ng/ml TNF for 30 and 60 min to induce necroptosis. In parallel, cells were additionally treated with 1 μ M birinapant. Western blot analyses were performed of whole cell lysates. The blots were incubated with antibodies detecting cIAP1 (62 kDa) and HtrA2/Omi (36 kDa). Arrows indicate the position of the analyzed proteins. Detection of actin served as a loading control.

Since dysregulation of IAPs has been associated to various cancers, tumor cell survival and chemo-resistance, IAPs have been used as anticancer drug targets. Consequently, Smac mimetics were utilized as pharmacological inhibitors of IAPs in clinical trials for cancer treatment (Silke and Meier 2013).

Here in this context, the Smac mimetic birinapant was used in combination with TNF and zVAD (and CHX) to induce necroptosis and to clarify if the use of Smac mimetics can override the protection from necroptosis caused by the deletion of the protease HtrA2/Omi. First, L929Ts wild type cells were compared to the L929Ts HtrA2/Omi $-/-$ clone C2 and HtrA2/Omi-deficient cells reconstituted with HtrA2/Omi (E12). When the cells were treated with TNF and zVAD alone, the HtrA2/Omi-deficient cells were completely protected from necroptosis, as expected, whereas wild type cells and reconstituted cells showed a similar sensitivity (Figure 33A). When the cells were additionally treated with the Smac mimetic birinapant, the HtrA2/Omi-deficient cells showed increased cell death in comparison to the treatment with TNF and zVAD alone (Figure 33A), indicating that the effect caused by the deletion of HtrA2/Omi can be neutralized upon usage of birinapant. The same experiment was performed for HtrA2/Omi-deficient MEF, wild type counterparts and HtrA2/Omi-deficient MEF reconstituted with HtrA2/Omi (D2). Again, the HtrA2/Omi-deficient cells were protected against necroptosis, when the cells were treated with TNF, zVAD and CHX (Figure 33B). When the cells were additionally treated with birinapant, HtrA2/Omi-deficient cells showed indeed increased cell death, but in comparison to wild type cells the HtrA2/Omi-deficient cells still showed a slight protection against necroptosis (Figure 33B).

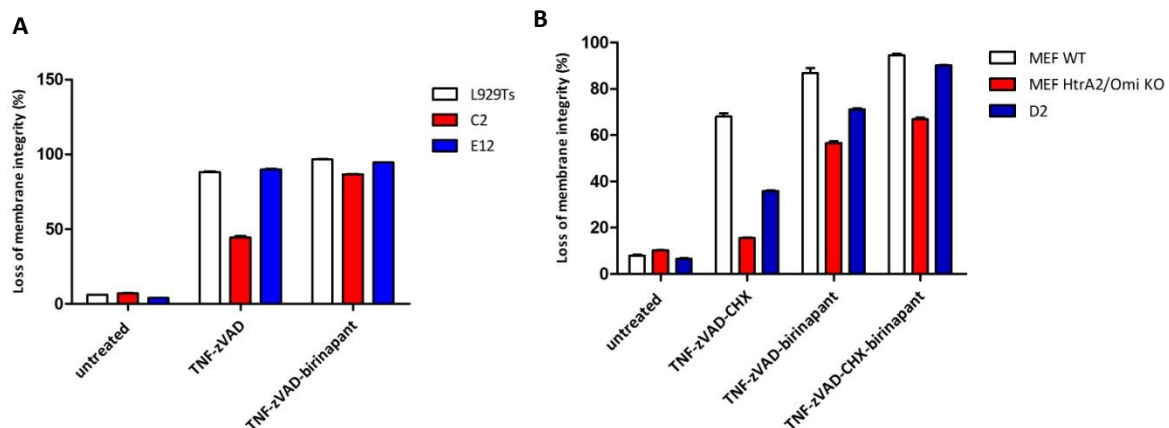


Figure 33: The Smac mimetic birinapant overcomes the protection from necroptosis caused by the deletion of HtrA2/Omi. (A) Flow cytometric analyses of HtrA2/Omi-deficient L929Ts cells (C2), HtrA2/Omi-deficient L929Ts cells reconstituted with HtrA2/Omi (E12) and L929Ts wild type cells were performed. Cells were left untreated or stimulated with 20 μ M zVAD-fmk (prestimulated for 30 min) and 100 ng/ml TNF for 5 h to induce necroptosis. In parallel, cells were additionally treated with 1 μ M birinapant to induce necroptosis. **(B)** Parallel analyses of HtrA2/Omi-deficient MEF, HtrA2/Omi-deficient MEF reconstituted with HtrA2/Omi (D2) and HtrA2/Omi wild type MEF. Cells were left untreated or stimulated with 20 μ M zVAD-fmk, 5 μ g/ml CHX (both prestimulated for 30 min) and 100 ng/ml TNF for 16 h to induce necroptosis. In parallel, cells were additionally treated with 1 μ M birinapant to induce necroptosis. Representative data from one out of three experiments are shown and error bars indicate SD from three measurements.

Altogether, these results lead to the assumption that inhibitor of apoptosis proteins are downstream mediators of HtrA2/Omi during necroptosis.

4.2.5 Identification of new potential substrates of HtrA2/Omi by mass spectrometric analysis

In contrast to apoptosis, it is described that HtrA2/Omi is not released from mitochondria during TNF-induced necroptosis (van Loo *et al.* 2002, Blink *et al.* 2004). Therefore, new potential substrates of HtrA2/Omi were identified in this thesis from mitochondrial fractions of necroptotic wild type and HtrA2/Omi-deficient MEF by mass spectrometric analysis in collaboration with the group of Prof Dr. Andreas Tholey (Institute for Experimental Medicine, Kiel). Table 3 shows a list of candidates that have been identified within the mass spectrometric analysis. Since the group of Prof. Dr. Andreas Tholey postulated that the dendritic polyglycerol aldehyde polymer used for the enrichment had production issues, a repetition of this experiment in the future is highly recommended.

Table 3: List of potential substrates of HtrA2/Omi during necroptosis which were identified by mass spectrometric analysis

Identified proteins	Accession number
FAU , ribosomal protein S30	P62861
ATP5A1 , ATP synthase subunit alpha	P25705-1
RPL9 , ribosomal protein L9	P32969
MTCH2 , mitochondrial carrier homolog 2	Q9Y6C9
EZR , Ezrin	P15311
EIF5A , eukaryotic translation initiation factor 5A-1	P63241-2
TAGLN2 , Transgelin-2	P37802-2
YBX3 , Y-box-binding protein 3	P16989-1
CRAT , Carnitine O-acetyltransferase	P43155
GATAD2B , transcriptional repressor p66-beta	Q8WXI9
CDC42BPB , serine/threonine-protein kinase MRCK beta	Q9Y5S2
RPS3A , ribosomal protein S3A	P61247
MYH9 , Myosin-9; MYH10, Myosin-10	P35579-1; P35580-4
RD3L , protein RD3-like	P0DJH9
HIST1H2BL , Histone H2B type 1-L	Q99880
EIF3CL , eukaryotic translation initiation factor 3 subunit C-like protein	B5ME19
PDLIM5 , PDZ and LIM domain protein5	Q96HC4-6

4.2.6 Conclusion

To conclude, the results indicate that some of the potential analyzed proteins like moesin, PSA1, LONP1 and PMPCA are unlikely downstream mediators of HtrA2/Omi during necroptosis, since siRNA knockdown of these proteins had no effect on cell death. For other proteins like VPS4B, DBC1, PDXDC1 and stathmin, Western blot analyses have been promising, but further analyses will be needed to draw a final conclusion, since again siRNA knockdown of these proteins had no effect on cell death. For all siRNA knockdown experiments the efficiency was very weak, recommending a repetition of these experiments with different siRNAs.

Since the effect caused by the deletion of HtrA2/Omi can be neutralized by usage of the Smac mimetic birinapant, it is likely that IAPs are downstream mediators of HtrA2/Omi. Western blot analyses of XIAP show that XIAP is cleaved by HtrA2/Omi during necroptosis, supporting the assumption that IAPs are substrates of HtrA2/Omi during necroptosis. Western blot analyses of cIAP1 have shown that HtrA2/Omi has an effect on the amount of cIAP1 present during necroptosis, but further experiments will be needed, since the results are inconsistent, which might have been due to problems with the antibody against cIAP1 in mouse cells.

5. Discussion

5.1 Necroptosis is differentially regulated by caspase-8 in mice and in humans

Since necroptosis is associated to various diseases, a precise knowledge of the necroptotic signaling pathway is crucial for the development of new therapeutic strategies. It is generally accepted that inhibition or genetic ablation of caspase-8 encourages death receptor-induced necroptosis (Feltham *et al.* 2017). This is highlighted by the fact that embryonic lethality of caspase-8 knockout mice is rescued by co-deletion of the necroptotic core proteins RIPK3 or MLKL (Kaiser *et al.* 2011, Alvarez-Diaz *et al.* 2016).

The critical role of caspase-8 in suppressing necroptosis is also confirmed by the results obtained in the presented dissertation, which demonstrate that the absence of caspase-8 in murine L929Ts cells promotes TNF-induced necroptosis. This finding is in line with a previous study by Oberst and colleagues, where it was also shown that knockdown of caspase-8 in murine L929 cells causes TNF-induced necroptosis (Oberst *et al.* 2011). In contrast, the data obtained during this thesis in human U-937 cells showed that genetic ablation of caspase-8 protected the cells from TNF-induced necroptosis instead of promoting cell death. This observation was confirmed in a second human cell line, in HT-29 cells. The results obtained in the presented dissertation showed that all HT-29 caspase-8 *-/-* cell clones generated by CRISPR/Cas9 technology were protected from TNF-induced necroptosis. Notably, this protection was obliterated when cells were additionally treated with the Smac mimetic birinapant, which is in line with a study of Tanzer and co-workers where they also used Smac mimetics to induce cell death, showing that three out of five HT-29 caspase-8 *-/-* cell clones generated by employing the CRISPR/Cas9 system were still sensitive to IFN γ -induced cell death (Tanzer *et al.* 2017).

Within the above mentioned study by Oberst and colleagues, it was demonstrated that the enzymatic activity of caspase-8 is required for the inhibition of TNF-induced necroptosis (Oberst *et al.* 2011). This was confirmed in this dissertation by the results of the experiments to reconstitute CRISPR/Cas knockout cells. When human and murine CRISPR/Cas caspase-8 *-/-* clones were reconstituted with enzymatically active and inactive caspase-8, only reconstitution with proteolytically active caspase-8 showed an effect on cell death. Therefore, caspase-8 enzymatic activity seems to be crucial for necroptosis induction in human cells as well as for the inhibition of TNF-induced necroptosis in murine cells. A scaffolding function of caspase-8 within the necroptotic signaling pathway seems to be unlikely.

Immunoprecipitations with caspase-8 in human HT-29 and U-937 cells performed within the presented dissertation showed that caspase-10 is recruited to the necrosome during TNF-induced necroptosis. Further results concerning necrosome analyses by immunoprecipitation obtained in this study revealed that core components of the necrosome do not associate during TNF-induced necroptosis when caspase-8 is deleted,

implying that the necrosome assembly is dependent on caspase-8 and that caspase-8 is essential for the initial recruitment of complex IIb proteins. This was also shown for apoptosis, in a study by Horn and colleagues, where caspase-8-deficient HeLa cells generated by employing the CRISPR/Cas system were fully protected from CD95L-induced death (Horn *et al.* 2017). Within this study, it was also demonstrated that only reconstitution with enzymatically active caspase-8 was able to restore sensitivity to CD95L-induced death. Furthermore, it was demonstrated that caspase-8 has a scaffolding function for DISC formation and recruitment of caspase-10. This is again in line with results of necrosome analyses by immunoprecipitation of the thesis presented here showing that deletion of caspase-8 in U-937 cells prevented the recruitment of caspase-10.

The results of experiments regarding the reconstitution of enzymatically active and inactive caspase-8 obtained within this study revealed that there is a difference between mouse and human caspase-8, since reconstitution of human caspase-8-deficient HT-29 cells with active human caspase-8 induced cell death, whereas reconstitution of these cells with active mouse caspase-8 reduced cell death. Until now, no differences between human and mouse caspase-8 have been reported regarding substrate specificity, but there is evidence that functional differences might emerge due to different post-translational modifications (Sakamaki *et al.* 2015). For example, in a previous study by Cursi and colleagues, it was demonstrated that human caspase-8 can be phosphorylated by the tyrosine kinase Src, causing the inhibition of apoptosis, which is not the case for mouse caspase-8 (Cursi *et al.* 2006). Another indication for a difference between human and mouse caspase-8 is the diverging phenotype (embryonic lethality in mice (Oberst *et al.* 2011) vs. immunodeficiency in humans (Chun *et al.* 2002)) in terms of functional mutations of caspase-8 in mice and in humans (Chun *et al.* 2002, Oberst *et al.* 2011).

5.2 Caspase-10 in humans cannot substitute the function that is held by caspase-8 in mice

As described above, in contrast to caspase-8, the impact of caspase-10 on necroptosis remains unknown. Mutations in caspase-10 are linked to autoimmune lymphoproliferative syndrome (ALPS) (Worth *et al.* 2006), and both caspases-8 and -10 are essential for normal human development.

The data obtained in the presented dissertation demonstrated that genetic ablation of caspase-10 in human HT-29 and U-937 cells promoted TNF-induced necroptosis, thus suggesting that caspase-10 has an inhibitory function for TNF-induced necroptosis. Since this is the effect that is described for genetic loss of caspase-8 in murine cells (Oberst *et al.* 2011), and since caspase-10 only exists in mammals but not in rodents (Salvesen and Walsh 2014), it can be assumed that caspase-10 in humans may substitute the function that is held by caspase-8 in mice. The fact that mutations affecting the function of caspase-8 in mice result in embryonic lethality (Sakamaki *et al.* 2002, Oberst *et al.* 2011), whereas humans with mutant caspase-8 only show a defect in activating lymphocytes resulting in

immunodeficiency (Chun *et al.* 2002), also leads to the assumption that caspase-10 can to some extent compensate caspase-8 in humans. An inhibiting function of caspase-10 on different forms of cell death was previously described. A study of Lamy and colleagues has demonstrated that caspase-10 inhibits autophagic cell death in myeloma cells (Lamy *et al.* 2013) while Horn and colleagues demonstrated that a caspase-10 knockdown enhanced CD95L-induced cell death (Horn *et al.* 2017).

In the literature, it is controversially discussed whether caspase-10 is able to substitute for the function of caspase-8 in death receptor signaling. In previous studies of Wang and colleagues and Kischkel and colleagues, it was shown that caspase-10 can promote ligand-induced apoptosis independently of caspase-8 (Kischkel *et al.* 2001, Wang *et al.* 2001). These results were confirmed by a study of Milhas and colleagues showing induction of apoptosis in caspase-8-deficient Jurkat cells and parallel activation of caspase-10, suggesting that caspase-10 can act as an initiator caspase in Fas signaling leading to apoptosis (Milhas *et al.* 2005). A study by Lafont and colleagues showed that FasL-induced cell death was blocked in cells double-deficient for caspase-8 and -10, but not in cells deficient only for caspase-8, indicating that caspase-10 is involved in FasL-induced death (Lafont *et al.* 2010). In contrast, the results of the siRNA knockdown experiments in caspase-8-deficient CRISPR/Cas cell clones obtained in the study presented here revealed that caspase-10 was not able to override the effect that was caused by the deletion of caspase-8 within the necroptotic signaling pathway, suggesting that, with regard to necroptosis, caspase-10 in humans cannot substitute the function that is held by caspase-8 in mice. This is in line with a previous study by Sprick and colleagues showing that caspase-10 cannot substitute the function of caspase-8 within the apoptotic signaling pathway (Sprick *et al.* 2002).

In the above mentioned study by Horn and colleagues, the authors demonstrated that caspase-10 acts as a negative regulator for caspase-8-mediated cell death (Horn *et al.* 2017). Within this study it was shown that knockdown of caspase-10 enhanced CD95L-induced cell death and that caspase-10 prevents DISC-mediated caspase-8 activation. Since a combined knockdown of caspase-10 and c-FLIP further increased sensitization to CD95L (Horn *et al.* 2017), it was proposed that caspase-10 might, similar to c-FLIP, act as a second and independent inhibitor of caspase-8. Possibly, this might also be the case for TNF-induced necroptosis. c-FLIP is a key regulator of caspase-8 activity, thus determining signaling outcome in terms of cell survival or several forms of cell death (Hughes *et al.* 2016, Dillon *et al.* 2012, Oberst *et al.* 2011). Two main isoforms of c-FLIP have been described, namely c-FLIP_S and c-FLIP_L (Hughes *et al.* 2016). Hughes and colleagues demonstrated that c-FLIP_S functions exclusively as an inhibitor of caspase-8 by inhibiting caspase-8 oligomerization and pro-caspase-8 activation, thereby inhibiting apoptosis and promoting necroptosis. On the contrary, in case of c-FLIP_L, the c-FLIP_L-pro-caspase-8 ratio determines signaling outcome. Low levels of c-FLIP_L cause pro-caspase-8 activation while high levels of c-FLIP_L inhibit pro-caspase-8 activation (Hughes *et al.* 2017). In the end, both ways of regulating caspase-8 and inhibiting cell death may be possible for caspase-10 as well. Caspase-10 may also either disrupt caspase-8 oligomerization or form inactive heterodimers with caspase-8 thereby

inhibiting necroptosis. It has been reported that caspase-10, like caspase-8, also forms heterodimers with c-FLIP (Raam and Salvesen 2012) and that the caspases-10 and -8 form inactive heterodimers as well (Humphreys *et al.* 2018), highlighting the possibility of caspase-10 being a regulator of caspase-8. The results of analyses of the necrosome formation by immunoprecipitation obtained during this thesis, revealed that caspase-8 and caspase-10 associate during TNF-induced necroptosis. Noteworthy, caspases-8 and -10 and c-FLIP are located at the same gene locus (Fischer *et al.* 2006) and co-regulated genes tend to be clustered in the same genetic neighborhood (Michalak 2008). Similar to c-FLIP, it has been reported that caspase-10 is overexpressed in tumor tissues (Qian *et al.* 2018). Within the study by Qian and colleagues it was demonstrated that caspase-10 is overexpressed in tumor tissues of clear cell renal cell carcinoma (ccRCC), suggesting that caspase-10 might be involved in the pathogenesis of ccRCC (Qian *et al.* 2018). Moreover, it has been described that loss of caspase-10 in cancer cells promotes a more effective mode of apoptosis upon usage of chemotherapeutic drugs and might therefore enhance effectiveness of cancer therapy (Mohr *et al.* 2018). All data concerning caspase-10 obtained within this thesis, hint to the possibility of using caspase-10 as a therapeutic target.

Furthermore, data obtained within this thesis demonstrated that the enzymatic activity of caspase-10 is essential for the inhibitory function of caspase-10 within the necroptotic signaling pathway. HT-29 CRISPR/Cas caspase-10 *-/-* clones reconstituted with enzymatically active and inactive caspase-10, only showed an effect on cell death when reconstituted with active caspase-10.

5.3 Identification of downstream mediators of the serine protease HtrA2/Omi

The serine protease HtrA2/Omi is located in the mitochondrial intermembrane space and enzymatically inactive mutations of HtrA2/Omi are related to neurodegenerative disorders such as Parkinson's disease and Alzheimer's disease (Jones *et al.* 2003, Martins *et al.* 2004, Strauss *et al.* 2005, Westerlund *et al.* 2011). It has been described that, during apoptosis, HtrA2/Omi is released from the mitochondria into the cytosol, where it interacts with IAPs via N-terminal IAP-binding motifs and inactivates IAPs, leading to activation of caspases and the induction of apoptosis (Suzuki *et al.* 2001, Hedge *et al.* 2002, Martins *et al.* 2002, van Loo *et al.* 2002, Verhagen *et al.* 2002, Verhagen *et al.* 2007). In previous studies by Srinivasula and colleagues and Yang and colleagues, it was shown that HtrA2/Omi promotes proteolytic degradation of bound IAPs (Srinivasula *et al.* 2003, Yang *et al.* 2003). In addition, previous studies have reported that HtrA2/Omi mediates caspase-independent cell death through its own serine protease activity (Suzuki *et al.* 2001, Hedge *et al.* 2002, Blink *et al.* 2004). In 2013, the serine protease HtrA2/Omi was identified as key mediator regulating TNF-induced necroptosis (Sosna *et al.* 2013), but the underlying mechanism through which HtrA2/Omi regulates necroptosis is still unknown.

Within the presented dissertation, several potential downstream mediators of HtrA2/Omi during TNF-induced necroptosis were therefore analyzed by Western blot and siRNA

knockdown experiments. The results obtained in this study demonstrated that LONP1, PSA1 and PMPCA do not seem to be substrates of HtrA2/Omi, since downregulation of these proteins had no effect on cell death. However, as knockdown efficiency was very weak, further experiments will be needed to draw a final conclusion. For DBC1, PDXDC1, VPS4B and stathmin1, the results of Western blot experiments performed within this thesis showed at least for MEF that the deletion of HtrA2/Omi influences the cleavage of these proteins. Since subsequent siRNA knockdown experiments showed that the downregulation of DBC1, PDXDC1 and VPS4B had no effect on cell death, they do not seem to be downstream mediators of HtrA2/Omi. Again, knockdown efficiency was very weak and further experiments will be needed. Since a previous study by Sundararajan and colleagues demonstrated that DBC1 promotes mitochondrial clustering, matrix condensation and TNF-mediated apoptosis (Sundararajan *et al.* 2005), this protein represents a promising candidate as substrate of HtrA2/Omi which is why it will be highly interesting to perform further analyses. The same applies to the mitochondrial protease LONP1, for which it has also been described that its stability is influenced by HtrA2/Omi and that HtrA2/Omi therefore might be an upstream regulator in maintaining mitochondrial homeostasis (Goo *et al.* 2014). Western blot analyses of moesin showed that there are no differences in protein expression between HtrA2/Omi wild type MEF and HtrA2/Omi-deficient MEF under necroptotic conditions, leading to the assumption that moesin can be excluded as substrate of HtrA2/Omi during TNF-induced necroptosis.

Within his PhD thesis in the group of Prof. Dr. Dieter Adam, Johaiber I. Fuchslocher Chico showed that HtrA2/Omi seems to be linked to necroptosis upstream of RIPK3 and MLKL. A previous study of Vande Walle and colleagues demonstrated that HtrA2/Omi cleaves RIPK1 during apoptosis in mice, but not in humans, and that HtrA2/Omi-generated RIPK1 cleavage fragments were not able to activate NF- κ B, thus increasing apoptosis (Vande Walle *et al.* 2010). This might also be one possibility how HtrA2/Omi regulates TNF-induced necroptosis.

As mentioned above, HtrA2/Omi has been described to regulate apoptosis through inactivation of IAPs (Suzuki *et al.* 2001, Hedge *et al.* 2002, Martins *et al.* 2002, van Loo *et al.* 2002, Verhagen *et al.* 2002, Verhagen *et al.* 2007). This represents another possibility how HtrA2/Omi regulates TNF-induced necroptosis.

Western blot analyses regarding IAPs performed within this thesis showed the most promising results. There were differences in the protein expression of cIAP1 between HtrA2/Omi wild type MEF and HtrA2/Omi-deficient MEF under necroptotic conditions, but it is hard to explain why the signal for cIAP1 was less pronounced in HtrA2/Omi-deficient cells, since these cells were protected from TNF-induced necroptosis and therefore the signal for cIAP1 should have been more pronounced in comparison to wild type counterparts. Recently, a study by Annibaldi and colleagues demonstrated that cIAP1-mediated ubiquitylation inhibits RIPK1 kinase auto-activation and targets it for proteasomal degradation (Annibaldi *et al.* 2018). As a consequence, lower amounts of cIAP1 would lead to accumulation of active RIPK1 and induction of cell death in response to TNF. Another

study by Dondelinger and colleagues demonstrated that the depletion of cIAP1/2 promoted TNF-induced necroptosis upon inhibition of caspase activity (Dondelinger *et al.* 2013). Both studies are inconsistent with the results obtained in the study here, where lower amounts of cIAP1 in HtrA2/Omi-deficient cells correlated with protection from TNF-induced necroptosis. At present, it cannot be excluded that these inconsistencies are due to technical issues, i.e., specificity problems of the antibody against cIAP1 in mouse cells.

The results of Western blot analyses of XIAP were more conclusive, since it was shown in this study that XIAP was only cleaved in HtrA2/Omi wild type cells but not in HtrA2/Omi-deficient MEF under necroptotic conditions and that this effect was even more prominent when the Smac mimetic birinapant was added, indicating that XIAP is a substrate of HtrA2/Omi during TNF-induced necroptosis. This is in line with former studies showing that HtrA2/Omi binds to XIAP during apoptosis (Suzuki *et al.* 2001, Martins *et al.* 2002, van Loo *et al.* 2002). Besides, a former study by Wicki and colleagues demonstrated that loss of XIAP promoted TNF-induced cell death and that it facilitated the switch to TNF-induced necroptosis in mouse neutrophils (Wicki *et al.* 2016). Additionally, results of flow cytometric analyses obtained in this study revealed that the protection of HtrA2/Omi-deficient cells against TNF-induced necroptosis could be neutralized upon usage of the Smac mimetic birinapant indicating once more that HtrA2/Omi may mediate TNF-induced necroptosis by proteolytic cleavage of IAPs. If HtrA2/Omi promotes cell death by inactivating IAPs, this would presume that HtrA2/Omi-deficient cells are resistant against apoptosis and necroptosis, since the inactivation of IAPs promotes cell death via both, apoptosis or necroptosis. Within the presented dissertation, it was demonstrated that HtrA2/Omi-deficient cells were protected from necroptosis. Two former studies additionally demonstrated that the downregulation of HtrA2/Omi via siRNA caused significant reduction of apoptosis in U2OS cells (Martins *et al.* 2002) and staurosporine-induced cell death in HeLa cells (Kuninaka *et al.* 2005), suggesting once more that IAPs are substrates of the serine protease HtrA2/Omi.

Within the presented dissertation, several potential substrates of HtrA2/Omi were identified by mass spectrometry from mitochondrial fractions of necroptotic wild type and HtrA2/Omi-deficient MEF (see Table 3). The experiment has to be repeated in the future due to production issues of employed material which may compromise the obtained results. Nevertheless, one of the proteins listed in Table 3, named mitochondrial carrier homologue 2 (MTCH2), might be a promising candidate. In a study by Zaltsman and colleagues, it was demonstrated that MTCH2 facilitates tBID recruitment to mitochondria (Zaltsman *et al.* 2010). In addition, a former study of van Loo and colleagues showed that tBID is essential for the release of HtrA2/Omi from mitochondria (van Loo *et al.* 2002). Combining both findings, MTCH2 might be a potential downstream mediator of HtrA2/Omi during TNF-induced necroptosis, promoting the release of HtrA2/Omi from mitochondria.

5.4 Biological relevance of the obtained results of this thesis and future perspectives

As described above, necroptosis has been associated to the pathogenesis of various human diseases like inflammatory bowel disease (Pierdomenico *et al.* 2014), Gaucher's disease (Vitner *et al.* 2014), sepsis (Linkermann *et al.* 2012) or cancer (He *et al.* 2013, Seifert *et al.* 2016). There exist different approaches to cancer treatment and classical cancer therapies include surgery, radiation and chemotherapy (Urruticoechea *et al.* 2010). To date, the common adjuvant strategy for cancer treatment of patients is the induction of tumor cell apoptosis by chemotherapeutic drugs like cisplatin or 5-fluorouracil (Dasari and Tchounwou 2014, Holohan *et al.* 2013, Gaijar *et al.* 2018). Since many cancer cells have primary or acquired resistance to apoptosis, available cancer therapies are currently limited in their effectiveness (Holohan *et al.* 2013). Various cancer cell lines are reported to have the components of the necroptotic cell death machinery and thus are able to undergo necroptosis (Su *et al.* 2016). Therefore, necroptosis has become a promising alternative as a target for cancer therapy. A study of Han and colleagues demonstrated that necroptosis was induced by shikonin in breast cancer cells that were resistant to proapoptotic drugs (Han *et al.* 2007). Moreover, a study by Metzigg and colleagues showed that colorectal cancer cells being resistant to the proapoptotic drug 5-fluorouracil underwent necroptosis upon treatment of pancaspase inhibitors (Metzigg *et al.* 2016). Several other studies also reported cases where necroptosis was triggered to kill cancer cells resistant to proapoptotic cancer therapy (Bonapace *et al.* 2010, Laukens *et al.* 2011, McCabe *et al.* 2014). Necroptosis is not only a promising approach to eliminate cancer cells but it has recently also been described that at least in mouse models the survival in neonatal sepsis is increased and that lung injuries are decreased when necroptosis is inhibited (Bolognese *et al.* 2018). Besides, it has been reported that targeting necroptosis might be an attractive therapeutic strategy to reduce plaque formation and the development of atherosclerosis (Coornaert *et al.* 2018). Therefore, it is essential to gain further insight into the necroptotic signaling pathway. The results obtained within this thesis regarding caspase-8 have revealed that there are differences between mouse and human caspase-8 and that the deletion or downregulation of caspase-8 protects human cells from TNF-induced necroptosis instead of enhancing cell death. This might be decisive regarding the use of caspase-8 as a target to trigger necroptosis in cancer cells. Moreover, the findings of the presented dissertation indicate that caspase-10 either partially substitutes the function of caspase-8 or acts as a regulator of caspase-8. Therefore, caspase-10 might be a new, promising target for cancer therapy. In general, findings of the presented dissertation regarding caspase-8 and -10 and the serine protease HtrA2/Omi provide new opportunities for more specific manipulation of necroptosis regarding the development of new therapeutic strategies.

6. References

- Aaes T.L, Kaczmarek A, Delvaeye T, De Craene B, De Koker S, Heyndrickx L, Delrue I, Taminau J, Wiernicki B, De Groote P, Garg A.D, Leybaert L, Grooten J, Bertrand M.J, Agostinis P, Berx G, Declercq W, Vandenabeele P, Krysko D.V** (2016) Vaccination with necroptotic cancer cells induces efficient anti-tumour immunity. *Cell Rep.* 15, 274-287.
- Afonso M.B, Rodrigues P.M, Carvalho T, Caridade M, Borralho P, Cortez-Pinto H, Castro R.E, Rodrigues C.M** (2015) Necroptosis is a key pathogenic event in human and experimental murine models of non-alcoholic steatohepatitis. *Clin. Sci. (Lond.)* 129, 721-739.
- Alvarez-Diaz S, Dillon C.P, Lalaoui N, Tanzer M.C, Rodriguez D.A, Lin A, Lebois M, Hakem R, Josefsson E.C, O'Reilly L.A, Silke J, Alexander W.S, Green D.R, Strasser A** (2016) The pseudokinase MLKL and the kinase RIPK3 have distinct roles in autoimmune disease caused by loss of death-receptor-induced apoptosis. *Immunity* 45, 513-526.
- Andrabi S.A, Dawson T.M, Dawson V.L** (2008) Mitochondrial and nuclear cross talk in cell death: parthanatos. *Ann. NY Acad. Sci.* 1147, 233-241.
- Annibaldi A, Meier P** (2018) Checkpoints in TNF-induced cell death: implications in inflammation and cancer. *Trends Mol. Med.* 24, 49-65.
- Annibaldi A, John S.W, Berghe T.V, Swatek K.N, Ruan J, Liccardi G, Bianchi K, Elliott P.R, Choi S.M, Coillie S, Bertin J, Wu H, Komander D, Vandenabeele P, Silke J, Meier P** (2018) Ubiquitin-mediated regulation of RIPK1 kinase activity independent of IKK and MK2. *Mol. Cell* 69, 566-580.
- Barros F.B.A, Assao A, Garcia N.G, Nonogaki S, Carvalho A.L, Soares F.A, Kowalski L.P, Oliveira D.T** (2018) Moesin expression by tumor cells is an unfavorable prognostic biomarker for oral cancer. *BMC Cancer* 18, 1-8.
- Benetatos C.A, Mitsuuchi Y, Burns J.M, Neiman E.M, Condon S.M, Yu G, Seipel M.E, Kapoor G.S, LaPorte M.G, Rippin S.R, Deng Y, Hendi M.S, Tirunahari P.K, Lee Y.H, Haimowitz T, Alexander M.D, Graham M.A, Weng D, Shi Y, McKinlay M.A, Chunduru S.K** (2014) Birinapant (TL32711), a bivalent SMAC mimetic, targets TRAF2-associated cIAPs, abrogates TNF-induced NF- κ B activation, and is active in patient-derived xenograft models. *Mol. Cancer Ther.* 13, 867-879.
- Blink E, Maianski N.A, Alnemri E.S, Zervos A.S, Roos D, Kuijpers T.W** (2004) Intramitochondrial serine protease activity of Omi/HtrA2 is required for caspase-independent cell death of human neutrophils. *Cell Death Differ.* 11, 937-939.
- Bolognese A.C, Yang W.L, Hansen L.W, Denning N.L, Nicastro J.M, Coppa G.F, Wang P** (2018) Inhibition of necroptosis attenuates lung injury and improves survival in neonatal sepsis. *Surgery* doi: 10.1016/j.surg.2018.02.017.
- Bonapace L, Bornhauser B.C, Schmitz M, Cario G, Ziegler U, Niggli F.K, Schäfer B.W, Schrappe M, Stanulla M, Bourquin J.P** (2010) Induction of autophagy-dependent necroptosis is required for childhood acute lymphoblastic leukemia cells to overcome glucocorticoid resistance. *J. Clin. Invest.* 120, 1310-1323.

- Brands R.C, Scheurer M.J.J, Hartmann S, Seher A, Kübler A.C, Müller-Richter U.D.A** (2017) Apoptosis-sensitizing activity of birinapant in head and neck squamous cell carcinoma cell lines. *Oncol. Letters* 15, 4010-4016.
- Brenner D, Blaser H, Mak T.W** (2015) Regulation of tumour necrosis factor signaling: live or let die. *Nature Reviews* 15, 362-374.
- Brinkman V, Reichard U, Goosmann C, Fauler B, Uhlemann Y, Weiss D.S, Weinrauch Y, Zychlinsky A** (2004) Neutrophil extracellular traps kill bacteria. *Science* 303, 1532-1535.
- Budd R.C, Wen-Chen Y, Tschopp J** (2006) cFLIP regulation of lymphocyte activation and development. *Nat. Rev. Immunol.* 6, 196-204.
- Cai Z, jitkaew S, Zhao J, Chiang H.C, Choksi S, Liu J, Ward Y, Wu L.G, Liu Z.G** (2014) Plasma membrane translocation of trimerized MLKL protein is required for TNF-induced necroptosis. *Nat. Cell Biol.* 16, 55-65.
- Chen W, Zhou Z, Li L, Zhong C.Q, Zheng X, Wu X, Zhang Y, Ma H, Huang D, Li W, Xia Z, Han J** (2013) Diverse sequence determinants control human and mouse receptor interacting protein 3 (RIPK3) and mixed lineage kinase domain-like (MLKL) interaction in necroptotic signaling. *J. Biol. Chem.* 288, 16247-16261.
- Chen X, Li W, Ren J, Huang D, He W, Song Y, Yang C, Li W, Zheng X, Chen P, Han J** (2014) Translocation of mixed lineage kinase domain-like protein to plasma membrane leads to necrotic cell death. *Cell Res.* 24, 105-121.
- Cho Y, Challa S, Moquin D, Genga R, Ray T.D, Guildford M, Chan F.K** (2009) Phosphorylation-driven assembly of RIP1-RIP3 complex regulates programmed necrosis and virus-induced inflammation. *Cell* 137, 1112-1123.
- Chun H.J, Zheng L, Ahmad M, Wang J, Speirs C.K, Siegel R.M, Dale J.K, Puck J, Davis J, Hall CG, Skoda-Smith S, Atkinson T.P, Straus S.E, Leonardo M.J** (2002) Pleiotropic defects in lymphocyte activation caused by caspase-8 mutations lead to human immunodeficiency. *Nature* 419, 395-399.
- Conrad M, Angeli J.P.F, Vandenabeele P, Stockwell B.R** (2016) Regulated necrosis: disease relevance and therapeutic opportunities. *Nat. Rev. Drug Discov.* 15, 348-366.
- Cookson B.T, Brennan M.A** (2001) Pro-inflammatory programmed cell death. *Trends Microbiol.* 9, 113-114.
- Coornaert I, Hofmans S, Devisscher L, Augustyns K, Van Der Veken P, De Meyer GRY, Martinet W** (2018) Novel drug discovery strategies for atherosclerosis that target necrosis and necroptosis. *Expert.Opin. Drug Discov.* 13, 477-488.
- Cursi S, Rufini A, Stagni V, Condò I, Matafora V, Bachi A, Bonifazi A.P, Coppola L, Superti-Furga G, Testi R, Barilà D** (2006) Src kinase phosphorylates caspase-8 on Tyr380: a novel mechanism of apoptosis suppression. *EMBO J.* 25, 1895-1905.
- Dasari S, Tchounwou P.B** (2014) Cisplatin and cancer therapy: molecular mechanisms of action. *Eur. J. Pharmacol.* 740, 364-378.

- Degterev A, Huang Z, Boyce M, Li Y, Jagtap P, Mizushima N, Cuny G.D, Mitchison T.J, Moskowitz M.A, Yuan J** (2005) Chemical inhibitor of nonapoptotic cell death with therapeutic potential for ischemic brain injury. *Nat. Chem. Biol.* 1, 112-119.
- Degterev A, Hitomi J, Gemscheid M, Ch'en I.L, Korkina O, Teng X, Abbott D, Cuny G.D, Yuan C, Wagner G** (2008) Identification of RIPK1 kinase as a specific cellular target of necrostatins. *Nat. Chem. Biol.* 4, 313-321.
- Dillon C.P, Oberst A, Weinlich R, Janke L.J, Kang T.B, Ben-Moshe T, Mark T.W, Wallach D, Green D.R** (2012) Survival function of the FADD-CASPASE-8-cFLIP_L complex. *Cell Rep.* 1, 401-407.
- Dixon S.J, Lemberg K.M, Lamprecht M.R, Skouta R, Zaitsev E.M, Gleason C.E, Patel D.N, Bauer A.J, Cantley A.M, Yang W.S, Morrison B 3rd, Stockwell B.R** (2012) Ferroptosis: an iron-dependent form of nonapoptotic cell death. *Cell* 149, 1060-1072.
- Dondelinger Y, Aguilera M.A, Goossens V, Dubuisson C, Grootjans S, Dejardin E, Vandenabeele P, Bertrand M.J.M** (2013) RIPK3 contributes to TNFR1-mediated RIPK1 kinase-dependent apoptosis in conditions of cIAP1/2 depletion or TAK1 kinase inhibition. *Cell Death Differ.* 20, 1381-1392.
- Dondelinger Y, Declercq W, Montessuit S, Roelandt R, Goncalves A, Bruggeman I, Hulpiau P, Weber K, Sehon C.A, Marquis R.W, Bertin J, Gough P.J, Savvides S, Martinou J.C, Bertrand M.J, Vandenabeele P** (2014) MLKL compromises plasma membrane integrity by binding to phosphatidylinositol phosphates. *Cell Rep.* 7, 971-981.
- Du C, Fang M, Li Y, Li L, Wang X** (2000) Smac, a mitochondrial protein that promotes cytochrome c-dependent caspase activation by eliminating IAP inhibition. *Cell* 102, 33-42.
- Egger L, Schneider J, Rheme C, Tapernoux M, Häcki J, Borner C** (2003) Serine proteases mediate apoptosis-like cell death and phagocytosis under caspase-inhibiting conditions. *Cell Death Differ.* 10, 1188-1203.
- Elmore S** (2007) Apoptosis: a review of programmed cell death. *Toxicol. Pathol.* 35, 495-516.
- Feltham R, Vince J.E, Lawlor K.E** (2017) Caspase-8: not so silently deadly. *Clin. Transl. Immunol.* 6, 1-13.
- Fischer U, Stroh C, Schulze-Osthoff K** (2006) Unique and overlapping substrate specificities of caspase-8 and caspase-10. *Oncogene* 25, 152-159.
- Fuchs Y, Steller H** (2015) Live to die another way: modes of programmed cell death and the signals emanating from dying cells. *Nat. Rev. Mol. Cell Biol.* 16, 329-344.
- Fuchslocher Chico J, Saggau C, Adam D** (2017) Proteolytic control of regulated necrosis. *Biochim. Biophys. Acta* 1864, 2147-2161.
- Fulda S, Vucic D** (2012) Targeting IAP proteins for therapeutic intervention in cancer. *Nat. Rev. Drug Disc.* 11, 109-124.

- Gaijar K.K, Vora H.H, Kobawala T.P, Trivedi T.I, Ghosh N.R** (2018) Deciphering the potential value of 5-flourouracil metabolic enzymes in predicting prognosis and treatment response of colorectal cancer patients. *Int. J. Biol. Markers* 33, 180-188.
- Galluzzi L, López-Soto A, Kumar S, Kroemer G** (2016) Caspases connect cell-death signaling to organismal homeostasis. *Immunity* 44, 221-231.
- Galluzzi L, Vitale I et al.** (2018) Molecular mechanisms of cell death: recommendations of the nomenclature committee on cell death 2018. *Cell Death Differ.*
- Goo H.G, Rhim H, Kang S** (2014) HtrA2/Omi influences the stability of LON protease 1 and prohibitin, proteins involved in mitochondrial homeostasis. *Exp. Cell Res.* 328, 456-465.
- Gray C.W, Ward R.V, Karran E, Turconi S, Rowles A, Viglienghi D, Southan C, Barton A, Fantom K.G, West A, Savopoulos J, Hassan N.J, Clinkenbeard H, Hanning C, Amegadzie B, Davis J.B, Dingwall C, Livi G.P, Creasy C.L** (2000) Characterization of human HtrA2, a novel serine protease involved in the mammalian cellular stress response. *Eur. J. Biochem.* 267, 5699-5710.
- Green D.R, Llambi F** (2015) Cell death signaling. *Cold Spring Harb. Perspect. Biol.* 7, 1-24.
- Grootjans S, VandenBerghe T, Vandenabeele P** (2017) Initiation and execution mechanisms of necroptosis: an overview. *Cell Death Differ.*, 1-12.
- Guo H, Omoto S, Harris P.A, Finger J.N, Bertin J, Gough P.J, Kaiser W.J, Mocarski E.S** (2015) Herpes simplex virus suppresses necroptosis in human cells. *Cell Host Microbe* 17, 243-251.
- Han W, Li L, Qui S, Lu Q, Pan Q, Gu Y, Luo J, Hu X** (2007) Shikonin circumvents cancer drug resistance by induction of a necroptotic death. *Mol. Cancer Ther.* 6, 1641-1649.
- He S, Wang L, Miao L, Wang T, Du F, Zhao L, Wang X** (2009) Receptor interacting protein kinase-3 determines cellular necrotic response to TNF- α . *Cell* 137, 1100-1111.
- He L, Peng K, Liu Y, Xiong J, Zhu F.F** (2013) Low expression of mixed lineage kinase domain-like protein is associated with poor prognosis in ovarian cancer patients. *Onco.Targets Ther.* 6, 1539-1543.
- He G, Günther C, Thonn V, Yu Y, Martini E, Buchen B, Neurath M.F, Stürzl M, Becker C** (2017) Regression of apoptosis-resistant tumors by induction of necroptosis in mice. *J. Exp. Med.*, 1-8.
- Hedge R, Srinivasula S.M, Zhang Z, Wassell R, Mukattash R, Cilenti L, Dubois G, Lazebnik Y, Zervos A.S, Fernandes-Alnemri T, Alnemri E.S** (2002) Identification of Omi/HtrA2 as a mitochondrial apoptotic serine protease that disrupts inhibitor of apoptosis protein-caspase interaction. *J. Biol. Chem.* 277, 432-438.
- Hildebrand J.M, Tanzer M.C, Lucet I.S, Young S.N, Spall S.K, Sharma P, Pierotti C, Garnier J, Dobson R.C.J, Webb A.I, Tripaydonis A, Babon J.J, Mulcair M.D., Scanlon M.J, Alexander W.S, Wilks A.F, Czabotar P.E, Lessene G, Murphy J.M, Silke J** (2014) Activation of the pseudokinase MLKL unleashes the four-helix bundle domain to induce membrane localization and necroptotic cell death. *Proc. Natl. Acad. Sci.* 111, 15072-15077.

- Holler N, Zaru R, Micheau O, Thome M, Attinger A, Valitutti S, Bodmer J.L, Schneider P, Seed B, Tschopp J** (2000) Fas triggers an alternative, caspase-8-independent cell death pathway using the kinase RIP as effector molecule. *Nat. Immunol.* 1, 489-495.
- Holohan C, Van Schaeybroeck S, Longley D.B, Johnston P.G** (2013) Cancer drug resistance: an evolving paradigm. *Nat. Rev. Cancer* 13, 714-726.
- Horn S, Hughes M.A, Schilling R, Sticht C, Tenev T, Ploesser M, Meier P, Sprick M.R, MacFarlane M, Leverkus M** (2017) Caspase-10 negatively regulates caspase-8-mediated cell death, switching the response to CD95L in favor of NF κ B activation and cell survival. *Cell Rep.* 19, 785-797.
- Huang Z, Wu S.Q, Liang Y, Zhou X, Chen W, Li L, Wu J, Zhuang Q, Chen C, Li J, Zhong C.Q, Xia W, Zhou R, Zheng C, Han J** (2015) RIP1/RIP3 binding to HSV-1 ICP6 initiates necroptosis to restrict virus propagation in mice. *Cell Host Microbe* 17, 229-242.
- Hughes M.A, Ian R, Powley I.R, Jukes-Jones R, Horn S, Feoktistova M, Fairall L, John W.R, Leverkus M, Cain K, MacFarlane M** (2016) Co-operative and hierarchical binding of c-FLIP and caspase-8: a unified model defines how c-FLIP isoforms differentially control cell fate. *Mol. Cell* 61, 834-849.
- Humphreys L, Espona-Fiedler M, Longley D.B** (2018) FLIP as a therapeutic target in cancer. *FEBS J.* doi: 10.1111/febs.14523 [Epub ahead of print].
- Ito Y, Ofengeim D, Najafov A, Das S, Saberi S, Li Y, Hitomi J, Zhu H, Chen H, Mayo L, Geng J, Amin P, DeWitt J.P, Mookhtiar A.K, Florez M, Ouchida A.T, Fan J.B, Pasparakis M, Kelliher M.A, Ravits J, Yuan J** (2016) RIPK1 mediates axonal degeneration by promoting inflammation and necroptosis in ALS. *Science* 353, 603-608.
- Jones J.M, Datta P, Srinivasula S.M, Ji W, Gupta S, Zhang Z, Davies E, Hajnóczky G, Saunders T.L, Van Keuren M.L, Fernandes-Alnemri T, Meisler M.H, Alnemri E.S** (2003) Loss of Omi mitochondrial protease activity causes the neuromuscular disorder of mnd2 mutant mice. *Nature* 425, 721-727.
- Joshi M, Anselm I, Shi J, Bale T.A, Towne M, Schmitz-Abe K, Crowley L, Giani F.C, Kazerounian S, Markianos K, Lidov H.G, Folkert R, Sankaran V.G, Agrawal P.B** (2016) Mutations in the substrate binding glycine-rich loop of the mitochondrial processing peptidase- α protein (PMPCA) cause a severe mitochondrial disease. *Cold Spring Harb. Mol. Case Stud.* 2, 1-11.
- Kaiser W.J, Upton J.W, Long A.B, Livingston-Rosanoff D, Daley-Bauer L.P, Hakem R, Caspary T, Mocarski E.S** (2011) RIP3 mediates the embryonic lethality of caspase-8-deficient mice. *Nature* 471, 368-372.
- Kaiser W.J, Sridharan H, Huang C, Mandal P, Upton J.W, Gough P.J, Sehon C.A, Marguis R.W, Bertin J, Mocarski E.S** (2013) Toll-like receptor 3-mediated necrosis via TRIF, RIP3, and MLKL. *J. Biol. Chem.* 288, 31268-31279.
- Keller N, Ozmadenci D, Ichim G, Stupack D** (2018) Caspase-8 function, and phosphorylation, in cell migration. *Semin. Cell Dev. Biol.*, Article in press.
- Kerr J.F, Wyllie A.H, Currie A.R** (1972) Apoptosis: a basic biological phenomenon with wide-ranging implications in tissue kinetics. *Br. J. Cancer* 26, 239-257.

- Kitur K, Parker D, Nieto P, Ahn D.S, Cohen T.S, Chung S, Wachtel S, Bueno S, Prince A** (2015) Toxin-induced necroptosis is a major mechanism of *Staphylococcus aureus* lung damage. *PLoS Pathog.* 11, 1-20.
- Kischkel F.C, Lawrence D.A, Tinel A, LeBlanc H, Virmani A, Schow P, Gazdar P, Blenis J, Arnott D, Ashkenazi A** (2001) Death receptor recruitment of endogenous caspase-10 and apoptosis initiation in the absence of caspase-8. *J. Biol. Chem.* 276, 46639-46646.
- Kuninaka S, Nomura M, Hirota T, Iida S, Hara T, Honda S, Kunitoku N, Sasayama T, Arima Y, Marumoto T, Koja K, Yonehara S, Saya H** (2005) The tumor suppressor WARTS activates the Omi/HtrA2-dependent pathway of cell death. *Oncogene* 24, 5287-5298.
- Lafont E, Milhas D, Teissié J, Therville N, Andrieu-Abadie N, Levade T, Benoist H, Ségui B** (2010) Caspase-10-dependent cell death in Fas/CD95 signalling is not abrogated by caspase inhibitor zVAD-fmk. *PLoS One* 5, e13638.
- Lamy L, Ngo V.N, Emre T.N.C, Shaffer A.L, Yang Y, Tian E, Nair V, Kruhlak J, Zingone A, Landgren O, Staudt L.M** (2013) Control of autophagic cell death by caspase-10 in multiple myeloma. *Cancer Cell* 23, 435-449.
- Laukens B, Jennewein C, Schenk B, Vanlangenakker N, Schier A, Cristofanon S, Zobel K, Deshayes K, Vucic D, Jeremias I, Bertrand M.J, Vandenabeele P, Fulda S** (2011) Smac mimetic bypasses apoptosis resistance in FADD- or caspase-8-deficient cells by priming for tumor necrosis factor α -induced necroptosis. *Neoplasia* 13, 971-979.
- Li J, McQuade T, Siemer A.B, Napetschnig J, Moriwaki K, Hsiao Y.S, Damko E, Moquin D, Walz T, McDermott A, Chan F.K, Wu H** (2012) The RIP1/RIP3 necrosome forms a functional amyloid signaling complex required for programmed necrosis. *Cell* 150, 339-350.
- Li J.X, Feng J.M, Wang Y, Li X.H, Chen X.X, Su Y, Shen Y.Y, Chen Y, Xiong B, Yang C.H, Ding J, Miao Z.H** (2014) The B-Raf (V600E) inhibitor dabrafenib selectively inhibits RIP3 and alleviates acetaminophen-induced liver injury. *Cell Death Dis.* 5, e1278.
- Li C, Liao J, Wu S, Fan J, Peng Z, Wang Z** (2017) Overexpression of DBC1, correlated with poor prognosis, is a potential therapeutic target for hepatocellular carcinoma. *Biochem. Biophys. Res. Commun.* 494, 511-517.
- Lin J, Li H, Yang M, Ren J, Huang Z, Han F, Huang J, Ma J, Zhang D, Zhang Z, Wu J, Huang D, Qiao M, Jin G, Wu Q, Huang Y, Du J, Han J** (2013) A role of RIPK3-mediated macrophage necrosis in atherosclerosis development. *Cell Rep.* 3, 200-210.
- Linkermann A, Bräsen J.H, De Zen F, Weinlich R, Schwendener R.A, Green D.R, Kunzendorf U, Krautwald S** (2012) Dichotomy between RIPK1- and RIPK3-mediated necroptosis in tumor necrosis factor- α -induced shock. *Mol. Med.* 18, 577-586.
- Linkermann A, Bräsen J.H, Darding M, Jin M.K, Sanz A.B, Heller J.O, De Zen F, Weinlich R, Ortiz A, Walczak H, Weinberg J.M, Green D.R, Kunzendorf U, Krautwald S** (2013) Two independent pathways of regulated necrosis mediate ischemia-reperfusion injury. *Proc. Natl. Acad. Sci. U. S. A.* 110, 12024-12029.

- Los M, Wesselborg S, Schulze-Osthoff K** (1999) The role of caspases in development, immunity, and apoptotic signal transduction. *Immunity* 10, 629-639.
- Luedde M, Lutz M, Carter N, Sosna J, Jacoby C, Vucur M, Gautheron J, Roderburg C, Borg N, Reisinger F, Hippe H.J, Linkermann A, Wolf M.J, Rose-John S, Lüllmann-Rauch R, Adam D, Flögel U, Heikenwalder M, Luedde T, Frey N** (2014) RIPK3, a kinase promoting necroptotic cell death, mediates adverse remodelling after myocardial infarction. *Cardiovasc. Res.* 103, 206-216.
- Martins L.M, Iaccarino I, Tenev T, Gschmeissner S, Totty N.F, Lemoine N.R, Savopoulos J, Gray C.W, Creasy C.L, Dingwall C, Downward J** (2002) The serine protease Omi/HtrA2 regulates apoptosis by binding XIAP through a reaper-like motif. *J. Biol. Chem.* 277, 439-444.
- Martins L.M, Morrison A, Kristina K, Fedele V, Moiso N, Teismann P, Abuin A, Grau E, Geppert M, Livi G.P, Creasy C.L, Martin A, Hargreaves I, Heales S.J, Okada H, Brandner S, Schulz J.B, Mak T, Downward J** (2004) Neuroprotective role of the reaper-related serine protease HtrA2/Omi revealed by targeted deletion in mice. *Mol. Cell Biol.* 24, 9848-9862.
- Matsushima Y, Goto Y, Kaguni L.S** (2010) Mitochondrial Lon protease regulates mitochondrial DNA copy number and transcription by selective degradation of mitochondrial transcription factor A (TFAM). *Proc. Natl. Acad. Sci.* 107, 18410-18415.
- McCabe K.E, Bacos K, Lu D, Delaney J.R, Axelrod J, Potter M.D, Vamos M, Wong V, Cosford N.D, Xiang R, Stupack D.G** (2014) Triggering necroptosis in cisplatin and IAP antagonist-resistant ovarian carcinoma. *Cell Death Dis.* 30, e1496.
- Metzig O.M, Fuchs D, Tagscherer K.E, Gröne H.J, Schirmacher P, Roth W** (2016) Inhibition of caspases primes colon cells for 5-fluorouracil-induced TNF- α -dependent necroptosis driven by RIP1 kinase and NF- κ B. *Oncogene* 35, 3399-3409.
- Meyer-Schwesinger C, Meyer T.N, Sievert H, Hocha E, Sachs M, Klupp E.M, Münster S, Balabanov S, Carrier L, Helmchen U, Thaiss F, Stahl R.A** (2011) Ubiquitin C-terminal hydrolase-L1 activity induces polyubiquitin accumulation in podocytes and increases proteinuria in rat membranous nephropathy. *Am. J. Pathol.* 178, 2044-2057.
- Michalak P** (2008) Coexpression, coregulation, and cofunctionality of neighboring genes in eukaryotic genomes. *Genomics* 91, 243-248.
- Milhas D, Cuvillier O, Therville N, Clavé P, Thomsen M, Levade T, Benoist H, Ségui B** (2005) Caspase-10 triggers Bid cleavage and caspase cascade activation in FasL-induced apoptosis. *J. Bio. Chem.* 280, 19836-19842.
- Mohr A, Deedigan L, Jencz S, Mehrabadi Y, Houlden L, Albarenque S, Zwacke R.M** (2018) Caspase-10: a molecular switch from cell-autonomous apoptosis to communal cell death in response to chemotherapeutic drug treatment. *Cell Death Differ.* 25, 340-352.
- Mompeàn M, Li W, Li J, Laage S, Siemer A.B, Bozkurt G, Wu H, McDermott A.E** (2018) The structure of the necrosome RIPK1-RIPK3 core, a human hetero-amyloid signaling complex. *Cell* 173, 1244-1253.
- Moon S.J, Jeong B.C, Kim H.J, Lim J.E, Kwon G.Y, Kim J.H** (2018) DBC1 promotes castration-resistant prostate cancer by positively regulating DNA binding and stability of AR-V7. *Oncogene* 37, 1326-1339.

- Moquin D.M, McQuade T, Chan F.K** (2013) CYLD deubiquitinates RIPK1 in the TNF α -induced necrosome to facilitate kinase activation and programmed necrosis. *PLoS One* 8, e76841.
- Moriwaki K, Bertin J, Gough P.J, Chan F.K** (2015) A RIPK3-caspase 8 complex mediates atypical pro-IL-1 β processing. *J. Immunol.* 194, 1938-1944.
- Moujalled D.M, Cook W.D, Okamoto T, Murphy J, Lawlor K.E, Vince J.E, Vaux D.L** (2013) TNF can activate RIPK3 and cause programmed necrosis in the absence of RIPK1. *Cell Death Dis.* 4, e465.
- Mühlethaler-Mottet A, Flahaut M, Bourlout K.B, Nardou K, Coulon A, Liberman J, Thome M, Gross N** (2011) Individual caspase-10 isoforms play distinct and opposing roles in the initiation of death receptor-mediated tumour cell apoptosis. *Cell Death Dis.* 2, 1-12.
- Murphy J.M, Czabotar P.E, Hildebrand J.M, Lucet I.S, Zhang J.G, Alvarez-Diaz S, Lewis R, Lalaoui N, Metcalf D, Webb A.I, Young S.N, Varghese L.N, Tannahill G.M, Hatchell E.C, Majewski I.J, Okamoto T, Dobson R.C.J, Hilton D.J, Babon J.J, Nicola N.A, Strasser A, Silke J, Alexander W.S** (2013) The pseudokinase MLKL mediates necroptosis via a molecular switch mechanism. *Immunity* 39, 443-453.
- Murphy J.M, Lucet I.S, Hildebrand J.M, Tanzer M.C, Young S.N, Sharma P, Lessene G, Alexander W.S, Babon J.J, Silke J, Czabotar P.E** (2014) Insights into the evolution of divergent nucleotide-binding mechanisms among pseudokinases revealed by crystal structures of human and mouse MLKL. *Biochem. J.* 457, 369-377.
- Nagata S, Tanaka M** (2017) Programmed cell death and the immune system. *Nat. Rev. Immunol.* 17, 333-340.
- Najafov A, Chen H, Yuan J** (2017) Necroptosis and cancer. *Trends in Cancer* 3, 294-301.
- Nogusa S, Thapa R.J, Dillon C.P, Liedmann S, Oquin T.H 3rd, Ingram J.P, Rodriguez D.A, Kosoff R, Sharma S, Sturm O, Verbist K, Gough P.J, Bertin J, Hartmann B.M, Sealfon S.C, Kaiser W.J, Mocarski E.S, López C.B, Thomas P.G, Oberst A, Green D.R, Balachandran S** (2016) RIPK3 activates parallel pathways of MLKL-driven necroptosis and FADD-mediated apoptosis to protect against influenza A virus. *Cell Host Microbe* 20, 13-24.
- Norbury C.J, Hickson I.D** (2001) Cellular responses to DNA damage. *Annu. Rev. Pharmacol. Toxicol.* 41, 367-401.
- Oberst A, Dillon C.P, Weinlich R, McCormick L.L, Fitzgerald P, Pop C, Hakem R, Salvesen G.S, Green D.R** (2011) Catalytic activity of the caspase-8-FLIP(L) complex inhibits RIPK3-dependent necrosis. *Nature* 471, 363-367.
- O'Donnell M.A, Perez-Jimenez E, Oberst A, Ng A, Massoumi R, Xavier R, Green D.R, Ting A.T** (2011) Caspase 8 inhibits programmed necrosis by processing CYLD. *Nat. Cell Biol.* 13, 1437-1442.
- Ofengeim D, Ito Y, Najafov A, Zhang Y, Shan B, DeWitt J.P, Ye J, Zhang X, Chang A, Vakifahmetoglu-Norberg H, Geng J, Py B, Zhou W, Amin P, Berlink L.J, Qi C, Yu Q, Trapp B, Yuan J** (2015) Activation of necroptosis in multiple sclerosis. *Cell Rep.* 11, 1836-1849.

- Osborn S.L, Diehl G, Han S.J, Xue L, Kurd N, Hsieh K, Cado D, Robery E.A, Winoto A** (2010) Fas-associated death domain (FADD) is a negative regulator of T-cell receptor-mediated necroptosis. *Proc. Natl. Acad. Sci. U. S. A.* 107, 13034-13039.
- Pasparakis M, Vandenabeele P** (2015) Necroptosis and its role in inflammation. *Nature* 517, 311-320.
- Pearson J.S, Murphy J.M** (2017) Down the rabbit hole: is necroptosis truly an innate response to infection? *Cell Microbiol.* 19.
- Peter B, Waddington C.L, Oláhová M, Sommerville E.W, Hopton S, Pyle A, Champion M, Ohlson M, Siibak T, Chrzanowska-Lightowlers Z.M.A, Taylor R.W, Falkenberg M, Lightowlers R.N** (2018) Defective mitochondrial protease LonP1 can cause classical mitochondrial disease. *Hum. Mol. Gen.* 27, 1743-1753.
- Pfeffer C.M, Singh A.T.K** (2018) Apoptosis: a target for anticancer therapy. *Int. J. Mol. Sci.* 19, 448.
- Pierdomenico M, Negroni A, Stronati L, Vitali R, Prete E, Bertin J, Gough P.J, Aloï M, Cucchiara S** (2014) Necroptosis is active in children with inflammatory bowel disease and contributes to heighten intestinal inflammation. *Am. J. Gastroenterol.* 109, 279-287.
- Poon I.K, Lucas C.D, Rossi A.G, Ravichandran K.S** (2014) Apoptotic cell clearance: basic biology and therapeutic potential. *Nat. Rev. Immunol.* 14, 166-180.
- Qian H, Li X, Zhang W, Ma L, Sun J, Tang X, Chen Y, Teng L, Wang W, Li D, Xu Y, Li C, Cao Y** (2018) Caspase-10, matrix metalloproteinase-9 and total laminin are correlated with the tumor malignancy of clear cell renal cell carcinoma. *Oncol. Lett.* 16, 2039-2045.
- Quin J, Long B, Luo L, Wei Y, Chen S, Li Y, Liang X, Zhang Z** (2017) Identification of proteasome subunit alpha type-1 as a novel biomarker in HBV-associated hepatocellular carcinoma tissue interstitial fluid by proteomic analysis. *Int. J. Clin. Exp. Pathol.* 10, 7812-7820.
- Qinli Z, Meiqing L, Xia J, Weili G, Xiuliang J, Junwei J, Hailan Y, Ce Y, Qiao N** (2013) Necrostatin-1 inhibits the degeneration of neural cells induced by aluminium exposure. *Restor. Neurol. Neurosci.* 31, 543-555.
- Raam B.J, Salvesen G.S** (2012) Proliferative versus apoptotic functions of caspase-8 hetero or homo: The caspase-8 dimer controls cell fate. *Biochim. Biophys. Acta* 1824, 113-122.
- Robinson N, McComb S, Mulligan R, Dudani R, Krishnan L, Sad S** (2012) Type I interferon induces necroptosis in macrophages during infection with *Salmonella enterica* serovar Thyphimurium. *Nat. Immunol.* 13, 954-962.
- Roca F.J, Ramakrishnan L** (2013) TNF dually mediates resistance and susceptibility to mycobacteria via mitochondrial reactive oxygen species. *Cell* 153, 521-534.
- Rodriguez D.A, Weinlich R, Brown S, Guy C, Fitzgerald P, Dillon C.P, Oberst A, Quarato G, Low J, Cripps J.G, Chen T, Green D.R** (2015) Characterization of RIPK3-mediated phosphorylation of the activation loop of MLKL during necroptosis. *Cell Death Differ.* 23, 76-88.

- Rosenbaum D.M, Degterev A, David J, Rosenbaum P.S, Roth S, Grotta J.C, Cuny G.D, Yuan J, Savitz S.I** (2010) Necroptosis, a novel form of caspase-independent cell death, contributes to neuronal damage in a retinal ischemia-reperfusion injury model. *J. Neurosci. Res.* 88, 1569-1576.
- Sakamaki K, Inoue T, Asano M, Sudo K, Kazama H, Sakagami J, Sakata S, Ozaki M, Nakamura S, Toyokuni S, Osumi N, Iwakura Y, Yonehara S** (2002) Ex vivo whole-embryo culture of caspase-8-deficient embryos normalize their aberrant phenotypes in the developing neural tube and heart. *Cell Death Differ.* 9, 1196-1206.
- Sakamaki K, Shimizu K, Iwata H, Imai K, Satou Y, Funayama N, Nozaki M, Yajima M, Nishimura O, Higuchi M, Chiba K, Yoshimoto M, Kimura H, Gracey A.Y, Shimizu T, Tomii K, Gotoh O, Akasaka K, Sawasaki T, Miller D.J** (2014) The apoptotic initiator caspase-8: its functional ubiquity and genetic diversity during animal evolution. *Mol. Biol. Evol.* 31, 3282-3301.
- Sakamaki K, Imai K, Tomii K, Miller D.J** (2015) Evolutionary analyses of caspase-8 and its paralogs: deep origins of the apoptotic signaling pathways. *Bioessays* 37, 1-10.
- Salvesen G.S, Walsh C.M** (2014) Functions of caspase 8: the identified and the mysterious. *Semin. Immunol.* 26, 246-252.
- Savill J, Fadok V** (2000) Corpse clearance defines the meaning of cell death. *Nature* 407, 784-788.
- Seifert L, Werba G, Tiwari S, Gao L.N, Allothman S, Alqunaibit D, Avanzi A, Barilla R, Daley D, Greco S.H, Torres-Hernandez A, Pergamo M, Ochi A, Zambirinis C.P, Pansari M, Rendon M, Tippens D, Hundeyin M, Mani V.R, Hajdu C, Engle D, Miller G** (2016) The necrosome promotes pancreatic oncogenesis via CXCL1 and mincle-induced immune suppression. *Nature* 532, 245-249.
- Seifert L, Miller G** (2017) Molecular pathways: the necrosome – a target for cancer therapy. *Clin. Cancer Res.* 23, 1132-1136.
- Shindo R, Yamazaki S, Ohmuraya M, Araki K, Nakano H** (2016) Short form FLICE-inhibitory protein promotes TNF α -induced necroptosis in fibroblasts derived from *CFLARs* transgenic mice. *Biochem. Biophys. Res. Commun.* 480, 23-28.
- Silke J, Meier P** (2013) Inhibitor of apoptosis (IAP) proteins – modulators of cell death and inflammation. *Cold Spring Harb. Perspect. Biol.* 5, 1-19.
- Sosna J, Voigt S, Mathieu S, Kabelitz D, Trad A, Janssen O, Meyer-Schwesinger C, Schütze S, Adam D** (2013) The proteases HtrA2/Omi and UCH-L1 regulate TNF-induced necroptosis. *Cell Commun. Signal.* 11, 76.
- Sprick M.R, Rieser E, Stahl H, Grosse-Wilde A, Weigand M.A, Walczak H** (2002) Caspase-10 is recruited to and activated at the native TRAIL and CD95 death-inducing signalling complexes in a FADD-dependent manner but cannot functionally substitute caspase-8. *EMBO J.* 21, 4520-4530.
- Sprick M.R and Walczak H** (2004) The interplay between the Bcl-2 family and death receptor-mediated apoptosis. *Biochim. Biophys. Acta* 1644, 125-132.

- Srinivasula S.M, Gupta S, Datta P, Zhang Z, Hegde R, Cheong N, Fernandes-Alnemri T, Alnemri E.S** (2003) Inhibitor of apoptosis proteins are substrates for the mitochondrial serine protease Omi/HtrA2. *J. Biol. Chem.* 34, 31469-31472.
- Strauss K.M, Martins L.M, Plun-Favreau H, Marx F.P, Kautzmann S, Berg D, Gasser T, Wszolek Z, Müller T, Bornemann A, Wolburg H, Downward J, Riess O, Schulz J.B, Krüger R** (2005) Loss of function mutations in the gene encoding Omi/HtrA2 in Parkinson's disease. *Hum. Mol. Genet.* 15, 2099-2111.
- Strilic B, Yang L, Albarran-Juarez J, Wachsmuth L, Han K, Müller U.C, Pasparakis M, Offermanns S** (2016) Tumour-cell-induced endothelial cell necroptosis via death receptor 6 promotes metastasis. *Nature* 536, 215-218.
- Su Z, Yang Z, Xie L, DeWitt J.P, Chen Y** (2016) Cancer therapy in the necroptosis era. *Cell Death Differ.* 23, 748-756.
- Sun L, Wang H, Wang Z, He S, Chen S, Liao D, Wang L, Yan J, Liu W, Lei X, Wang X** (2012) Mixed lineage kinase domain-like protein mediates necrosis signalling downstream of RIPK3 kinase. *Cell* 148, 213-227.
- Sun L, Wang X** (2014) A new kind of cell suicide: mechanisms and functions of programmed necrosis. *Trends Biochem. Sci.* 39, 587-593.
- Sundararajan R, Chen G, Mukherjee C, White E** (2005) Caspase-dependent processing activates the proapoptotic activity of deleted in breast cancer-1 during tumor necrosis factor-alpha-mediated death signaling. *Oncogene* 24, 4908-4920.
- Suzuki Y, Imai Y, Nakayama H, Takahashi K, Takio K, Takahashi R** (2001) A serine protease, HtrA2, is released from the mitochondria and interacts with XIAP, inducing cell death. *Mol. Cell* 8, 613-621.
- Takahashi N, Duprez L, Grootjans S, Cauwels A, Nerinckx W, DuHadaway J.B, Goossens V, Roelandt R, Van Hauwermeiren F, Libert C, Declercq W, Callewaert N, Prendergast G.C, Degterev A, Yuan J, Vandenabeele P** (2012) Necrostatin-1 analogues: critical issues on the specificity, activity and in vivo use in experimental disease models. *Cell Death Dis.* 29, e437.
- Tanzer M.C, Khan N, Rickard J.A, Etemadi N, Lalaoui N, Spall S.K, Hildebrand J.M, Segal D, Miasari M, Chau D, Wong W, McKinlay M, Chunduru S.K, Benetatos C.A, Condon S.M, Vince J.E, Herold M.J, Silke J** (2017) Combination of IAP antagonist and IFN γ activates novel caspase-10- and RIPK1-dependent cell death pathways. *Cell Death Differ.*, 1-11.
- Urruticoechea A, Alemany R, Balart J, Villanueva A, Vinals F, Capella G** (2010) Recent advances in cancer therapy: an overview. *Bentham Sc.* 16, 3-10.
- Vanlangenakker N, Vanden Berghe T, Vandenabeele P** (2012) Many stimuli pull the necrotic trigger, an overview. *Cell Death Differ.* 19, 75-86.
- van Loo G, van Gurp M, Depuydt B, Srinivasula S.M, Rodriguez I, Alnemri E.S, Gevaert K, Vandekerckhove J, Declercq W, Vandenabeele P** (2002) The serine protease Omi/HtrA2 is released from mitochondria during apoptosis. Omi interacts with caspase-inhibitor XIAP and induces enhanced caspase activity. *Cell Death Differ.* 9, 20-26.

- Vande Walle L, Van Damme P, Lamkanfi M, Saelens X, Vandekerckhove J, Gevaert K, Vandenabeele P** (2007) Proteome-wide identification of HtrA2/Omi Substrates. *Journal of Proteome Research* 6, 1006-1015.
- Vande Walle L, Wirawan E, Lamkanfi M, Festjens N, Verspurten J, Saelens X, VandenBerghe T, Vandenabeele P** (2010) The mitochondrial serine protease HtrA2/Omi cleaves RIP1 during apoptosis of Ba/F3 cells induced by growth factor withdrawal. *Cell Research* 20, 421-433.
- Verhagen A.M, Silke J, Ekert P.G, Pakusch M, Kaufmann H, Connolly L.M, Day C.L, Tikoo A, Burke R, Wrobel C, Moritz R.L, Simpson R.J, Vaux D.L** (2002) HtrA2 promotes cell death through its serine protease activity and its ability to antagonize inhibitor of apoptosis proteins. *J. Biol. Chem.* 277, 445-454.
- Verhagen A.M, Kratina T.K, Hawkins C.J, Silke J, Ekert P.G, Vaux D.L** (2007) Identification of mammalian mitochondrial proteins that interact with IAPs via N-terminal IAP binding motifs. *Cell Death Differ.* 14, 348-357.
- Vitner E.B, Salomon R, Farfel-Becker T, Meshcheriakova A, Ali M, Klein A.D, Platt F.M, Cox T.M, Futerman A.H** (2014) RIPK3 as a potential therapeutic target for Gaucher's disease. *Nat. Med.* 20, 204-208.
- Wang J, Chun H.J, Wong W, Spencer D.M, Leonardo M.J** (2001) Caspase-10 is an initiator caspase in death receptor signaling. *Proc. Natl. Acad. Sci.* 98, 13884-13888.
- Wang H, Sun L, Su L, Rizo J, Liu L, Wang L.F, Wang F.S, Wang X** (2014) Mixed lineage kinase domain-like protein MLKL causes necrotic membrane disruption upon phosphorylation by RIP3. *Mol. Cell* 54, 133-146.
- Wang S, Ni H.M, Dorko K, Kumer S.C, Schmitt T.M, Nawabi A, Komatsu M, Huang H, Ding W.X** (2016) Increased hepatic receptor interacting protein kinase 3 expression due to impaired proteasomal functions contributes to alcohol-induced steatosis and liver injury. *Oncotarget* 7, 17681-17698.
- Weinlich R, Oberst A, Beere H.M, Green D.R** (2017) Necroptosis in development, inflammation and disease. *Cell Death Autophagy* 18, 127-136.
- Westerlund M, Behbahani H, Gellhaar S, Forsell C, Belin A.C, Anvret A, Zettergren A, Nissbrandt H, Lind C, Sydow O, Graff C, Olson L, Ankarcrona M, Galter D** (2011) Altered enzymatic activity and allele frequency of OMI/HTRA2 in Alzheimer's disease. *FASEB J.* 4, 1345-1352.
- Wicki S, Gurzeler U, Wie-Lynn Wong W, Jost P.J, Bachmann D, Kaufmann T** (2016) Loss of XIAP facilitates switch to TNF α -induced necroptosis in mouse neutrophils. *Cell Death Dis.* 7, e2422.
- Willingham S.B, Bergstralh D.T, O'Connor W, Morrison A.C, Taxman D.J, Duncan J.A, Barnoy S, Venkatesan M.M, Flavell R.A, Deshmukh M, Hoffman H.M, Ting J.P** (2007) Microbial pathogen-induced necrotic cell death mediated by the inflammasome components CIAS1/cryopyrin/NLRP3 and ASC. *Cell Host Microbe* 2, 147-159.
- Witt A, Vucic D** (2017) Diverse ubiquitin linkages regulate RIP kinases-mediated inflammatory and cell death signaling. *Cell Death Differ.*, 1-12.

- Worth A, Thrasher A.J, Gaspar H.B** (2006) Autoimmune lymphoproliferative syndrome: molecular basis of disease and clinical phenotype. *Br. J. Haematol.* 133, 124-140.
- Xu L, Zhai L, Ge Q, Liu Z, Tao R** (2017) Vacuolar protein sorting 4B (VPS4B) regulates apoptosis of chondrocytes via p38 mitogen-activated protein kinases (MAPK) in osteoarthritis. *Inflammation* 6, 1924-1932.
- Yan L, Dong X, Gao J, Liu F, Zhou L, Sun Y, Zhao X** (2018) A novel rapid quantitative method reveals stathmin-1 as a promising marker for esophageal squamous cell carcinoma. *Cancer Med.* 7, 1802-1813.
- Yang Q.H, Church-Hajduk R, Ren J, Newton M.L, Du C** (2003) Omi/HtrA2 catalytic cleavage of inhibitor of apoptosis (IAP) irreversibly inactivates IAPs and facilitates caspase activity in apoptosis. *Genes Dev.* 17, 1487-1496.
- Zaltsman Y, Shachnai L, Yivgi-Ohana N, Schwarz M, Maryanovich M, Houtkooper R.H, Vaz F.M, De Leonardis F, Fiermonte G, Palmieri F, Gillissen B, Daniel P.T, Jimenez E, Walsh S, Koehler C.M, Roy S.S, Walter L, Hajnóczky G, Gross A** (2010) MTCH2/MIMP is a major facilitator of tBID recruitment to mitochondria. *Nature Cell Biol.* 12, 553-562.
- Zaman S, Wang R, Gandhi V** (2014) Targeting the apoptosis pathway in hematologic malignancies. *Leuk. Lymphoma* 55, 1980-1992.
- Zhang D.W, Shao J, Lin J, Zhang N, Lu B.J, Lin S.C, Dong M.Q, Han J** (2009) RIP3, an energy metabolism regulator that switches TNF-induced cell death from apoptosis to necrosis. *Science* 325, 332-336.
- Zhu S, Zhang Y, Bai G, Li H** (2011) Necrostatin-1 ameliorates symptoms in R6/2 transgenic mouse model of Huntington's disease. *Cell Death Dis.* 2, e115.
- Zhu X, Shen X, Qu J, Straubinger R.M, Jusko W.J** (2018) Proteomic analysis of combined gemcitabine and birinapant in pancreatic cancer cells. *Front. Pharmacol.* 9, 1-14.

7. List of publications

Sosna J, Philipp S, Fuchslocher Chico J, Saggau C, Fritsch J, Föll A, Plenge J, Arenz C, Pinkert T, Kalthoff H, Trauzold A, Schmitz I, Schütze S, Adam D (2016) Differences and similarities in TRAIL- and TNF-mediated necroptotic signalling in cancer cells. *Mol. Cell. Biol.* 36(20), 2626-2644.

Fuchslocher Chico J, Saggau C, Adam D (2017) Proteolytic control of regulated necrosis. *Biochim. Biophys. Acta* 1864, 2147-2161.

Fuchslocher Chico J, Falk-Paulsen M, Luzius A, Saggau C, Ruder B, Bolik J, Schmidt-Arras D, Linkermann A, Becker C, Rosenstiel P, Rose-John S, Adam D (2018) The enhanced susceptibility of ADAM-17 hypomorphic mice to DSS-induced colitis is not ameliorated by loss of RIPK3, revealing an unexpected function of ADAM-17 in necroptosis. *Oncotarget* 9(16), 12941-12958.

8. Eidesstattliche Erklärung

Hiermit erkläre ich, Carina Saggau, dass ich die vorliegende wissenschaftliche Abhandlung mit dem Titel:

„The species-specific role of caspase-8 as a regulator of necroptosis“

nach den Regeln guter wissenschaftlicher Praxis eigenständig verfasst und keine anderen als die angegebenen Hilfsmittel und Quellen benutzt habe. Dabei habe ich keine Hilfe, außer der wissenschaftlichen Beratung durch meinen Doktorvater Prof. Dr. rer. nat. Dieter Adam und durch die namentlich erwähnten Kooperationspartner in Anspruch genommen.

Diese Arbeit wurde bisher an keiner Stelle im Rahmen eines Prüfungsverfahrens vorgelegt. Teile dieser Arbeit wurden bereits publiziert.

Kiel, im September 2018

Carina Saggau

9. Danksagung

Besonderer Dank gilt meinem Betreuer Prof. Dr. rer. nat. Dieter Adam für die Bereitstellung meines interessanten Dissertationsthemas, die intensive Betreuung und vor allem die sowohl kritischen wie auch unterstützenden und motivierenden Ratschläge und wissenschaftlichen Diskussionen, die maßgeblich zum Gelingen der vorliegenden Arbeit beigetragen haben. Vielen Dank auch für das Vertrauen, welches mir über die Jahre entgegen gebracht wurde und welches sichtlich zu meiner persönlichen und wissenschaftlichen Entwicklung beigetragen hat.

Herrn Prof. Dr. Axel Scheidig danke ich für seine Bereitschaft, die Begutachtung dieser Arbeit zu übernehmen.

Des Weiteren danke ich den Direktoren des Institutes für Immunologie Prof. Dr. med. Dieter Kabelitz und Prof. Dr. rer. nat. Alexander Scheffold für die Möglichkeit, diese Doktorarbeit anzufertigen.

Weiterhin bedanke ich mich herzlich bei allen Mitarbeitern des Institutes für Immunologie für ein freundschaftliches Arbeitsklima. Ich habe mich immer sehr gut aufgehoben gefühlt.

Mein besonderer Dank gilt Sabine Mathieu-Grützmacher und vor allem Parvin Davarnia (meiner „Labormutti“) für ihre exzellente technische Unterstützung, aber vor allem für die vielen motivierenden und aufbauenden Gespräche. Ohne euch wäre ich nicht da, wo ich heute bin. Ebenfalls danken möchte ich Johaiber Fuchslocher Chico, der für mich zu einem Freund geworden ist und ohne den der Laboralltag sehr viel trister gewesen wäre. Ein herzlicher Dank geht in diesem Zusammenhang auch an die jetzigen und ehemaligen Kollegen der Arbeitsgruppe von Prof. Dr. rer. nat. Dieter Adam für die gute Zusammenarbeit und die großartige Unterstützung im Laboralltag (besonders zu erwähnen an dieser Stelle: Jaqueline Klausewitz, die mich im Rahmen ihrer medizinischen Doktorarbeit tatkräftig unterstützte, Justus Hoyer und Justyna Sosna).

Besonders erwähnen möchte ich ebenfalls Dr. Jürgen Fritsch für seine wissenschaftliche Unterstützung und technische Hilfestellung im Rahmen dieser Arbeit, Philipp Zingler für die beste Zusammenarbeit in Bezug auf das Lager und die Entwicklermaschine, Dr. Susanne Quabius für die großartigen Gespräche und Doreen Gänslar und Heike Ebeling für ihre Fürsorge und Unterstützung in jeder Lebenslage.

Mein tiefer Dank gilt meiner gesamten Familie und der meines Freundes, meiner Mutter Veronica, meiner Schwester Julia und meinem Freund Patrick, für ihre Liebe, ihr Vertrauen in mich und meine Fähigkeiten und ihre unermüdliche Unterstützung. Dieser Dank gilt ebenso meinen Freunden (Marius, Momme, Felix, Julian, Lulu, Kathrin, Jessi, Svea, Philipp, Anne, Christian, Erik, Eva, Olli, Lotte) ohne die ich diesen Abschnitt meines Lebens niemals hätte bewältigen können.

10. Wissenschaftlicher Werdegang

Persönliche Daten

Name: Carina Saggau
Geburtsdatum und -ort: 07.06.1987 in Preetz
Adresse: Klüver Kamp 2a in 24326 Kalübbe
Staatsangehörigkeit: deutsch

Akademische Ausbildung

seit 05/2015 Promotions-Arbeit im Rahmen des Exzellenzclusters „*Inflammation at Interfaces*“ in der Arbeitsgruppe von Prof. Dr. Dieter Adam, Christian-Albrechts-Universität zu Kiel

04/2012 – 11/2014 Master-Studium der Ökotoxikologie an der Christian-Albrechts-Universität zu Kiel Fachrichtung Ernährungswissenschaften

10/2014 Abschluss: *Master of Science*
Thema der Masterarbeit: *“Regulation of a novel cytokine in low-grade inflammation of adipose tissue by fatty acids”*

10/2007 – 03/2012 Bachelor-Studium der Biologie an der Georg-August-Universität, Göttingen

03/2012 Abschluss: *Bachelor of Science*
Thema der Bachelorarbeit: *“Female sexual behaviour as an indicator of the timing of ovulation in crested black macaques (Macaca nigra)”*

10/2006 – 09/2007 Magister-Studium an der Christian-Albrechts-Universität zu Kiel

08/1997 – 06/2006 Gymnasium Schloss Plön
Abschluss: Abitur